공 학 박 사 학 위 논 문

Development of radical-stable peroxidases based on peroxidase inactivation mechanism

퍼옥시다제 비활성화 메커니즘에 기반한
퍼옥시다제의 래디컬 안정성 향상

2015년 2월

서울대학교 대학원

협동과정 바이오엔지니어링 전공

김 수 진

Development of radical-stable peroxidases based on peroxidase inactivation mechanism

By

Su Jin Kim

Advisor: Professor Ji Sook Hahn

Submitted in Partial Fulfillment of the Requirements
for the Degree of Doctor of Philosophy
in Seoul National University

February, 2015

Interdisciplinary Program of Bioengineering
Graduate School
Seoul National University

Development of radical-stable peroxidases based on peroxidase inactivation mechanism

퍼옥시다제 비활성화 메커니즘에 기반한
퍼옥시다제의 래디컬 안정성 향상

지도교수 한지숙

이 논문을 공학박사학위 논문으로 제출함

2015년 2월

서울대학교 대학원
협동과정 바이오엔지니어링 전공
김 수 진

김 수 진 의 박사학위논문을 인준함

2014년 12월

위 원 장 _____

부위원장 _____

위 원 _____

위 원 _____

위 원 _____

ABSTRACT

Development of radical-stable peroxidases based on peroxidase inactivation mechanism

Su Jin Kim

Interdisciplinary Program of Bioengineering
Graduate School
Seoul National University

Peroxidases catalyze a variety of oxidative transformations of many aromatic compounds and thus have potential in biosynthesis and other biotechnological applications. However, the usefulness of these versatile enzymes is limited, as the enzyme is quickly inactivated during the oxidation reaction of aromatic compounds. This low stability of peroxidases results in low product yield due to the incomplete reaction and increased production costs. Many researchers have studied this, and three possible pathways for peroxidase inactivation have been proposed: reaction with excess hydrogen peroxide, sorption by polymer product, and reaction with radical intermediates. The first two pathways have been corroborated with extensive evidence; however, the free radical-mediated mechanism of peroxidase inactivation has not been fully elucidated.

Thus, the dominant inactivation mechanism in the oxidation reaction of phenolic compounds must be revealed. An understanding of the molecular mechanism of radical-mediated inactivation is necessary for protein engineering to improve peroxidase stability.

Firstly, the dominant mechanism of peroxidase inactivation during phenol oxidation was determined. Two peroxidases, *Coprinus cinereus* peroxidase (CiP) and horseradish peroxidase isozyme C (HRPC), showed much higher inactivation rates after the simultaneous addition of phenol and hydrogen peroxide. After the oxidation reaction of phenol, the molecular weights of polypeptides originating from the inactivated peroxidases were slightly increased, and a large fraction of heme from the two inactivated peroxidases remained intact. These findings support the hypothesis that the inactivation of peroxidase during the oxidation of phenol occurs by the coupling of phenoxyl radicals with peroxidase polypeptides.

Secondly, the radical coupling site of CiP was identified, and the radical stability of CiP was improved by site-directed mutagenesis. The residue F230 of CiP modified with the phenoxyl radical was mutated to amino acids (Ala) that resist radical coupling. The F230A mutant showed the highest stability against the radical attack, retaining 80% of its initial activity, while the wild-type protein was almost completely inactivated. In addition, no structural changes were observed in CiP after radical coupling.

Thirdly, HRPC was also engineered to enhance the radical stability. Phenylalanine residues that are vulnerable to modification by phenoxyl radicals were identified and then changed to Ala to prevent radical coupling. The F68A/F142A/F143A/F179A mutant

exhibited dramatic enhancement of radical stability, retaining 41% of its initial activity compared to the wild type, which was completely inactivated. Radical coupling did not change the secondary structure or the active site structure of HRPC. Structure and sequence alignment revealed that radical-vulnerable Phe residues were conserved in homologous peroxidases.

Fourthly, the radical-stable CiP mutant, F230A, was applied to the major practical applications, such as the removal of phenol, the decolorization of dye, and the synthesis of polymers. As expected, the removal efficiency of phenol and the decolorization efficiency of Reactive Black 5 were increased four- and five-fold, respectively, compared with that of the wild type. In addition, the phenolic polymer having the highest molecular mass (8850 Da) was synthesized by the F230A mutant in a 50% v/v isopropanol-buffer mixture.

A novel engineering strategy to eliminate the radical coupling site increased the radical stability of two peroxidases, CiP and HRPC. This implies that phenoxyl radicals covalently bind to critical Phe residues and inactivate peroxidase by blocking substrate access to the active site of the enzyme.

Keywords **:** Peroxidase inactivation, Radical stability, Radical coupling, Mass spectrometry, Site-directed mutagenesis, *Coprinus cinereus* peroxidase, Horseradish peroxidase

Student Number: 2010-31018

CONTENTS

LIST OF TABLES

LIST OF FIGURES

LIST OF ABBREVIATIONS

Amino acid

Ala	Alanine
Arg	Arginine
Asn	Asparagine
Asp	Aspartate
Cys	Cysteine
Gln	Glutamine
Glu	Glutamate
Gly	Glycine
His	Histidine
Ile	Isoleucine
Leu	Leucine
Lys	Lysine
Met	Methionine
Phe	Phenylalanine
Pro	Proline
Ser	Serine
Thr	Threonine
Trp	Tryptophan
Tyr	Tyrosine
Val	Valine

ABTS	*2,2'-azino-bis(3-ethylbenz-thiazoline-6-sulfonic acid)*
ARP	*Arthomyces ramosus* peroixdase
BHA	Benzhydroxamic acid
4-CA	4-chloroaniline
CD	Circular dichroism
CiP	*Coprinus cinereus* peroxidas
DE	Decoloriztion efficiency
Endoproteinase GluC	*Staphylococcus aureus* protease V8
FPLC	Fast protein liquid chromatography
HPLC	High-performance liquid chromatography
HRPC A2	Horseradish peroxidase isozyme A2
HRPC	Horseradish peroxidase isozyme C
LC-MS/MS	Liquid chromatography-tandem mass spectrometry
LiP	Lignin peroxidase
LPO	Lactoperoxidase
Mn	Molar mass averages of the number
MnP	Manganese peroxidase
Mw	Molar mass averages of the weight
NCBI	National Center for Biotechnology Information
NMR	Nuclear magnetic resonance
Pd	Polydispersity index
PEG	Polyethylene glycol
RB5	Reactive Black 5
RCSB	Research Collaboratory for Structural Bioinformatics
RE	Removal efficiency

SBP	Soybean peroxidase
SDS	Sodium dodecyl sulfate
SHA	Salicylhydroxamic acid
THF	Tetrahydrofuran
VA	Veratryl alcohol
VP	Versatile peroxidase

CHAPTER 1

INTRODUCTION

1. 1 Research Backgrounds

Enzymes catalyze a huge number of chemical reactions. The advantages of enzymes as catalysts of chemical transformations are now widely recognized. They show remarkable chemo-, region-, and stereospecificity, and enzyme-mediated reactions are more convenient, effective, and eco-friendly than conventional chemical catalysis (Schmid et al., 2001). Peroxidases are one of the most extensively studied groups of enzymes. Peroxidases have already promoted their introduction into several industrial processes, and they have occupied a prominent position in the field of radical polymerization (Azevedo et al., 2003; Hollmann and Arends, 2012). Peroxidases catalyze the oxidation of a wide variety of substrates using hydrogen peroxide or other peroxides. The catalytic properties of peroxidases to catalyze the free-radical formation of a variety of aromatic compounds followed by spontaneous polymerization have resulted in many applications (Regalado et al., 2004). For example, peroxidases have been used to polymerize the phenolic and aromatic amines in water and water-miscible organic solvents, which has led to new types of aromatic polymers, such as polycardanol and polyaniline (Kim et al., 2003; Shan and Cao, 2000). In addition, peroxidases have the potential to decrease environmental pollutants by the bioremediation of wastewater contaminated with phenols, cresols, and chlorinated phenols (Kobayashi and Makino, 2009; Regalado et al., 2004).

In spite of the promises of peroxidase-based technology, there

is a significant problem in the utilization of peroxidases. Peroxidases are inactivated by hydrogen peroxide and by reaction products such as free radicals and polymeric products. There have been numerous efforts to describe the peroxidase inactivation mechanism in the past two decades, and three possible pathways for peroxidase inactivation have been described. First, the active enzyme may be transformed to the inactive species by reacting with excess hydrogen peroxide (Arnao et al., 1990; Baynton et al., 1994). Second, peroxidase may be absorbed and entrapped by polymeric products, resulting in the occlusion of the enzyme's active site (Nakamoto and Machida, 1992). Third, the enzyme may be modified or the heme may be destroyed by the free phenoxyl radicals generated during enzyme catalysis (Chang et al., 1999). The first two pathways have been corroborated by numerous experimental studies (Valderrama et al., 2002); however, the third is not yet fully understood.

Many practical approaches have been developed to mitigate peroxidase inactivation. For example, the in-situ hydrogen peroxide generation method (Pricelius et al., 2011), the addition of polyethylene glycol (PEG) (Wu et al., 1993), and the immobilization and microencapsulation of peroxidase (Shutava et al., 2004) have been found to enhance peroxidase stability during the oxidation reactions of aromatic substrates. In addition to these methods, there have been some attempts to improve peroxidase stability based on the protein engineering method. Hiner et al. (1995) tried to increase the stability of horseradish peroxidase (HRP) against hydrogen peroxide through site-directed mutagenesis, but the results were not satisfactory. Morawski et al. (2001) obtained mutated HRP with

higher hydrogen peroxide stability through random mutagenesis. The resistance toward hydrogen peroxide of the manganese peroxidase (MnP) of *Phanerochaete chrysosporium* was highly increased by site-specific mutagenesis. To date, most of the efforts to improve peroxidase stability have been mainly limited to the improvement of the hydrogen peroxide stability of peroxidase rather than the radical stability. There have been no reports on strengthening peroxidase stability against radical attacks during the oxidation of aromatic compounds due to a lack of understanding of peroxidase inactivation by free-radical intermediates.

1. 2 Research Objectives

The low stability of peroxidase during the oxidation of phenolic substrates is a difficult problem to solve. In spite of its low stability, peroxidase can be an efficient biocatalyst for the production of industrially relevant compounds. Therefore, protein engineering could be successful in improving peroxidase stability, rendering a peroxidase mutant useful for industrially relevant applications. In order to develop a stable peroxidase, the molecular mechanism of peroxidase inactivation by radical attack must be understood and described.

Firstly, a dominant inactivation mechanism of peroxidase in the oxidation reaction was proposed using the two model enzymes, CiP and HRPC. To determine the main inactivation factor, two peroxidases were treated with high concentrations of hydrogen peroxide, the polymeric precipitates, and hydrogen peroxide and phenol. The changes in the molecular weights of the polypeptides and the intact heme contents of peroxidases were measured to reveal the attack site of phenoxyl radicals on peroxidases. From these results, the overall inactivation mechanism by radical attack was established; the covalent binding of phenoxyl radicals to the polypeptides of enzymes was found to be associated with the peroxidase inactivation.

Secondly, the proposed inactivation mechanism was proved by analyzing CiP as a model enzyme. The radical coupling site on the peroxidase polypeptide was identified, and the radical-stable mutant of CiP was obtained. The effect of radical coupling on the protein

structure was investigated using the spectrometry method. Additionally, the mutational effect on the kinetic properties of CiP was analyzed using molecular docking simulation.

Thirdly, the inactivation mechanism was applied to another peroxidase, HRPC. Multiple radical binding sites were identified, and then HRPC was engineered to have high radical stability. In addition, the conserved residue to be a radical binding site was observed in the multiple sequence and structure alignment for other peroxidases.

Fourthly, the developed radical-stable CiP was applied to the practical applications (i.e., the removal of phenol, the decolorization of dye, and the polymerization reaction of phenol). The efficiency of the radical-stable mutant was evaluated and compared with that of wild-type CiP.

In summary, the goal of this research was to propose the general radical-mediated inactivation mechanism of peroxidase and suggest a novel protein engineering strategy for improving the radical stability of peroxidase. Based on the new engineering strategy, the highly radical-stable CiP and HRPC were obtained, indicating the possibility of applying this strategy to other peroxidases. The overall scheme of this research is depicted in Figure 1-1. The objectives of this work are as follows.

■ To suggest the molecular mechanism for peroxidase inactivation by radical attack during the oxidation reaction of phenol

■ To develop a novel protein engineering strategy for increasing the radical stability of peroxidase

■ To generate engineered peroxidase with improved stability against radical attack

■ To evaluate the radical-stable CiP in practical applications

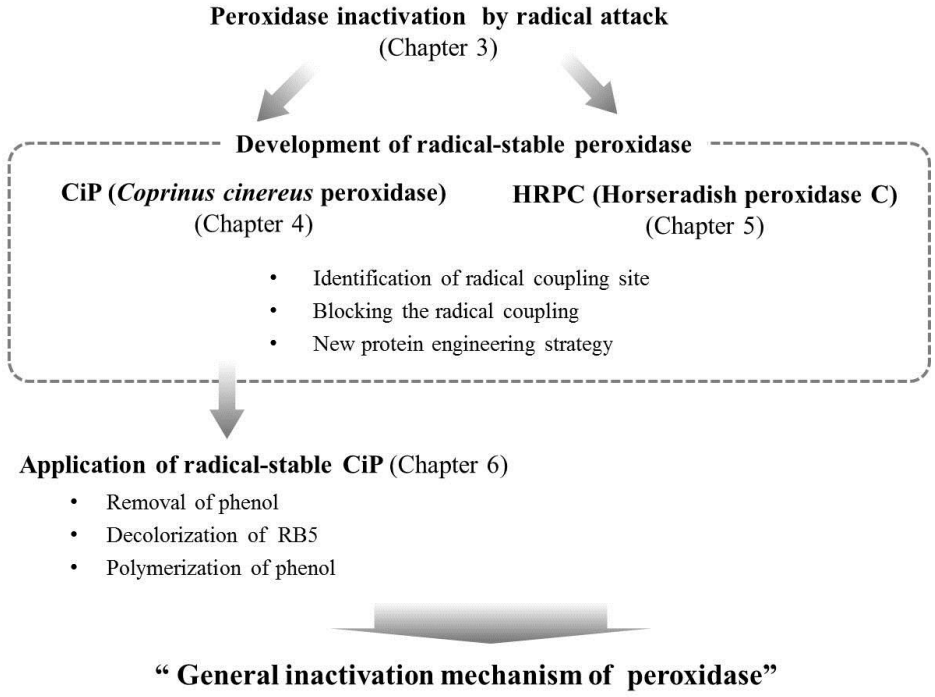

Figure 1-1. Overall scheme of study.

CHAPTER 2

LITERATURE SURVEY

2. 1 Peroxidase

Peroxidases (EC 1.11.1.7) are widely distributed throughout bacteria, fungi, plants, and vertebrates, and they are involved in several physiological processes (Jacks et al., 1991; Wallace and Fry, 1999). This extensive distribution suggests that peroxidases play important roles in many biological processes in living systems, such as plant growth, defense against pathogens, and thyroid hormone synthesis (Jacks et al., 1991; Veitch, 2004). Peroxidases are one of the most widely studied groups of enzymes, and their ability to oxidize various substrates makes them useful in a number of biotechnology applications (Regalado et al., 2004). In this literature review, the general properties of peroxidases and those of the two commercially important peroxidases investigated here, CiP and HRPC, are overviewed. The inactivation mechanisms of peroxidases that have been studied so far are discussed, and examples of using protein engineering to improve enzyme stability are summarized.

2. 1. 1 Heme peroxidase classification

Peroxidases are divided into two main superfamilies based on their primary sequence: plant peroxidases and animal peroxidases. The plant peroxidase superfamily can be further divided into three classes based on structural homology, sequence homology, and posttranslational modifications (Welinder et al., 1992): the

intracellular peroxidases (Class I, EC 1.11.1.5/.6/.11), extracellular fungal peroxidases (Class II, EC 1.11.1.13/.14), and secretory plant peroxidases (Class III, EC 1.11.1.7).

Class I includes yeast cytochrome C peroxidase, ascorbate peroxidase, and bacterial catalase-peroxidases. Peroxidases in Class I have a conserved proximal tryptophan residue; however, they lack carbohydrates, disulfide bridges, calcium ions, and signal peptides for secretion. Class II consists of secretory fungal peroxidases: the lignin and manganese peroxidases from *P. chrysosporium* and the peroxidase from *Coprinus cinereus* or *Arthromyces ramosus*. They contain about 5% carbohydrate, two calcium ions, four conserved disulfide bridges, and a signal peptide for secretion in the endoplasmic reticulum. Class III, the secretory plant peroxidases, includes peroxidases from horseradish, peanuts, and barley. Class III peroxidases contain a wide range of carbohydrate content, two calcium ions, and four conserved disulfide bridges in different positions from those in Class II peroxidases. Moreover, they have an N-terminal signal peptide for secretion and a C-terminal vacuolar targeting peptide (Dunford, 2010).

2. 1. 2 Catalytic mechanism of peroxidase

Peroxidases are oxidoreductases that catalyze the oxidation of numerous organic and inorganic compounds utilizing peroxides, such as hydrogen peroxide (Hamid and Khalil-ur-Rehman, 2009). The catalytic reaction mechanism of peroxidases can be expressed by

the following equation in which AH_2 and $AH^{\bullet}$ represent a reducing substrate and its radical product, respectively. Typical reducing substrates include aromatic phenols, phenolic acids, indoles, amines, and sulfonates.

$$2AH_2 + H_2O_2 \rightarrow 2\ AH^{\bullet} + 2H_2O$$

Most peroxidases are heme proteins and contain iron (III) protoporphyrin IX (ferriprotoporphyrin IX) as the prosthetic group. The catalytic cycle of peroxidase involves distinct intermediate enzyme forms (Wong, 1995) (Figure 2-1). The first step in the catalytic cycle is the reaction between hydrogen peroxide and the Fe(III) resting state of the enzyme. The native ferric enzyme is oxidized by hydrogen peroxide to form Compound I (CoI), an unstable intermediate with a heme structure of FeIV=O-porphyrin π-cation radical, with a consequent reduction of hydrogen peroxide to water. CoI is two oxidizing equivalents above the resting state. CoI oxidizes the electron-donor substrate to give Compound II (CoII), releasing a free radical. CoII is a Fe(IV) oxoferryl species one oxidizing equivalent above the resting state. CoII is further reduced by a second substrate molecule, regenerating the iron (III) state and producing another free radical.

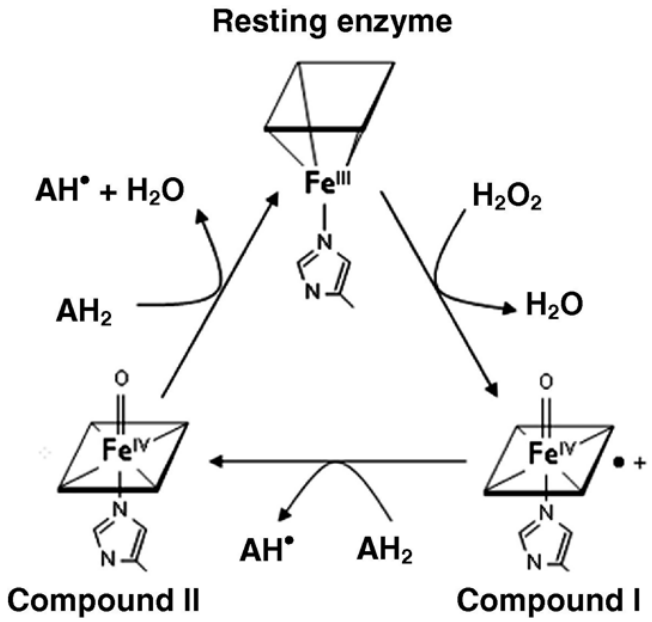

Figure 2-1. Catalytic cycle of heme peroxidases.

2. 1. 3 Horseradish peroxidase (HRP)

HRP is a well-known and important enzyme obtained from a plant source. HRP belongs to Class III (secretory plant peroxidases) of the plant peroxidase superfamily (Welinder et al., 1992). The HRP family consists of at least 15 isoforms with different catalytic properties (Veitch et al.,, 2004), and our knowledge of HRP comes mainly from studies with horseradish peroxidase isozyme C (HRPC), as it is the most abundant isoform and it produces its corresponding recombinant enzyme (Veitch et al., 2004).

Recombinant HRPC has been successfully produced in Escherichia coli with low yield (typically 2–4 mg/l) (Smith et al., 1990). The weight of HRPC is 34,000 Daltons, comprising 308 amino acids. It contains a heme-group, two endogenous calcium ions (Ca^{2+}), four disulfide bridges (between cysteines 11-91, 44-49, 97-301, and 177-209), and a single buried salt bridge (between Asp99-Arg123). The calcium ions play an important role in maintaining the protein structure, catalytic activity, and thermal stability of HRPC (Shiro et al., 1986). The N-terminal residue is blocked by pyroglutamate, and the C-terminus is heterogeneous, with some molecules lacking the terminal residue Ser308 (Ammosova et al., 1997; Welinder, 1979). HRPC has nine potential N-glycosylation sites recognized in the primary sequence, and of these, eight are occupied by the sugar moiety (Yang et al., 1996). The total carbohydrate content of HRPC ranges between 18 and 22%, depending on the source of the enzyme.

The protein crystal structure of HRPC was first determined by

Gajhede et al. in 1997 using X-ray crystallography, and the structure of the HRPC−benzhydroxamic acid (BHA) complex was solved by Henriksen et al. (1998). These reports identified the key residue involved in direct interactions with aromatic donor molecules. The reducing substrate (BHA) interacts with the hydrophobic pocket provided by residues H42, F68, G69, A140, P141, and F179 and heme C18, 18-methyl, and C20. After the BHA binds to the active site, Phe68 is reoriented into hydrophobic contact with BHA to form a lid on the hydrophobic pocket. The hydrophilic portion of the bound BHA molecule forms an extensive hydrogen bonding network with the H42 (distal catalytic residue), R38, P139, and the distal water molecule above the heme iron, which makes the extended interaction between BHA and the distal heme crevice of HRPC possible. The interaction between BHA and the hydrophobic pocket of HRPC is supported by the increase in the k_d (dissociation constant) of the HRPC F68A−BHA mutant complex from 2.4 μM in the wild type to 11 μM in the mutant (Veitch et al., 1996). In addition, F179A mutation results in an 80-fold decrease (k_d: 74 μM) in the binding affinity of HRPC for BHA, which means that F179 residue is more important for hydrophobic interactions with peroxidase substrates (Veitch et al., 1997). Another phenylalanine residue, F142, indirectly participates in the aromatic substrate binding. An NMR study showed that the structural integrity of the aromatic donor molecule binding site is altered as a result of the substitution of Phel42 by Ala, and the k_d of the HRPC F142A−BHA mutant complex is increased from 2.1 μM to 2.8 μM (Veitch et al., 1995).

2. 1. 4 Peroxidase from *C. cinereus*

In 1988, Morita et al. discovered a novel peroxidase, CiP, which is produced extracellularly by the ink cap basidiomycete *C. cinereus* (Petersen et al., 1994). CiP was purified to homogeneity from the culture filtrate of *C. cinereus* by anion exchange and affinity chromatographies, with an activity yield of 50%. The total number of acid residues of CiP was found to be 381, and the molecular weight of CiP is was 33,000 Daltons with a pI value of 3.5. (Morita et al., 1988). The glycine-rich N-terminal extension of CiP was blocked with a pyroglutamate residue that is absent in other fungal peroxidases (Morita et al., 1988). In addition, the rate constants of CiP for hydrogen peroxide and guaiacol were found to have similar values to those for the higher plant peroxidase, HRP (Morita et al., 1988).

The CiP gene shows a limited genetic polymorphism encoding one major and one minor isoform of the peroxidase (Baunsgaard et al., 1993), which is an advantageous feature in the industrial production and application of this peroxidase. The production of CiP has been achieved by heterologously expression in the *Aspergillus oryzae* transformants under the *A. oryzae* TAKA amylase promoter (Dalboge et al., 1992). The relative yield of CiP production in *A. oryzae* approached 2000%, compared to that in original strain *C. cinereus*. Recently, recombinant CiP was also successfully expressed using the *Pichia* expression system (Kim et al., 2009).

Primary and tertiary structure analysis showed that CiP belongs to Class III (extracellular fungal peroxidases) of the plant

peroxidase superfamily (Welinder, 1992). The cDNA sequence of CiP is 99% identical to the amino sequence of *Arthomyces ramosus* peroxidase (ARP) (Kjalke et al., 1992). An amino acid residue corresponding to Val99 of CiP is substituted by Ile in ARP. There are some minor differences between CiP and ARP. CiP and ARP have a tetraglycine and a pentaglycine segment, respectively, in the N-terminal glycine-rich extension, and they also vary in their degree of N-glycosylation (Kjalke et al., 1992).

CiP shows 40–50% sequence identity to the lignin-degrading peroxidases (LiPs) isolated from the white-rot fungi, *P. chrysosporium*. The folding and active sites of CiP are almost identical to those of LiP however, CiP lacks the ligninolytic activity. The crystal structure of CiP shows that the folding of CiP is almost identical to the folding of LiP with slight differences only in the loop and C-terminal regions. Moreover, the active sites of CiP and LiP are similar with respect to the position, orientation, and hydrogen bond pattern of the active site residues. However, CiP and LiP differ in their substrate specificity due the difference in their active site channels. The active site of CiP is much larger than that of LiP. Hence, the large opening to the active site in CiP makes the heme group accessible to substrate binding at different sites of the heme edge, which may explain the broad substrate specificity of CiP (Petersen et al., 1994). Although CiP is much more similar to HRPC in terms of substrate specificity, specific activity, and pH optimum than to white-rot fungal peroxidases, the sequences of CiP and HRPC showed only 18% identity (Welinder, 1992).

The crystal structure analysis of the complex of salicylhydroxamic acid (SHA) with ARP (Tsukamoto et al., 1999) offers the information about the binding mode of aromatic substrate to CiP. The SHA molecule is located in the heme cavity on the distal side, and the aromatic ring of SHA is accommodated in a hydrophobic region created by the heme pyrrole ring D and nearby hydrophobic amino acids (Ala92, Pro156, Leu192, and Phe230). The hydroxamic acid group of SHA is located in the distal cavity and is hydrogen-bonded to His56, Arg52, and Pro154. The hydroxyl group on the benzene ring of SHA does not form hydrogen bonds with any amino acid residues in the heme cavity. The binding mode of BHA to ARP is very similar to that of the ARP−SHA complex (Itakura et al., 1997).

2. 2 Applications of Peroxidases

Nowadays, the development of environmentally friendly technologies is critical and essential for sustainable industrial development (DeSimone and Popoff, 2000). Many researchers are seeking promising biocatalysts for green chemistry (Bornscheuer and Buchholz, 2005). Among the various enzymes, peroxidases have long been of interest from a practical biotechnological perspective. The important advantages of peroxidases include their broad range of substrate specificity (van de Velde et al., 2001) and high redox potential (McEldoon et al., 1995; Russ et al., 2002). Accordingly, peroxidases have been successfully used in a large number of

applications in diverse fields, which are summarized in Table 2-1.

The peroxidases, with their degrading and bleaching effects, are used in detergents. The first patent on peroxidases used as detergent additives was that by Kirk et al. (Damhus et al., 1989). The peroxidase oxidizes or bleaches the dye and inhibits the transfer of the textile dye from one dyed fabric to another during the washing process. Peroxidases derived from *Coprinus* or *Bacillus pumilus* and microperoxidase were used for this application (Pedersen et al., 1993). Peroxidases can be used in the treatment of wool fibers or animal hair to improve shrink resistance, stretch, burst strength, and dyeing characteristics (Patrick and Jakob, 2000).

Furthermore, peroxidases have been developed to treat pollutants derived from industrial activities. Wastewater is contaminated with various problematic pollutants, such as synthetic dye, phenolic compounds, pesticides, endocrine disruptive chemicals (EDCs), and other xenobiotics. Peroxidases are able to transform these pollutants and reduce their toxicity (Hamid and Khalil-ur-Rehman, 2009). To achieve the biodegradation of dyes, oxidative enzymes (laccase, MnP, and LiP) from white-rot fungi appear to be a valuable alternative (Heinfling et al., 1998; Muñoz et al., 1997). These oxidases and peroxidases have been reported to be excellent oxidant agents for degrading dyes (Kirby et al., 1995). Maximum decolorization achieved by partially purified LiP was 80% for Procion Brilliant Blue HGR, 83% for Ranocid Fast Blue, 70% for Acid Red 119, and 61% for Navidol Fast Black MSRL. Phenols are known to be toxic and carcinogenic, and they can be removed by the oxidative coupling

reactions of peroxidases (Nicell et al., 1993). For example, Mamatha et al. (2012) treated a laboratory phenol with turnip peroxidase and then efficiently removed the polymer precipitates by centrifugation. EDCs are widely dispersed in the environment, but they can mainly be found in wastewater. Huang and Weber (2005) reported that the EDC oxidation by MnP and the 10 unit/ml of MnP from *Pleurotus ostreatus* eliminated 0.4 mM bisphenol A in 1 h. In addition, peroxidases extracted from some fungal species have great potential to transform several pesticides into harmless forms. The transformation of organophosphorus pesticides by white-rot fungi has been studied (Jauregui et al., 2003), and the transformation of several organophosphorus pesticides by the chloroperoxidase from *Caldariomyces fumago* has been reported (Jauregui et al., 2003).

Peroxidases have been used to synthesize the polymers of phenolic and aromatic amine compounds, and the new types of polymers have been synthesized by peroxidase. In the presence of an oxidation reagent, peroxidase catalyzes the oxidation of phenol and its derivatives, which eventually give rise to high molecular weight polymers (Reihmann and Ritter, 2006). This peroxidase-mediated polymerization method could be used as an alternative to the conventional process using toxic chemicals. Polyaniline is a conducting polymer with high environmental stability and promising electronic properties that is synthesized using HRP (Lim et al., 2000). Oguchi et al. (1999) synthesized the phenol polymer using HRPC and soybean peroxidase (SBP), and a new phenol polymer possessing high thermal stability was obtained (Ghoul and Chebil, 2012). Another useful polymer, polycardanol, was produced

by SBP (Ikeda et al., 2000) and HRPC (Kim et al., 2003) in aqueous/organic solvents. Kim et al. (2005) successfully synthesized the polycardanol by using CiP, and they used cashew nut shell liquid (a byproduct from the mechanical processing of the cashew nut) (Phani Kumar et al., 2002) instead of purified cardanol. Polycardanol has potential use in surface coatings and flame retardants (Mahanwar and Kale, 1998).

Biopulping is a process in which fungi are used to produce extracellular enzymes (hydrolytic and oxidative) to degrade wood as well as the lignin constituents of wood (Singh et al., 2010). The pulping byproducts (black liquor) cause serious environmental problems due to their high pollution load. In order to solve this environmental problem, two bacterial strains, *Citrobacter freundii* (FJ581026) and *Citrobacter* sp. (FJ581023), were applied in axenic and mixed conditions for the degradation of the pulping byproduct. The bacterial strains reduced chemical oxygen demand by 82%, adsorbable organic halides by 79%, color by 79%, and lignin by 60% after a 144 h incubation period, and the optimum activity of the lignin-degrading enzyme was noted at 96 h and characterized as MnP by SDS-PAGE analysis. The biological method is both economical and ecofriendly (Chandra and Abhishek, 2011). Additionally, LiPs can be used in the treatment of black liquor. LiPs have been shown to be able to efficiently break down pulping byproducts due to their high redox potential and specialized catalytic mechanisms (Hammel and Cullen, 2008).

Table 2-1. Applications of peroxidases in various fields.

Application	Peroxidase type	Organism type	Organism	Reference
Detergent additive	Peroxidase	Fungus	*Coprinus macrorhizus*	Pedersen et al., 1993
	Microperoxidase	Bacteria	*Bacillus pumilis*	
Dye degradation	LiP, MnP	Fungus	*Pleurotus eryngii*	Heinfling et al., 1998;
	LiP	Fungus	*Phanerochaete chrysosporium*	Kirby et al., 1995
Phenol removal	Peroxidase	Plant	Horseradish	Nicell et al., 1993
	Peroxidase	Plant	Turnip root	Mamatha et al., 2012
EDC oxidation	MnP	Fungus	*Pleurotus ostreatus*	Huang and Weber, 2005
Pesticide degradation	Chloroperoxidase	Fungus	*Caldariomyces fumago*	Longoria et al., 2008
	LiP, MnP	Fungus	*Ganoderma applanatum* *Bjerkandera adusta*	Jauregui et al., 2003

Table 2-1. Applications of peroxidases in various fields. (continued)

Application	Peroxidase type	Organism type	Organism	Reference
Polymer synthesis	Peroxidase	Plant	HRPC SBP	Oguchi et al, 1999
	Peroxidase	Plant	SBP	Ikeda et al., 2000
	Peroxidase	Plant	HRPC	Kim et al., 2003
Degradation of pulping by product	Peroxidase	Bacteria	*Citrobacter freundii* *Citrobacter* sp.	Chandra and Abhishek, 2011

2. 3 Inactivation Mechanism of Peroxidase

Although peroxidases have enormous potential, their commercial uses are hampered by their low stability during oxidation reactions of aromatic substrates. Peroxidases are inactivated by their natural substrate and reaction products, such as hydrogen peroxide, free radicals, and polymer products. This process is referred to as suicide inactivation, and unfortunately, it has not been fully elucidated (Valderrama et al., 2002). Until recently, three possible pathways for peroxidase inactivation have been proposed: inactivation by hydrogen peroxide, by reaction products, and by free phenoxyl radicals. The molecular mechanism of each inactivation pathway is described below.

2. 3. 1 Inactivation by hydrogen peroxide

Peroxidases are irreversibly inactivated by exposure to excess hydrogen peroxide (the suicide substrate) (Arnao et al., 1990; Baynton et al., 1994). The molecular mechanism of peroxidase inactivation by hydrogen peroxide is complicated, because a multitude of interactions exists between the heme iron and hydrogen peroxide. In the absence of a reducing substrate, or when exposed to high concentrations of hydrogen peroxide, active intermediate species CoII is converted into a highly reactive peroxy-iron(III)porphyrin free radical called Compound III (CoIII) (Nakajima and Yamazaki, 1987).

CoIII is not involved in the normal catalytic cycle of peroxidase. However, it is produced via the reaction of hydrogen peroxide and intermediate species generated by the interaction between CoII and the superoxide anion (Adediran and Lambeir, 1989). Previous reports confirmed the CoIII in the HRPC, MnP (Wariishi et al., 1988), and LiP (Wariishi and Gold, 1990) treated with excess hydrogen peroxide.

CoIII can be further oxidized until bleaching and irreversible inactivation (Wariishi and Gold, 1990), and it is decomposed following one of the three possible pathways (Figure 2-2). The first pathway involves the reaction of the peroxyl radical in CoIII with the tetrapyrrole structure. Heme groups are susceptible to oxidative attacks at the meso positions. The peroxyl radical of porphyrin in CoIII attacks and oxidizes the porphyrin moiety. This oxidation reaction breaks the carbon bridges linking the pyrrole rings, and the porphyrin macrocycle is cleaved. Subsequently, an open-chain tetrapyrrole is formed, which is characterized by heme bleaching, and free iron is released (O'Carra, 1975). Heme bleaching has been observed in many peroxidases—such as HRP (Nakajima and Yamazaki, 1980), CiP (Chang et al., 1999), and ascorbate peroxidase (Hiner et al., 2000)—after treatment with excess hydrogen peroxide.

In the second pathway, CoIII returns to the ground state by the oxidation of the surrounding amino acid. In LiP, the surface tryptophan 171 residue is hydroxylated, and it functions as the endogenous electron donor for CoI reduction (Blodig et al., 2001; Piontek et al., 2001). Long-range electron transfer exists between the surrounding amino acid and the porphyrin of peroxidase (Blodig et

al., 2001). Accordingly, it is feasible that CoIII is reduced and then returns to the resting state by electron transfer from the amino acid side chain.

In the last pathway, the porphyrin moiety in CoIII is repaired by a reducing substrate (electron donor) and converted to a resting state of peroxidase. The addition of veratryl alcohol (VA), an electron donor, causes the rapid conversion of CoIII of LiP to native LiP (Wariishi and Gold, 1989). The VA binds to the porphyrin in CoIII and then leads the transformation to the native enzyme, releasing hydroxyl/superoxide anion radicals. The reversion of CoIII to the native state of enzymes by phenolic substrates has been observed in HRP (Gross et al., 1977; Halliwell, 1978).

It is well known that the addition of a reducing substrate protects the enzyme from inactivation. The reducing substrate competes with hydrogen peroxide for CoII, which would preclude the peroxidase inactivation by hydrogen peroxide (Hiner et al., 1995). In studies that incubated HRP (Hiner et al., 1995) and ascorbate peroxidase (Hiner et al., 2000) with excess substrates, the inactivation rate by hydrogen peroxide was decreased in both cases..

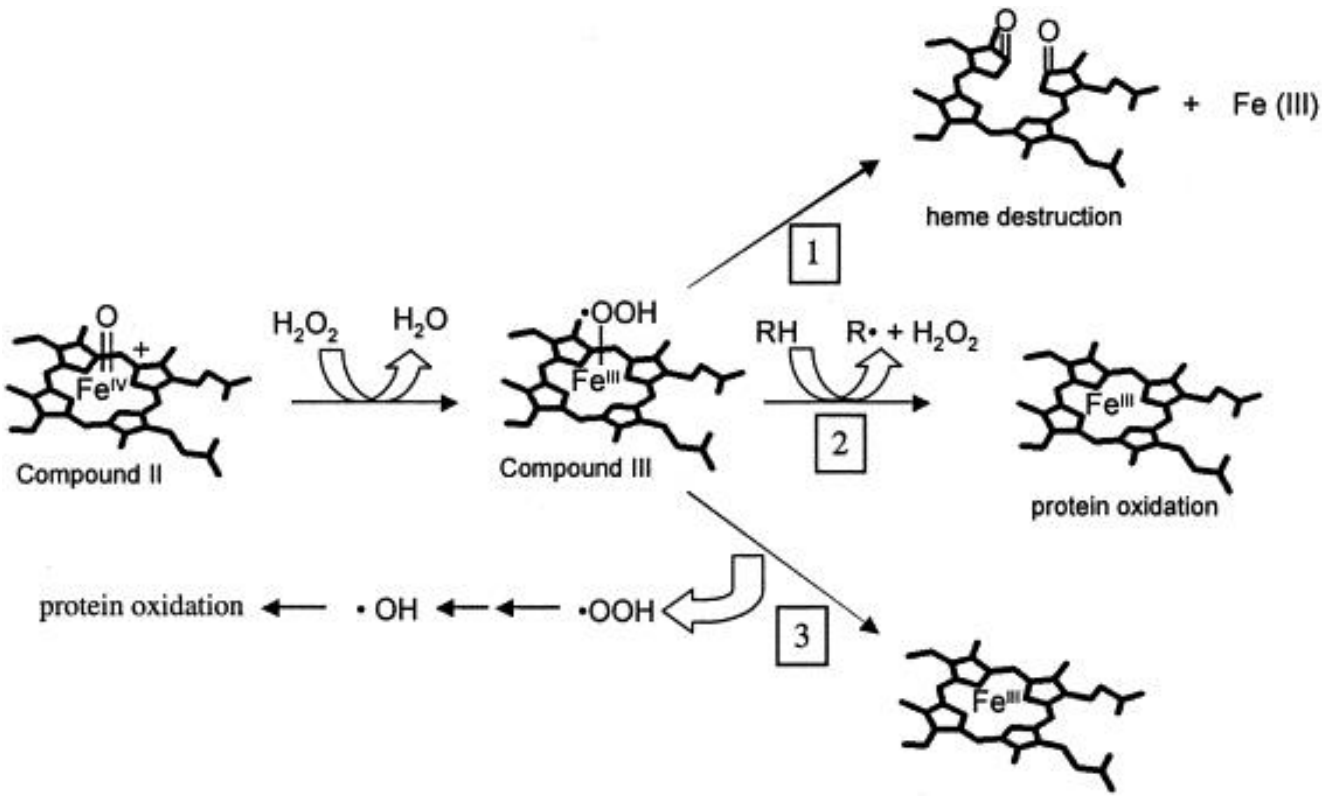

Figure 2-2. Alternative inactivation pathways from compound III intermediate (Valderrama et al., 2002).

2. 3. 2 Inactivation by reaction product

Numerous studies have reported that the addition of additives—such as PEG (Nakamoto and Machida, 1992), sodium dodecyl sulfate (SDS), and Triton X-100 (Triton) (Al-Ansari et al., 2010)—protects peroxidase against peroxidase inactivation. In an early study, the addition of PEG had a significant protective effect on the activity of HRP, and the amount of peroxidase required to remove phenol was decreased 40-fold compared to without PEG (Wu et al., 1993). Furthermore, it has been reported that the pre-addition of Triton relieves the inactivation of CiP during phenol-polymerizing reactions (Sakurai et al., 2003), and Triton added after phenol polymerization causes the inactivated CiP to reincorporate into the enzyme catalytic cycle via its desorption (Sakurai et al., 2003).

The studies of additive effects elucidate the inactivation mechanism by phenolic polymers. Peroxidase adsorption on phenolic polymers has been observed in many cases (Feng et al., 2013; Masuda et al., 2001; Sakurai et al., 2003; Wu et al., 1998). Nakamoto and Machida (1992) suggested peroxidase inactivation by reaction product (end product). They proposed that the active peroxidase is adsorbed/trapped in the polymer precipitate, and the substrate access to the enzyme active site is hindered, which results in the peroxidase inactivation. The phenolic polymers form from phenol by coupling between the phenoxyl radicals generated from peroxidase catalysis. The radical–radical coupling occurs non-enzymatically through C–C and C–O coupling with *o*-, *p*-orientation on the benzene rings (Ghoul and Chebil, 2012), and the structure of phenolic

polymers is random. The increased molecular weight increases the hydrophobicity of the forming products that are eventually precipitated. The hydrophobicity of phenolic polymers is important for the interaction with peroxidase.

Additives, including PEG, act as "sacrificial polymers". They partition into solid polymer products instead of enzymes, thus preventing the peroxidase inactivation by polymer products. It has been reported that polymer precipitate formed in the absence of PEG inactivates peroxidase (Wu et al., 1998). On the contrary, in the presence of PEG, polymer precipitate generated during a reaction has been found to be inert to peroxidase (Wu et al., 1998). This phenomenon can be explained by the competition of two molecules, the enzyme and PEG, for the phenolic polymer. When the peroxidase catalyzes the polymerization reaction in the presence of PEG, the surface of the enzyme is saturated with PEG, which is absorbed instead of the enzyme, thus minimizing enzyme adsorption.

Furthermore, different enzymes vary in their relative affinities for the precipitate (Wu et al., 1998). In addition, the relative hydrophobicity of different polymer precipitates is related to the structure of the corresponding monomer (Steevensz et al., 2012). Consequently, it has been suggested that the additive effect depends on the interaction between the enzyme or additive and the polymer product, and inactivation by a polymer product is not a universal occurrence (Wu et al., 1998). For example, enzymes having no hydrophobic part on their surface or phenolic polymers with less hydrophobicity lead to less significant inactivation of enzymes, and the additive effect is also diminished.

2. 3. 3 Inactivation by free phenoxyl radical

In the presence of reducing substrates, peroxidase is irreversibly inactivated. In early studies, Klibanov et al. (1982) suggested that this inactivation was the result of interactions with phenoxyl radicals, and peroxidase inactivation by free radicals has been predicted from kinetic data modeling (Baynton et al., 1994). Unfortunately, its molecular mechanism remains unclear.

When hydrogen peroxide presents in excess over donor substrates or alone, peroxidase inactivation occurs by the hydrogen peroxide-mediated mechanism described in Section 2.3.1. However, at low hydrogen to donor substrate concentration ratios, peroxidase could be dominantly inactivated by the free radicals produced during peroxidase catalysis (Ma and Rokita, 1988). The inactivation of HRP by radicals has been observed with phenylhydrazines and alkylhydrazines (Ator and Ortiz de Montellano, 1987) and sodium azide (Ortiz de Montellano et al., 1988). In addition, many peroxidases—ascorbate peroxidase (Chen and Asada, 1990), lactoperoxidase (LPO) and thyroid peroxidase (Divi and Doerge, 1994), and CiP (Aitken and Heck, 1998; Kim et al., 2009)—have also been shown to suffer from radical-meditated inactivation.

Chang et al. (1999) investigated and suggested the mechanisms for the inactivation of CiP, LPO, and HRP during the oxidative oligomerization of 4-chloroaniline (4-CA). In this study, HPLC and MALDI-TOF/MS analysis of proteolytic digests of CiP, LPO, and HRP that had been inactivated during the oxidation of 4-

CA revealed that the peptide residues of all peroxidases are covalently bound with 4-CA oligomers. It was proposed that free radicals or reactive oligomers are formed by the one-electron oxidation of 4-CA (Simmons et al., 1987), and the inactivation occurs because of the covalent modification of the polypeptide chain and heme destruction.

Recently, researchers elucidated the mechanisms of peroxidase inactivation by radical attacks (Huang et al., 2005; Mao et al., 2013). The hypothesis that HRP is inactivated by heme destruction was supported by measuring the quantity of iron released from HRP upon the reaction with hydrogen peroxide and phenol (Huang et al., 2005; Mao et al., 2013). Additionally, resonance Raman and Fourier transform infrared spectroscopy measurements showed no structural changes of the enzyme during the reaction and a significant amount of phenoxylphenol-type oligomers in solution and probably also in the heme pocket (Huang et al., 2005). The prosthetic group change was identified by UV-vis spectrum changes. The product of heme destruction generated by the oxidative attack of phenoxyl radicals on the heme vinyl group was identified by LC-MS analysis of extracted heme from HRP after turnover of phenol (Mao et al., 2013). These observations prove the radical-mediated inactivation of HRP accompanies heme destruction.

2. 4 Improvement of Peroxidase Stability through Protein Engineering

Industry needs stable enzymes as biocatalysts to reduce operation costs. However, wild peroxidases are not well suited for industrial use due to their low operation stability (Colonna et al., 1999). Thus, improving peroxidase stability is a prerequisite for industrial applicability (Valderrama et al., 2002). Protein engineering is generally required to obtain highly produced and efficient biocatalysts (Ayala et al., 2008). There have been many efforts based on protein engineering to enhance the stability of peroxidase during the oxidation reaction process, although a large number of reports have been limited in considering the peroxidase inactivation by hydrogen peroxide.

Li et al. (2001) improved the stability of cytochrome P450BM-3 by site-directed mutagenesis. P450BM-3 was extremely unstable in hydrogen peroxide; however, the stability of a F87A mutant in hydrogen peroxide solutions increased significantly. While the wild type lost about 55% of its activity in 1 mM hydrogen peroxide within 7 min, F87A only lost 45% in 16 mM hydrogen peroxide during the same period. Moreover, the F87A mutation also increased the hydrogen peroxide-supported substrate hydroxylation activity of cytochrome P450BM-3, whose original hydrogen peroxide-supported activity was hardly detectable. It was proposed that the free space size near the heme iron is critical for the stability of P450BM-3, and a bigger free space size near the heme iron makes the enzyme more stable in hydrogen peroxide solution.

Villegas et al. (2000) reported that some iso-1-cytochrome c variants constructed by site-directed mutagenesis are more stable in the presence of hydrogen peroxide than the wild type. K73A/C102T,

K87A/C102T, and N52I/C102T variants were significantly more stable in the presence of hydrogen peroxide. A triple mutant (N52L/Y67F/C102T) had a slightly lower inactivation rat, and a higher turnover rate than the wild type. In addition, the heme prosthetic in the triple mutant was not degraded at catalytic concentrations of hydrogen peroxide. By electron spin resonance spectroscopy experiments, the protein radical formation was identified in the wild type but not in the triple variant, because variants contain no tyrosine residues, which are known to generate free radicals in hemoproteins. Consequently, it was suggested that the heme degradation process is a result of protein radical formation.

The resistance toward hydrogen peroxide of MnP produced by *P. chrysosporium* was increased by the conversion of unstable amino acid residues around the hydrogen peroxide-binding region to stable amino acid residues (Miyazaki and Takahashi, 2001). Met273 residue is the nearest residue to the active site and faces the active site pocket, so this residue is solvent-accessible and easily oxidized. The M273L mutation showed high hydrogen peroxide resistance (i.e. 4.1-fold higher than that of the wild type) and prevented conformational changes near the active site caused by chemical oxidation. The conversion of oxidizable methionine residue around the pocket to non-oxidizable residue was critical to the improvement of the oxidative resistance. Furthermore, the N81S mutant retained more than 99% of its initial activity at a concentration of 1 mM hydrogen peroxide for 1 h, while the wild type was completely inactivated. The N81S mutation caused a hydrogen bond interaction between the –OH group of Ser81 and the main peptide chain of Asn76. The hydrogen

bond interactions might have caused conformational stabilization and increased hydrogen peroxide resistance.

A protein engineering strategy similar to that used to engineer the unstable residues to hydrogen peroxide was applied to *Pleurotus eryngii* versatile peroxidase (VP) (Bao et al., 2014). Target residues such as methionine were easily oxidized and closed to the hydrogen peroxide-binding pocket and heme. The VP mutants (A79L, P141A, M247L, M265L, M247L/M265L, A77E/I81L, A77E/A79S/I81L, A77S/A79L/I81L, A77E/A79S/I81L/M265L, A77E/A79S/I81L/M247L/M265L, and A77E/A79S/I81L/S168A) showed significantly increased oxidative tolerance. It was shown that oxidizable residues (Met247 and Met265), residues close to heme (Pro141), and residues close to the hydrogen peroxide-binding pocket (Ala77, Ala79, and Ile81) had important effects on hydrogen peroxide stability. These mutations might alter the intramolecular electron transfer pathways or affect different stages of the VP catalytic cycle, consequently delaying or suppressing CoIII formation and/or heme bleaching and the self-inactivation process.

The fungal peroxidase from *C. cinereus* was engineered using a combination of approaches, site-directed and random mutagenesis, to increase protein stability toward hydrogen peroxide (Cherry et al., 1999). Based on the crystal structure analysis, the target amino acid residues susceptible to oxidation by hydrogen peroxide were identified and subjected to site-directed mutagenesis. The mutants (M166F, E239K, M242I, and Y272F) were generated with an oxidative stability 5-fold higher and a thermostability 124-fold higher than that of the wild-type enzyme. The E239G mutant generated by random

mutagenesis using the error-prone PCR showed a 146-fold increase in thermostability. The best mutant in this study was I49S/V53A/T121A/M166F/E239G/M242I/Y272, which showed the most dramatic improvements in oxidative stability, yielding a mutant with 174 times the thermal stability and 100 times the oxidative stability of wild-type CiP. The M166, M242, and Y272 mutants were close to the active site, which was directly exposed to the oxidizing effects of the substrate. The replacement of these oxidizable residues was beneficial to oxidative stability. For example, the replacement of E239 with Gly improved the thermostability of CiP, which resulted from relief of the charge repulsion between E239 and E214, which lay in close proximity. Finally, the I49, V53, and T121 residues formed the contact point between helices B and D in the peroxidase. The mutations on these residues reduced the distance between helices B and D, which led to the reduction in the accessibility of hydrogen peroxide to the interior of the protein and then protected the enzyme from the attack by hydrogen peroxide.

CHAPTER 3

PEROXIDASE INACTIVAION BY COVALENT MODIFICATION WITH PHENOXYL RADICAL DURING PHENOL OXIDATION

3. 1 Introduction

Peroxidases are heme enzymes that contain a ferric protoporphyrin IX prosthetic group and use hydrogen peroxide and other peroxides to catalyze the oxidation of a large number of aromatic compounds (Dunford, 1999). The catalytic cycle of peroxidase occurs in three distinct steps. Peroxidase is oxidized by hydrogen peroxide and is converted to Compound I. Compound I oxidizes an aromatic substrate into a free radical, whereas Compound I is reduced to Compound II. Compound II is further reduced by another aromatic substrate, returning to its native form of peroxidase and producing another free radical (Yu et al., 1994).

Peroxidases have attracted industrial attention because of their usefulness as catalysts in the pulp, paper, textile and laundry industries and for their use as biosensors and in other applications (Harazono et al., 1996; Vyas and Molitoris, 1995). The ability of peroxidases to catalyze free radical formation from a variety of aromatic compounds, followed by spontaneous polymerization, can be used in the bio-remediation of water and soil containing phenolic compounds (Bollag, 1992; Klibanov et al., 1983) and in the synthesis of various aromatic polymers (Hollmann and Arends, 2012; Won et al., 2004). Despite their potential applications, the commercial uses of peroxidases are limited by their rapid inactivation during reactions (Aitken, 1993).

Three mechanisms of horseradish peroxidase (HRP) inactivation have been proposed (Figure 3-1). The first is associated

with excess peroxide. Active intermediate peroxidase compounds react with excess peroxide, which results in the formation of inactive species (Arnao et al., 1990; Nakajima and Yamazaki, 1987). The second involves absorption by polymeric products. Peroxidase is absorbed on a polymeric product, and its active sites are occluded (Nakamoto and Machida, 1992). In the third mechanism, free phenoxyl radicals generated by the oxidation reaction attack peroxidase, leading to its inactivation (Klibanov et al., 1983). The severity of inactivation from each mechanism depends on the reaction conditions.

It is necessary to understand the factors involved in the inactivation process and to describe the molecular mechanism underlying peroxidase inactivation. The overall objective of the present study was to evaluate the dominant mechanism of peroxidase inactivation during the oxidation of phenol. Using two types of peroxidases, *Coprinus cinereus* peroxidase (CiP) and horseradish isozyme C (HRPC), we investigated the effects of hydrogen peroxide and polymeric products on peroxidase activity. Modifications that were made to the peroxidases and the proportion of intact hemes were measured using electrophoresis and high-performance liquid chromatography (HPLC). This work provides a basis for understanding the molecular mechanism of peroxidase inactivation and for the rational protein engineering of peroxidases to improve their stability in the phenol oxidation process.

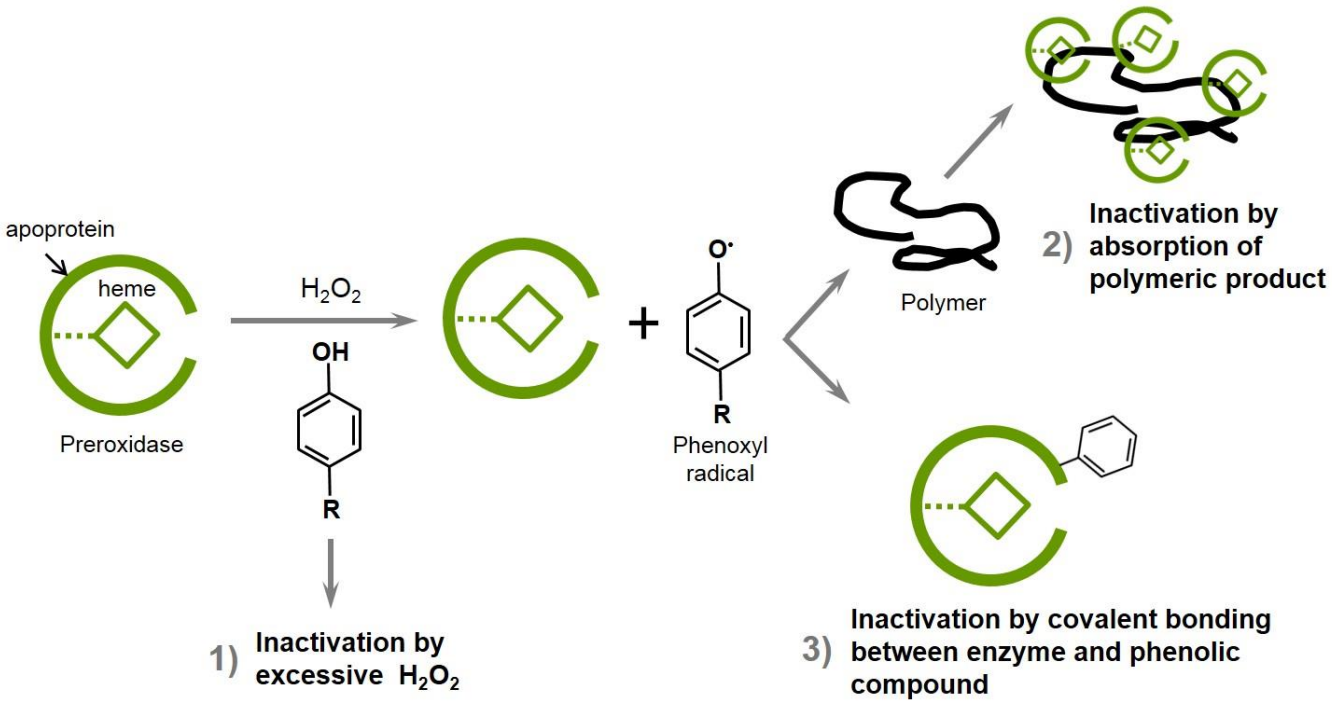

Figure 3-1. Inactivation pathways of HRP during the oxidation of phenolic compounds.

3. 2 Materials and Methods

3. 2. 1 Chemicals and reagents

Phenol (≥99%), 2,2'-azino-bis(3-ethylbenz-thiazoline-6-sulfonic acid) (ABTS) (98%, in diammonium salt form), formic acid (≥96%), hemin (bovine, ≥90%) and Pronase (from *Streptomyces griseus*) were purchased from Sigma-Aldrich (USA). Hydrogen peroxide (H_2O_2, 30%, v/v) was obtained from Junsei Chemical Co., Ltd. (Japan). HPLC-grade water, acetonitrile, and formic acid were supplied by Honeywell Burdick & Jackson (USA). A Bradford protein assay kit was purchased from Bio-Rad (USA).

3. 2. 2 Enzymes

Horseradish peroxidase isozyme C (HRPC, P8415) was purchased from Sigma-Aldrich (USA) and used without any further purification. The heterologous expression and purification of CiP was performed as previously described (Kim et al., 2010). Briefly, the synthetic CiP gene was expressed in the supernatants of *Pichia pastoris* cell cultures using a pPICZαA vector-based expression system (Invitrogen, USA). CiP was purified with a size exclusion column (Superose™ 6 10/300 GL, GE Healthcare, USA) using an FPLC system (GE Healthcare, USA).

3. 2. 3 Peroxidase stability

To investigate the effect of substrates and reaction products on peroxidase activity, CiP and HRPC were treated with hydrogen peroxide, polymer products and phenol. CiP and HRPC were diluted in 100 mM phosphate buffer, pH 7.0, to yield a concentration of 1 U/mL, and enzyme solutions were then treated by the addition of the following solutions: 0.5 mM hydrogen peroxide, phenol polymer or 0.5 mM hydrogen peroxide plus 0.5 mM phenol. Each reaction mixture was incubated and stirred for 20 min at room temperature. Samples were taken every 5 min after initiating the reaction. Peroxidase activity was assayed by mixing enzyme samples with 2 mL of ABTS-H_2O_2 (0.18 mM ABTS and 2.2 mM H_2O_2, pH 5.0), and changes in absorbance at 420 nm (molar extinction coefficient of ABTS, 34,700 M^{-1} cm^{-1}) were determined using a UV-Vis spectrometer (Japan) at room temperature. One unit of activity (U) is defined as the amount of enzyme that catalyzes the oxidation of 1 μmol ABTS for 1 minute at 25 °C.

The phenol polymer used to estimate peroxidase stability was obtained using CiP and HRPC catalysis. The reaction solution was a mixture of 100 mM potassium phosphate buffer at pH 7.0, 10 mM phenol and 20 U/mL of CiP or HRPC. Each reaction was initiated by adding 10 mM hydrogen peroxide to the reaction solution. After the reaction was complete, the precipitates were collected by centrifugation for 15 min at 13,000 rpm. The collected materials were washed twice with deionized distilled water to remove residual peroxidases and then dried in an oven at 100 °C for 1 day. The

precipitate was added to the reaction mixture to give a final concentration of 0.1 mg/mL.

3. 2. 4 Peroxidase-catalyzed reactions

The phenol oxidation reaction was initiated by adding 0.5 mM hydrogen peroxide to a reaction mixture containing 100 mM phosphate buffer (pH 7.0) and 10 U/mL of CiP or HRPC. The control reaction was performed without hydrogen peroxide. After stirring vigorously at room temperature for 1 h, the precipitates were eliminated by centrifugation at 13,000 rpm for 20 min. The reaction supernatants were desalted through a HiTrap desalting column (GE Healthcare, USA) to remove the remaining hydrogen peroxide and phenol. Protein samples were concentrated with an Amicon concentrator (Millipore, USA) and analyzed by sodium dodecyl sulfate polyacrylamide gel electrophoresis (SDS-PAGE) and HPLC.

3. 2. 5 SDS-PAGE

Concentrated samples from CiP- and HRPC-mediated oxidation reactions were subjected to SDS-PAGE using a 4% stacking gel and a 15% running gel. A total of 10 μg of each protein was loaded, and protein bands were visualized by Coomassie Brilliant Blue staining.

3. 2. 6 HPLC analysis

CiP and HRPC samples that were separated from the phenol oxidation reactions were concentrated to approximately 1 mg/mL. Pronase (0.25 mg/mL) was added to the protein samples, which were incubated overnight at 37 °C. Hemes were analyzed by HPLC using an OptimaPak C18, 4.6×250 mm column (RS tech Co., Korea). The heme was eluted with a linear gradient of 20-80% acetonitrile in water (0.1% formic acid) for over 50 min. The flow rate was 1 mL/min, and the elution was monitored at 400 nm. Under the HPLC gradient, the heme group was detected at a retention time of 44.8 min. The heme content was calculated according to the relative peak areas, and 100 μM hemin was used as a control.

3. 3 Results and Discussion

3. 3. 1 Inactivation factors for peroxidase during the phenol oxidation reaction

There are three proposed pathways for peroxidase inactivation during phenol oxidation. The first is a reaction with excess hydrogen peroxide, the second is the absorption by polymeric products, and the third is a reaction with free phenoxyl radicals produced by the oxidation reactions (Arnao et al., 1990; Klibanov et al., 1983; Nakajima and Yamazaki, 1987; Nakamoto and Machida, 1992). To determine which factor is dominant during the oxidation of phenol, the inactivation of two types of peroxidases, CiP and HRPC, was observed under various conditions; CiP and HRPC yielded the same result under each reaction condition (Figure 3-2). The activity of each peroxidase was decreased by approximately 20% due to hydrogen peroxide-mediated inactivation (Figure 3-2, B). It is well-known that peroxidases are inactivated by hydrogen peroxide (Arnao et al., 1990; Nakajima and Yamazaki, 1987; Valderrama et al., 2002); however, at a low concentration of hydrogen peroxide (0.5 mM), the contribution of hydrogen peroxide-mediated inactivation was small (Figure 3-2. B).

After the addition of a phenol polymer, the peroxidases maintained their initial level of activity (Figure 3-2. C). The inactivating effect of phenol polymer is not obvious unless a large amount (grams per liter) of precipitated polymer product is formed

(Huang et al., 2005; Nakamoto and Machida, 1992). The amount of phenol polymers used in the present study was not sufficient to affect peroxidase activity, even the added phenol polymers formed with 20-fold higher concentrations of substrates and enzyme. This result indicated that the precipitated polymeric product barely inactivated the peroxidase at a low substrate concentration.

In contrast, in the presence of hydrogen peroxide and phenol, CiP and HRPC were inactivated to a dramatic extent within 5 min (Figure 3-2. D). The hydrogen peroxide-mediated inactivation of peroxidase is largely suppressed by the addition of a reducing substrate because it competes with hydrogen peroxide for Compound II (Arnao et al., 1990; Choi et al., 1999). However, phenol did not prevent CiP and HRPC inactivation by hydrogen peroxide, and the peroxidases were more rapidly inactivated by the addition of phenol. Thus, the main factor causing the inactivation of CiP and HRPC was the phenoxyl radical attacking the peroxidase.

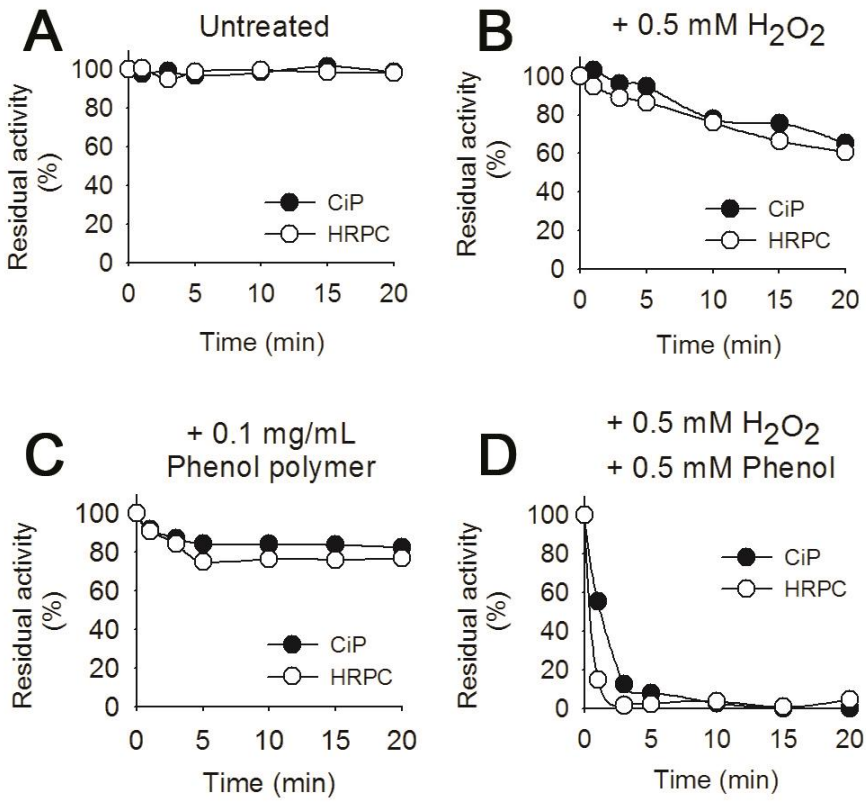

Figure 3-2. Peroxidase inactivation in various reaction conditions. CiP and HRPC were incubated in (A) phosphate buffer, pH 7.0, (B) 0.5 mM H_2O_2, (C) 0.1 mg/mL phenol polymer, (D) or 0.5 mM H_2O_2 and 0.5 mM phenol.

3. 3. 2 The modification of peroxidase polypeptide

Peroxidase can be inactivated by covalent bonding between the peroxidase and a phenoxyl radical (Chang et al., 1999; Huang et al., 2005; Kim et al., 2009). There are two possible outcomes if a radical attacks the peroxidase during the oxidation of phenol (Figure 3-3): a critical amino acid residue in the polypeptide is modified, or the heme is modified or destroyed via covalent bonding between the phenoxyl radical and the enzyme.

To determine if the polypeptide was modified by a phenoxyl radical, samples of CiP and HRPC that had been inactivated during the phenol oxidation reaction were analyzed by SDS-PAGE. CiP and HRPC were separated from the phenol oxidation reaction mixture, and subjected to SDS-PAGE. Figure 3-4 shows that the molecular weights of inactivated CiP and HRPC shifted slightly upward compared to those of the native controls, suggesting that the reacted CiP and HRPC polypeptides were modified by phenoxyl radicals. Covalent modifications by a phenolic substrate at the heme edge of HRPC have been identified by Gilfoyle at al. (1996). However, the molecular weight changes in CiP and HRPC confirmed by SDS-PAGE were not due to the heme modification, because the heme moiety of peroxidase would have been released from the polypeptide during denaturation by sodium dodecyl sulfate. This result showed that the phenoxyl radical was covalently bound to the polypeptide rather than the heme moiety of peroxidase.

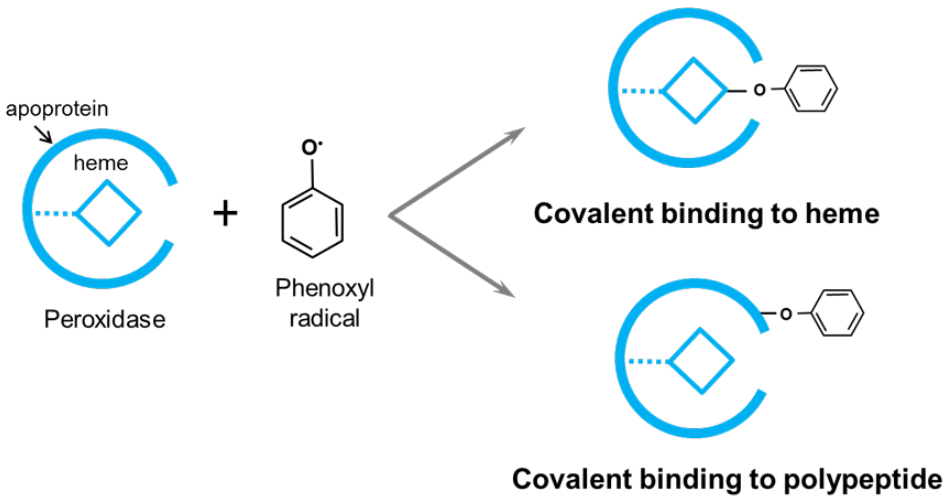

Figure 3-3. Inactivation of peroxidase by radical coupling during the oxidation reaction of phenol.

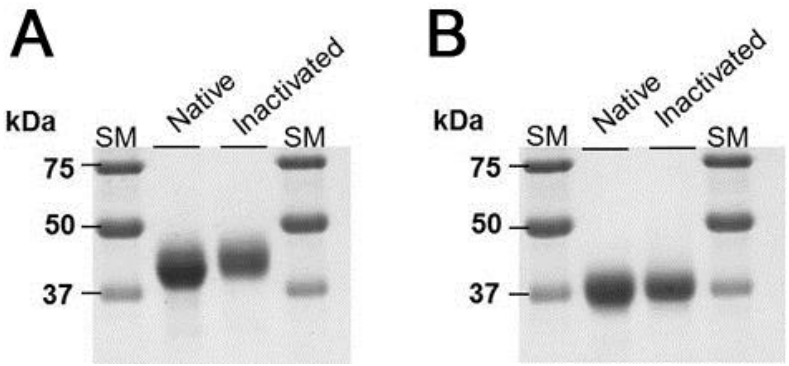

Figure 3-4. Molecular weights of inactivated peroxidase polypeptides after phenol oxidation reactions. (A) CiP and (B) HRPC were incubated with 0.5 mM H_2O_2 and 0.5 mM phenol, and the molecular weight of each peroxidase was analyzed by 15% SDS-PAGE. SM; size-marker.

3. 3. 3 Heme destruction of peroxidase

In order to further investigate the heme destruction by phenoxyl radical attack, intact hemes from peroxidases were quantified following the peroxidase-catalyzed oxidation of phenol. The proportions of intact heme groups from native, hydrogen peroxide-incubated, and phenoxyl radical-inactivated CiP and HRPC are shown in Table 3-1. Following treatment with hydrogen peroxide alone, the amount of intact hemes from CiP and HRPC decreased to 87 and 73%, respectively, of those found in native peroxidases. This result is in accord with the stability of peroxidase after treatment with hydrogen peroxide (Figure 3-2. B). When CiP and HRPC were treated with hydrogen peroxide and phenol, the amount of intact hemes decreased to 75 and 48%, respectively. Although CiP and HRPC were completely inactivated (Figure 3-2. D), CiP and HRPC maintained a high proportion of intact hemes in the presence of 0.5 mM phenol and hydrogen peroxide (Table 3-1). The activity loss is substantially greater than that caused by heme destruction during the phenol oxidation reaction. This result suggests that the phenoxyl radicals are associated with the loss of intact heme groups; however, the loss of catalytic activity is primarily caused by a modification of the peroxidase polypeptide rather than heme destruction by radical attack.

During the oxidation of phenolic compounds, peroxidase inactivation can occur as a result of phenoxyl radicals interacting with

hydrogen peroxide and a phenolic substrate (Baynton et al., 1994; Huang et al., 2005; Klibanov et al., 1983; Nakamoto and Machida, 1992). Theses previous report claimed that HRPC can be inactivated through heme destruction by radical attack. However, neither a direct interaction between a phenoxyl radical and heme nor a phenol-modified heme from a phenolic substrate-reacted HRPC or CiP could be detected by Raman spectrometry (Gilfoyle et al., 1996; Huang et al., 2005; Mao et al., 2013). Although there was a modified heme compound (20-phenyl heme) in phenylhydrazine-treated HRPC, but the modified heme of the perfectly inactivated HRPC constituted less than 10% of the total heme (Gilfoyle et al., 1996)

On the other hand, the covalently binding of substrate radicals generated by oxidation reactions with to peptide residues was observed in many peroxidases (Chang et al., 2011; Chang et al., 1999; Cohen-Yaniv and Dosoretz, 2009; Kim et al., 2009). The polypeptides in 4-chloroanillin-inactivated HRP, CiP, and lactoperoxidase (LPO) are covalently modified by 4-chloroanillin derivatives (Chang et al., 1999). In addition, a covalent link is generated between the HRP polypeptide and a bromophenol intermediate generated during the oxidation reaction of bromophenol (Cohen-Yaniv and Dosoretz, 2009). LPO is inactivated by the irreversible covalent binding of genistein to a particular peptide fragment (Chang et al., 2011). These reports also supported the peroxidase inactivation mechanism associated with covalent bounding between the polypeptide and phenoxyl radicals.

Table 3-1. The proportions of intact hemes from CiP and HRPC following the phenol oxidation by peroxidase.

Peroxidase	Proportion of intact heme (%)		
	Native	H_2O_2-incubated	Phenoxyl radical-inactivated
CiP	100	86.6	74.6
HRPC	100	72.9	48.3

3. 4 Conclusion

The two types of peroxidases, CiP and HRPC catalyzed phenol oxidation, and were subject to rapidly inactivation. After incubation with hydrogen peroxide and phenol, CiP and HRPC had slightly higher molecular weights. Although heme destruction occurred, more of enzyme catalytic activity was lost than could be accounted for by heme destruction alone. From these results, I suggested that phenoxyl radicals produced by peroxidase-mediated phenol oxidation were covalently bound to the peroxidase polypeptides and that these covalent attachments were the dominant source of enzyme inactivation. Many previous reports showed the covalent biding of the substrate intermediate radicals to the polypeptide in the many peroxidases, and the modified polypeptides of CiP and HRPC with phenoxyl radical were also confirmed in this study.

CHAPTER 4

DEVELOPMENT OF THE RADICAL-STABLE *COPRINUS CINEREUS* PEROXDIASE (CIP) BY BLOCKING THE RADICAL ATTACK

4. 1 Introduction

Peroxidases (EC 1.11.1.7) are heme-containing enzymes that catalyze the oxidation of a wide variety of phenolic compounds by utilizing hydrogen peroxide as oxidant (Dunford, 1999). For every one equivalent of hydrogen peroxide consumed, two equivalents of phenol are converted into a highly reactive radical species. These unstable radicals react with one another to yield phenolic polymers. The radical coupling reaction can potentially be used to remove phenolic and aromatic pollutants from wastewater (Aitken, 1993; Al-Ansaria et al., 2009; Steevensz et al., 2009). Peroxidases also can be used for the biocatalytic synthesis of green chemicals, such as conducting polymers, phenolic fine chemicals, and pharmaceuticals (Antoniotti and Dordick, 2005; Khmelnitsky et al., 1997; Kim et al., 2007; Sigoillot et al., 2005). For example, the fungal peroxidase CiP catalyzes the synthesis of useful polymers, such as polycardanol and poly(bisphenol A) (Kim et al., 2007; Kim et al., 2005; Park et al., 2009).

Despite the versatile catalytic ability of peroxidases, their industrial applications are quite limited by their rapid inactivation during oxidative reactions (Klibanov et al., 1983). The peroxidases are inactivated by their natural substrate or reaction intermediates during the oxidation of phenolic compounds, which is referred to as suicide inactivation. This process involves reactions between peroxidase and hydrogen peroxide or radical intermediates generated from enzyme catalysis (Hiner et al., 1995; Kohler and Jenzer, 1989). Excess hydrogen peroxide is the suicide substrate, yielding inactive Compound III and generating hydroxyl free

radicals that result in heme destruction or protein oxidation (Nakajima and Yamazaki, 1987; Ward et al., 2002). To minimize the inactivation by excess hydrogen peroxide, a low hydrogen peroxide concentration is maintained by controlling the addition rate of hydrogen peroxide using a hydrogen peroxide sensor or by adding sufficient reducing substrates, such as phenolic compounds (Seelbach et al., 1997; van de Velde et al., 1999; Van Deurzen et al., 1997).

Despite the presence of a sufficient amount of phenolic compound to serve as a reducing substrate, peroxidase activity is significantly reduced by its interactions with phenoxyl radicals (Baynton et al., 1994; Nakamoto and Machida, 1992). Phenoxyl radicals inactivate many peroxidases, including ascorbate peroxidase (Chen and Asada, 1990), lactoperoxidase (LPO) and thyroid peroxidase (Divi and Doerge, 1994), and CiP (Aitken and Heck, 1998; Kim et al., 2009). Huang investigated possible inactivation mechanisms of horseradish peroxidase isoenzyme C (HRPC) during phenol oxidation e.g., radical attack on the heme pocket or binding of phenol oligomers (Huang et al., 2005). In addition to heme destruction by phenoxyl radicals, the modification of amino acids in the active site by ^{14}C-labelled substrate radical intermediates was also observed during inactivation of other peroxidases e.g., CiP, HRPC, and LPO (Chang et al., 1999). Despite the experimental evidence of the radical attack on peroxidase involving the heme destruction or amino acid modification in the active site, however, no effort has been made to identify radical-coupling (modified) residues of peroxidase and to perform site-directed mutagenesis of them for further understanding the effect of radical modification on peroxidase

inactivation or for engineering radical-stable peroxidases.

CiP is a class II fungal peroxidase (Welinder, 1992) with versatile properties, including high specific activity and broad substrate specificity (Nakayama and Amachi, 1999). Moreover, CiP has higher thermostability than HRP (Ryu et al., 1995), and its thermostability is further improved by protein engineering (Cherry et al., 1999). Therefore, a stable CiP mutant against radical attack could serve as an alternative to HRP in industrial applications, such as the synthesis of fine chemicals including phenolic polymers.

Using CiP as a model enzyme, a novel protein engineering strategy was proposed to stabilize peroxidases against radical attack. Mass spectrometry analysis of inactive CiP isolated after phenol oxidation reactions revealed that CiP was predominantly inactivated by a covalent modification of F230 with a phenoxyl radical. Radical-stable CiP mutants were obtained by mutating F230 to amino acids less susceptible to radical attack. This study is the first use of protein engineering to improve peroxidase stability against radical attack, and this strategy could be widely applicable to other peroxidases that are inactivated by radicals.

4. 2 Materials and Methods

4. 2. 1 Peroxidase expression, purification, and activity assay

The CiP gene (GenBank Accession No. X70789) was ordered as a synthetic gene (GenScript Inc., USA). For site-directed mutagenesis, the synthetic CiP gene was used as a template, and the primers used to generate mutations are listed in Table 4-1. The wild-type and mutant CiPs were expressed in the supernatant of *Pichia pastoris* X-33 cultures via a pPICZαA vector (Invitrogen, USA), and expressed CiPs were purified with a size exclusion column (GE Healthcare, USA) as previously described (Kim et al., 2010). Peroxidase activity was measured using ABTS (2,2'-azino-bis(3-ethylbenzothiazoline-6-sulphonic acid)), a widely used substrate for peroxidase (Childs and Bardsley, 1975), as previously described (Kim et al., 2010). All experimental results presented in this study were average values obtained from triplicate measurements.

4. 2. 2 Mass spectrometry analysis

The reaction mixture was prepared with 18 mM phenol in 100 mM phosphate buffer (pH 7.0). CiP and F230A proteins were added to the each reaction mixture to a final concentration of 0.3 μM, and enzyme reaction was initiated with the addition of 18 mM hydrogen peroxide. The reaction mixture was incubated for 40 min at room temperature with gentle stirring, and the proteins were precipitated

by the rapid addition of four volumes of ice-cold acetone. The mixture was incubated at -20 °C overnight and centrifuged at 13,000 g at 4 °C for 20 min. The supernatant was removed, and 1 mL of ice-cold acetone was added to wash the precipitate. The precipitated sample was incubated on ice for 15 min and centrifuged at 13,000 g at 4 °C for 20 min. The acetone-containing supernatant was removed, and the precipitate was lyophilized. The precipitate obtained from the acetone precipitation was analyzed by 10% (w/v) sodium dodecyl sulfate polyacrylamide gel electrophoresis. The gel was stained with colloidal Coomassie Brilliant Blue G-250 for 30 min, and excess dye was removed with 10% methanol containing 8% acetic acid. The protein bands containing CiP or F230A (46 kDa) were excised and subjected to proteolytic digestion with trypsin or Glu-C (*Staphylococcus aureus* Protease V8). Gel slices containing CiP and F230A (46 kDa) were digested in-gel with sequencing grade modified trypsin (Promega, USA) and endoproteinase Glu-C (Promega, USA), respectively. In brief, each protein spot was excised from the gel, and washed 4-5 times (until the gel was clear) with 200 μL of 1:1 acetonitrile/25 mM ammonium bicarbonate, pH 7.8. The gel slices were dried in a Speedvac concentrator, and then rehydrated in 30 μL of 25 mM ammonium bicarbonate, pH 7.8, containing 20 ng of trypsin or 5 ng of endoproteinase Glu-C. After incubation at 37 °C for 20 hrs, digested peptides remaining in the gel matrix were extracted for 40 min at 30 °C with 20 μL of 50% (v/v) aqueous acetonitrile containing 0.1% (v/v) formic acid. The combined supernatants were evaporated in a Speedvac concentrator and dissolved in 2 μL of 5 % (v/v) aqueous acetonitrile solution containing 0.1% (v/v) formic acid for

mass spectrometric analysis.

The peptides were analyzed on an HP 1100 HPLC nano-flow system using a splitter (Agilent, USA) coupled on-line to an LCQ DECA ion trap (Thermo Fisher Scientific, USA). Zorbax 300SB-C18 resin (particle size 5 μm, Agilent Technologies, USA) was packed into a home-built fused silica column (100 mm length × 75 μm I.D., tip diameter 10 μm). Peptides were bound in a flow of buffer A (0.1% (v/v) formic acid and 5% acetonitrile in water) for 10 min at 600 nL/min. The gradient was employed with buffer B (0.1% (v/v) formic acid in 95% acetonitrile) at a constant flow rate of 200 nL/min: 5–12% in 10 min, 12–35% in 25 min, 35–90% in 5 min, 90% for 10 min. A 1.7 kV spray voltage was applied at the ESI source and the transfer capillary temperature was set at 180 °C. MS scan events in positive ion mode were controlled by Xcalibur 1.2 software. Precursor ions were selected over the range m/z 350–2,000 for MS/MS fragmentation within a ±3 m/z window for subsequent MS/MS scans in a data-dependent mode. An exclusion dynamic mode was applied to exclude the selected most intense ion from further selection over 2 min period. MS/MS data were acquired using a 2 m/z unit ion isolation window in the automated gain control (AGC) mode where AGC values of 5.00e + 05 and 1.00e + 04 were set for full MS and MS/MS, respectively. The normalized CID was set to be 35.0.

Peak lists from MS/MS spectra were exported as individual files in DTA format using Bioworks 3.3 software (Thermo Fisher Scientific, USA) under the following settings: peptide mass range, 500–3500 Da; minimal total ion intensity threshold, 10000; minimal number of fragment ions, 20; precursor mass tolerance, 1.4 amu;

group scan, 1; minimum group count, 1. A single text file, which was generated by the automatic combination of the resulting DTA files from each analysis, was searched against either the National Center for Biotechnology Information (NCBI) non-redundant or the peroxidase protein database using Mascot (Perkins et al., 1999) operating on a local server (version 2.1; Matrix Science, UK) with the following parameters; trypsin or endoproteinase Glu-C as the enzyme with one potential missed cleavages; monoisotope mass selected, a 2-2.5 Da peptide mass tolerance and a 1 Da MS/MS tolerance; carbamidomethylation of cysteines, oxidation of methionine, deamidation of asparagine/glutamine (formally 'deamidation', but due to deisotoping artefact during data extraction), 1 × to 9 phenylene(s) modification of aromatic amino acid (phenylalanine, histidine, tryptophan, tyrosine) as variable modifications; singly, doubly, or triply charged state. Only significant hits as defined by MASCOT probability analysis ($p<0.05$) were considered.

4. 2. 3 Molecular docking simulation

Molecular docking simulations for peroxidases with a phenol molecule were performed using Discovery Studio (version 3.1; Accelrys, USA). The structures of CiP (pdb code: 1ARP) was downloaded from the Protein Data Bank (http://www.rcsb.org), and a phenol molecule was constructed using the Fragment Builder tools of Discovery Studio. Molecular docking simulation was conducted

for the wild-type and F230A. F230A mutant was modeled by the SCRWL 3.0 program based on the combination of rotamer libraries (Canutescu et al., 2003). The CHARMm force field was applied to the molecules, and the CDOCKER module was used for molecular docking simulation. For the docking of the CiP enzymes, the phenol molecule was manually docked into the F230 and F230A. All possible complexes of the peroxidase-phenol were generated. Residues within 8 Å from the initial docking position of the wild type and corresponding sites on the F230A mutant were selected for the binding site, and the other residues of the peroxidases were fixed. The molecular docking simulations were performed with the default parameters of the CDOCKER module. The top 10 hits with the lowest docking scores were selected for calculating the binding free energy of the complexes. The binding free energy of the complexes was calculated using a Discovery Studio protocol with default parameters. The complex of peroxidase and a phenol molecule with the lowest binding free energy was used as the modeled docking structure of the peroxidase for the structure analysis. The binding distance for peroxidase was determined by calculating the distance between the εN atom of the catalytic His residue (His56) (Itakura et al., 1997) and the reactive OH group of phenol using the modeled structures of the complex.

4. 2. 4 Turnover capacity and radical stability

Batch reactors consisted of a 50 mL glass vial containing 20 mL

of 0.5 mM phenol in 100 mM phosphate buffer (pH 7.0). The peroxidase was added to the batch reactor to a final concentration of 12 nM. A total of 0.5 mM of hydrogen peroxide was added to the reactor to initiate phenol oxidation. The reaction was sampled every 5 min after the initiation of phenol oxidation, and samples were centrifuged for 15 min at 13,000 g to remove polymerized precipitates. The phenol concentration was determined using an Agilent model 1200 liquid chromatograph (Agilent Technologies, USA) with a diode-array detector working at 280 nm. Separation was carried out using a Zorbax XDB-C18 column (150 × 0.3 mm, 3.5 m; Agilent Technologies, USA) at 25 °C, with a mobile phase of 0.3% (v/v) acetic acid (70%) and methanol (30%) at a flow rate of 1.0 mL/min. The phenol concentration was quantified using calibration curves prepared from external standards. The turnover capacity was expressed as the ratio of exhausted phenol (ΔS) per enzyme lost activity (ΔE) during 20 min of reaction.

4. 2. 5 Kinetic parameters

The kinetic properties of the wild-type CiP and mutants were measured as previously described (Kim et al., 2010). In brief, the peroxidase reaction rate was measured with 100 μM hydrogen peroxide, indicated substrates (ABTS in the final concentration rage from 0 to 100 μM and guaiacol in the final concentration range from 0.4 to 20 mM), and peroxidase (0.3 μM). The k_{cat} and K_m of each peroxidase were derived by the Michaelis-Menten equation based on

the corresponding Hanes-Woolf plots from three independent experiments.

4. 2. 6 Spectroscopic analysis

The concentrated CiP was diluted to approximately 0.12 μM in 100 mM phosphate buffer (pH 7.0). CiP was treated with 0.5 mM phenol and 0.5 mM hydrogen peroxide for 20 min at 25 °C. The solution was filtered and concentrated with an Amicon ultrafiltration device (Millipore, USA). The absorption spectral changes in CiP were recorded in the range of 350-700 nm using a UV-Vis spectrophotometer (Multiskan GO; Thermo Scientific, USA). Circular dichroism (CD) spectra were obtained from 1 mg/ml of sample protein and recorded on a J-815 CD spectropolarimeter (150-L Type; Jasco Inc., Japan) in 1 mM potassium phosphate (pH 7.0) at room temperature. CD in the far-UV range (190-260 nm) was measured using a quartz cell with a 1 mm optical path length. CD in near-UV region (260-320 nm) was monitored using a cuvette with a path length of 10 mm. Measurements were taken every 1 nm at a scan rate of 100 nm/min. The secondary structure percentages were predicted CDSSTR algorithms via Dichroweb (http://www.cryst.bbk.ac.uk/ cdweb/html/home.html) (Johnson, 1999; Whitmore and Wallace, 2004).

Table 4-1. Primers used for site-directed mutagenesis of CiP.

Primer	Sequence	Mutation sequence[a]	Mutant
Mutagenic primers	M1-F	5′- CCCGGTCCTTCATTGGGTGCTGCAGAAGAATTGTCTCCG-3′	F230A
	M1-R	5′- CGGAGACAATTCTTCTGCAGCACCCAATGAAGGACCGGG-3′	
	M2-F	5′- CCCGGTCCTTCATTGGGTTTGGCAGAAGAATTGTCTCCG-3′	F230L
	M2-R	5′- CGGAGACAATTCTTCTGCCAAACCCAATGAAGGACCGGG-3′	
	M3-F	5′- CCCGGTCCTTCATTGGGTATTGCAGAAGAATTGTCTCCG-3′	F230I
	M3-R	5′- CGGAGACAATTCTTCTGCAATACCCAATGAAGGACCGGG-3′	
	M4-F	5′- CCCGGTCCTTCATTGGGTGTTGCAGAAGAATTGTCTCCG-3′	F230V
	M4-R	5′- CGGAGACAATTCTTCTGCAACACCCAATGAAGGACCGGG-3′	
	M5-F	5′- CCCGGTCCTTCATTGGGTTACGCAGAAGAATTGTCTCCG-3′	F230Y
	M5-R	5′- CGGAGACAATTCTTCTGCGTAACCCAATGAAGGACCGGG-3′	
	M6-F	5′- CCCGGTCCTTCATTGGGTTGGGCAGAAGAATTGTCTCCG-3′	F230W
	M6-R	5′- CGGAGACAATTCTTCTGCCCAACCCAATGAAGGACCGGG-3′	
	M7-F	5′- CCCGGTCCTTCATTGGGTCATGCAGAAGAATTGTCTCCG-3′	F230H
	M7-R	5′- CGGAGACAATTCTTCTGCATGACCCAATGAAGGACCGGG-3′	
Flanking primers	5′ *Eco*RI	5′-GCGCGAATTCCAAGGTCCTGGTGGTGGTGGATCTG-3′	
	3′ *Not*I	5′-GCGCGCGGCCGCTTATGGAGCAGGAGCAAGTGATGGC-3′	

[a] Mutated sequences are underlined.

4. 3 Results and Discussion

4. 3. 1 Inactivation of CiP during phenol oxidation

CiP was incubated with 0.5 mM phenol and 0.5 mM hydrogen peroxide, and the remaining activity of peroxidase was determined at regular intervals. Figure 4-1 shows that in the absence of phenol, approximately 30% of the enzyme activity was lost by oxidant substrate hydrogen peroxide. However, the inclusion of phenol in the reaction solution completely eliminated enzymatic activity. The reducing substrate phenol did not prevent the inactivation by hydrogen peroxide, and increased the inactivation of peroxidase. It implied that the phenoxyl radical generated during peroxidase catalysis is closely associated with CiP inactivation, as previously reported (Aitken and Heck, 1998; Kim et al., 2009).

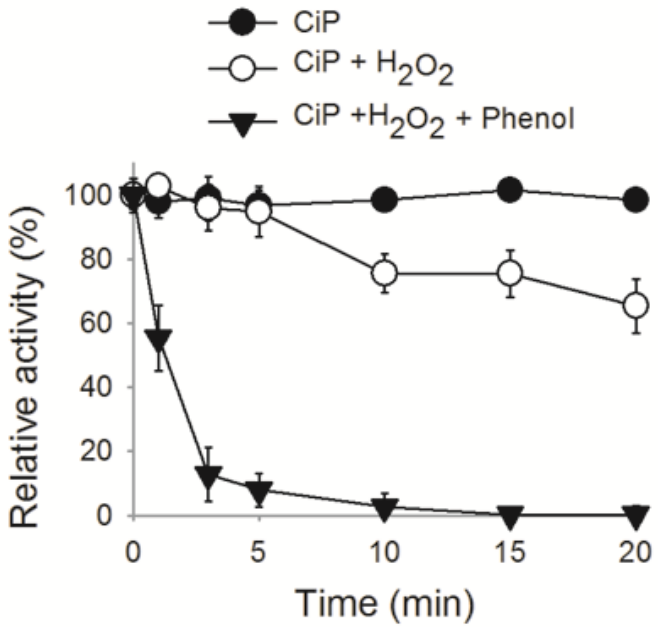

Figure 4-1. Residual activity of CiP during the oxidation reaction of phenol. The enzyme solution was incubated with 0.5 mM H_2O_2 in the absence or presence of 0.5 mM phenol. Samples were withdrawn at each indicated time, and the peroxidase activity was assayed using ABTS. Relative activity was calculated as enzymatic activity at indicated time divided by activity at time zero.

4. 3. 2 Formation of an inactive adduct between F230 and the phenoxyl radicals

To explore the inactivation of peroxidase by phenoxyl radical attack, the modification of CiP by phenoxyl radicals was investigated by mass spectrometry, after the phenol oxidation reaction. CiP was incubated with 18 mM phenol in the absence or presence of 18 mM hydrogen peroxide. The native CiP, treated with 18 mM phenol alone, and the inactivated CiP, reactivated with 18 mM phenol and 18 mM hydrogen peroxide, were isolated from the reaction solutions and analyzed by LC-MS/MS after tryptic digestion. Figure 4-2 shows the LC-MS/MS result from the inactivated CiP and their sequences derived through de novo sequencing. The sequence of the phenol-modified fragment (m/z 838.880) was KGTTQPGPSLGFAEELSPFPG EFRM (residues 219-241), whereas a fragment of native CiP (m/z 1211.621) was not modified (Tables 4-2 and 4-3). In the modified CiP peptide, a phenylalanine residue (F230) formed an inactive adduct with a phenoxyl radical (Figure 4-2). The phenoxyl radical coupling site, the F230 residue of CiP, was identified by mass spectrometry analysis. The peroxidase modification with the substrate-derived radicals was also reported in other previous studies (Chang et al., 2011; Chang et al., 1999; Cohen-Yaniv and Dosoretz, 2009; Kim et al., 2009).

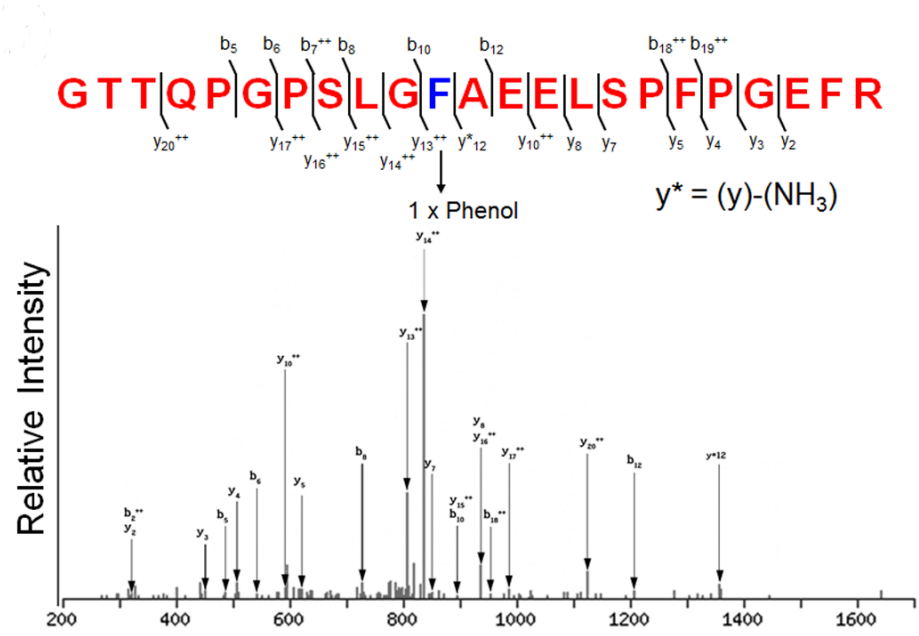

Figure 4-2. LC-MS/MS analysis of peptides from inactivated CiP. Modified peptide from the inactivated CiP was identified by mass spectrometry after incubation with 18 mM H_2O_2 and 18 mM phenol. The MS/MS spectrum was acquired from m/z 838.880 of the trypsin-digest fragment of the inactivated CiP.

Table 4-2. Modified residues of CiP (m/z 838.880) identified by mass spectrometry.

#	b	b^{++}	b*	b^{*++}	b^{0}	b^{0++}	Seq.	y	y^{++}	y*	y^{*++}	y^{0}	y^{0++}	#
1	58.029	29.518					G							23
2	159.076	80.042			141.066	71.037	T	2456.177	1228.592	2439.150	1220.079	2438.166	1219.587	22
3	260.124	130.566			242.114	121.560	T	2355.129	1178.068	2338.103	1169.555	2337.119	1169.063	21
4	388.183	194.595	371.156	186.082	370.172	185.590	Q	2254.082	1127.544	2237.055	1119.031	2236.071	1118.539	20
5	485.235	243.121	468.209	234.608	467.225	234.116	P	2126.023	1063.515	2108.996	1055.002	2108.012	1054.510	19
6	542.257	271.632	525.230	263.119	524.246	262.627	G	2028.970	1014.989	2011.944	1006.475	2010.960	1005.983	18
7	639.310	320.159	622.283	311.645	621.299	311.153	P	1971.949	986.478	1954.922	977.965	1953.938	977.473	17
8	726.342	363.675	709.315	355.161	708.331	354.669	S	1874.896	937.952	1857.869	929.438	1856.885	928.946	16
9	839.426	420.217	822.399	411.703	821.415	411.211	L	1787.864	894.436	1770.837	885.922	1769.853	885.430	15
10	896.447	448.727	879.421	440.214	878.437	439.722	G	1674.780	837.894	1657.753	829.380	1656.769	828.888	14
11	1135.542	568.275	1118.515	559.761	1117.531	559.269	F	1617.758	809.383	1600.732	800.870	1599.748	800.378	13
12	1206.579	603.793	1189.552	595.280	1188.568	594.788	A	1378.664	689.836	1361.637	681.322	1360.653	680.830	12
13	1335.622	668.314	1318.595	659.801	1317.611	659.309	E	1307.627	654.317	1290.600	645.804	1289.616	645.312	11
14	1464.664	732.836	1447.638	724.322	1446.654	723.830	E	1178.584	589.796	1161.558	581.282	1160.574	580.790	10
15	1577.748	789.378	1560.722	780.865	1559.738	780.373	L	1049.541	525.274	1032.515	516.761	1031.531	516.269	9
16	1664.780	832.894	1647.754	824.381	1646.770	823.889	S	936.457	468.732	919.431	460.219	918.447	459.727	8
17	1761.833	881.420	1744.806	872.907	1743.822	872.415	P	849.425	425.216	832.399	416.703	831.415	416.211	7
18	1908.901	954.954	1891.875	946.441	1890.891	945.949	F	752.373	376.690	735.346	368.177	734.362	367.685	6
19	2005.954	1003.481	1988.928	994.967	1987.944	994.475	P	605.304	303.156	588.278	294.642	587.294	294.150	5
20	2062.976	1031.991	2045.949	1023.478	2044.965	1022.986	G	508.251	254.629	491.225	246.116	490.241	245.624	4
21	2192.018	1096.513	2174.992	1088.000	2174.008	1087.508	E	451.230	226.119	434.203	217.605	433.219	217.113	3
22	2339.087	1170.047	2322.060	1161.534	2321.076	1161.042	F	322.187	161.597	305.161	153.084			2
23							R	175.119	88.063	158.092	79.550			1

The matched fragment ions are presented and the ion series were in the upper row. The sequence of matched peptide is shown in 1-letter code and matched values are highlighter in bold.

Table 4-3. LC-MS/MS analysis of peptide from native and inactivated CiP.

Peroxidase	Observed peak (m/z)	Molecular weights (Da)		Sequence and modification[a]
		Expected	Calculated	
Native	1,211.621	2,421.227	2,421.149	KGTTQPGPSLGFAEELSPFPGEFRM
Inactivated	838.880	2,513.618	2,512.191	KGTTQPGPSLGFAEELSPFPGEFRM F with 1xPhenol

[a] The modification residue is underlined.

4. 3. 3 Improving radical stability by engineering F230 mutants

In order to reduce radical inactivation of CiP, the phenol-modified Phe residue (F230), located at the entrance of the active site, was subjected to site-directed mutagenesis. The F230 residue was substituted with two types of amino acids to observe the effect of properties of amino acid residues on the radical stability of peroxidase. The first group substituted hydrophobic amino acids with different carbon lengths: F230G, F230A, F230V, F230I, and F230L. Except for F230G, these mutations conserved the native structure by maintaining hydrophobic interactions with other residues in CiP. The second group exchanged F230 with bulky-aromatic amino acids: F230H, F230Y, and F230W. Aromatic amino acids (e.g., Phe, Trp, Tyr, or His) may be susceptible to covalent bonding with free radicals (Hawkins and Davies, 2001). While the histidine residue was charged, its size and orientation were similar to those of phenylalanine. F230Y and F230W were designed to compare and characterize the pattern of radical inactivation of aromatic residues. All CiP mutants were expressed in *P. pastoris* as soluble proteins, however, the F230G, F230V, and F230Y mutants secreted from *Pichia* exhibited no enzyme activity against ABTS as substrate. Specific activities of the purified CiP wild-type and five mutants towards ABTS were summarized in Table 4-4. Specific activities on ABTS was lower for the all mutants (F230A: 405 U/mg, F230I: 124 U/mg, F230L: 494 U/mg, F230H: 591 U/mg, and F230W; 73 U/mg) compared with the wild-type CiP (3812 U/mg).

The wild-type and F230 mutants were incubated in phosphate buffer (100 mM, pH 6.0) containing 0.5 mM phenol and 0.5 mM hydrogen peroxide for 20 min at 25°C. Figure 4-3 shows the remaining peroxidase activity and phenol concentration at regular time intervals during the oxidative reaction of phenol. Compared to the wild-type, the F230A mutant showed remarkably improved radical stability. The wild-type was almost inactivated within 10 minutes, while the F230A mutant retained approximately 80% of its initial activity after 20 minutes. The residual peroxidase activity of other hydrophobic mutants, such as F230I and F230L, was approximately 40-fold higher than the wild-type (Figure 4-3. A and Table 4-5). However, other mutants containing aromatic amino acids, such as F230H and F230W, were similar to the wild-type enzyme, and were completely inactivated within 20 min (Figure 4-3. A).

Almost 90% of the initial phenol was oxidized to produce phenol polymer with the F230A mutant, while wild-type consumed only 20% of the initial phenol (Figure 4-3. B). Similar to F230A, the hydrophobic mutants F230I and F230L efficiently catalyzed the phenol oxidation reaction, whereas the F230H and F230W mutants consumed approximately 50% of the initial phenol (Figure 4-3. B and Table 4-5). In addition, the F230A mutant showed a higher turnover capacity, i.e., 16-fold higher than the wild-type, and both the F230I and F230L mutants had increased turnover capacity, as shown in Table 4-5. The F230 mutants showed the tendency that the aliphatic amino acid mutants (F230A, F230I, and F230L) were more robust against the radical attack than the wild-type and aromatic amino acid mutants (F230H and F230W). It is known that aliphatic amino acid

reacts with the free radical such as hydroxyl radical at relatively slow rates compared with aromatic amino acids (Stadtman, 1993).

Moreover, we confirmed that the F230A residue was not modified with a phenoxyl radical during the phenol oxidation reaction (Figure 4-4 and Tables 4-6 and 4-7). This result supports that the mutation of Phe to Ala at the F230 residue can block the modification of Phe residue by radical attack. In addition, these experiment results suggest that radical coupling between peroxidase and phenolic substrates contributes substantially to peroxidase inactivation, and the radical coupling-resistant mutant is a stable enzyme because it escapes suicide inactivation by phenoxyl radicals.

Table 4-4. Enzymatic specific activity of purified CiP wild-type and mutants.

Enzyme	Specific activity (U/mg)
CiP	3812
F230A	405
F230L	494
F230I	124
F230H	591
F230W	73

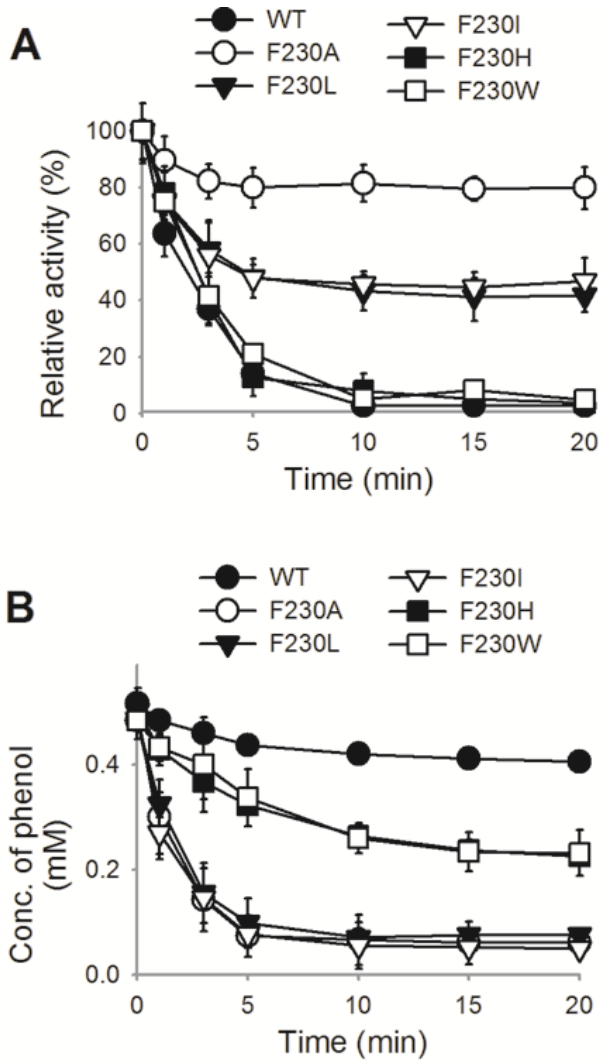

Figure 4-3. The stability of F230X mutants during the oxidation reaction of phenol. (A) The remaining peroxidase activity of the wild-type CiP (WT) and F230X mutants during the oxidation reaction of phenol. (B) Removal of phenol by the wild-type CiP (WT) and F230X mutants. Peroxidase activity and phenol concentrations were measured after incubation with 0.5 mM H_2O_2 and 0.5 mM phenol. Relative activity was calculated as enzymatic activity at indicated time divided by activity at time zero.

Table 4-5. Phenol-polymerization catalyzed by wild-type CiP and the F230 mutants.

Enzyme	Enzyme activity (U ml^{-1})			Phenol concentration (mM)			Turnover capacity[a] (mM U^{-1}) (fold increase)
	Initial	Final	Residual activity (%)	Initial	Final	Consumed phenol (%)	
CiP	0.9 ± 0.10	0.01 ± 0.001	≤1	0.51 ± 0.003	0.41 ± 0.01	20	0.11 (1.0)
F230A	1.16 ± 0.01	0.93 ± 0.04	80	0.48 ± 0.004	0.06 ± 0.002	88	1.83 (16.3)
F230L	1.07 ± 0.03	0.45 ± 0.05	42	0.48 ± 0.01	0.08 ± 0.01	83	0.65 (5.7)
F230I	0.99 ± 0.02	0.46 ± 0.01	46	0.48 ± 0.01	0.05 ± 0.002	83	0.81 (7.2)
F230H	0.86 ± 0.09	0.03 ± 0.018	3	0.51 ± 0.003	0.2 ± 0.02	61	0.37 (3.3)
F230W	1.09 ± 0.04	0.05 ± 0.02	5	0.48 ± 0.005	0.2 ± 0.004	58	0.27 (2.4)

[a] The turnover capacity is expressed as the ratio of exhausted phenol (mM) per consumed enzyme activity (U).

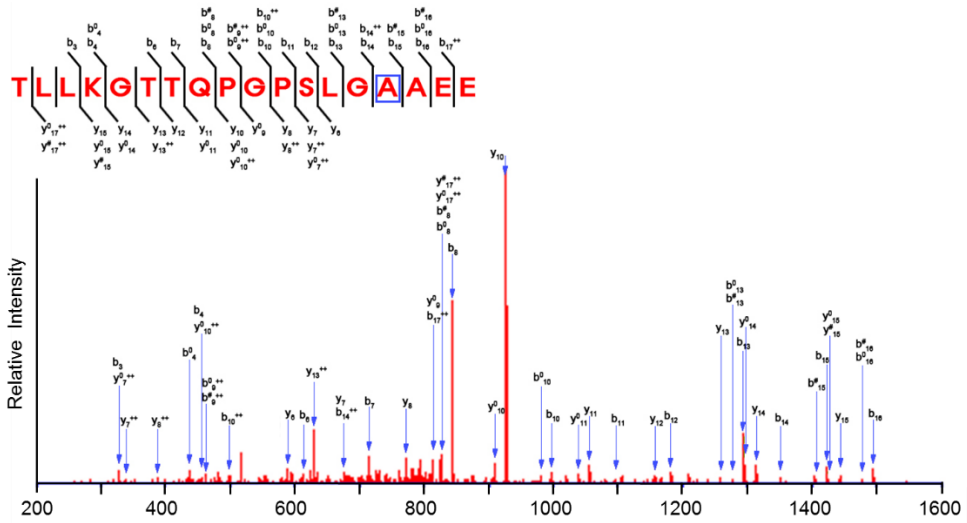

Figure 4-4. LC-MS/MS analysis of peptides from F230A mutant. Peptide of F230A mutant was identified by mass spectrometry after incubation with 18 mM H_2O_2 and 18 mM phenol. The MS/MS spectrum was acquired from m/z 886.832 of the Glu-C digested fragment of F230A mutant. The primary peptide structure was derived from de novo sequencing. The mutated residue (F230A) is marked with a square.

Table 4-6. Mutated residue of F230A (m/z 886.832) identified by mass spectrometry.

#	b	b^{++}	b*	b^{*++}	b^{0}	b^{0++}	Seq.	y	y^{++}	y*	y^{*++}	y^{0}	y^{0++}	#
1	102.0550	51.5311			84.0444	42.5258	T							23
2	215.1390	108.0731			197.1485	99.0679	L	1669.8643	835.4358	1652.8377	826.9225	1651.8537	826.4305	22
3	328.2231	164.6152			310.2125	155.6099	L	1556.7802	778.8937	1539.7537	770.3805	1538.7696	769.8885	21
4	456.3180	228.6627	439.2915	220.1494	438.3075	219.6574	K	1443.6961	722.3517	1426.6696	713.8384	1425.6856	713.3464	20
5	513.3395	257.1734	496.3129	248.6601	495.3289	248.1681	G	1315.6012	658.3042	1298.5746	649.7910	1297.5906	649.2989	19
6	614.3872	307.6972	597.3606	299.1840	596.3766	298.6919	T	1258.5759	629.7935	1241.5532	621.2802	1240.5692	620.7882	18
7	715.4349	358.2211	698.4083	349.7078	697.4243	349.2158	T	1157.5320	579.2697	1140.5055	570.7564	1139.5215	570.2644	17
8	844.4774	422.7424	827.4509	414.2291	826.4669	413.7371	Q	1056.4844	528.7458	1039.4578	520.2325	1038.4738	519.7405	16
9	941.5302	471.2687	924.5037	462.7555	923.5196	462.2635	P	927.4418	464.2245			909.4312	455.2192	15
10	998.5517	499.7795	981.5251	491.2662	980.5411	490.7742	G	830.3890	145.6981			812.3784	406.6929	14
11	1095.6044	548.3059	1078.5779	539.7926	1077.5939	539.3006	P	773.3676	387.1874			755.3570	378.1821	13
12	1182.6365	591.8219	1165.6099	583.3086	1164.6259	582.8166	S	676.3148	338.6610			658.3042	329.6558	12
13	1295.7205	648.3639	1278.6940	639.8506	1277.7100	639.3586	L	589.2828	295.1450			571.2722	286.1397	11
14	1352.7420	676.8746	1335.7154	668.3614	1334.7314	667.8693	G	476.1987	238.6030			458.1881	229.5977	10
15	1423.7791	712.3932	1406.7525	703.8799	1405.7685	703.3879	A	419.1772	210.0923			401.1667	201.0870	9
16	1494.8162	747.9117	1477.7896	739.3985	1476.8056	738.9065	A	348.1401	174.5737			330.1296	165.5684	8
17	1623.8588	812.4330	1606.8322	803.9198	1605.8482	803.4277	E	277.1030	139.0551			259.0925	130.0499	7
18							E	148.0604	74.5339			130.0499	65.5286	6

The matched fragment ions are presented and the ion series were in the upper row. The sequence of matched peptide is shown in 1-letter code and matched values are highlighter in bold.

Table 4-7. LC-MS/MS analysis of peptides from native and reacted F230A mutant.

Peroxidase	Observed peak (m/z)	Molecular weights (Da)		Sequence and modification
		Expected	Calculated	
Native[a]	886.322	1770.629	1768.921	E.TLLKGTTQPGPSLGAAEE.L
Reacted[b]	886.832	1771.650	1769.905	E.TLLKGTTQPGPSLGAAEE.L

[a] 'Native' is just purified F230A protein.

[b] 'Reacted' is the phenol-oxidation mediated F230A protein. The F230A mutant was incubated with 18 mM phenol and 18 mM hydrogen peroxide.

4. 3. 4 Kinetic studies.

The kinetic parameters of ABTS oxidation by F230A mutants were compared with wild-type to evaluate the effect of the mutation at F230 on peroxidative catalysis (Table 4-8). The F230 mutants showed much higher K_m values than the wild-type CiP, indicating that the F230 residue has an important role in the binding of aromatic substrates. The F230A mutant also had decreased substrate binding affinity but its k_{cat} value (2.02 s^{-1}) was comparable to that of wild-type (1.77 s^{-1}). Consequently, the ABTS oxidation efficiency of the F230A mutant was 5-fold lower than that of wild-type.

This kinetic study revealed that the F230 residue is already optimized in terms of enzyme catalysis, but can be further engineered for improving the enzyme stability. Previous studies revealed that the Phe residues situated at the entrance of the peroxidase heme access channel have a crucial role in the binding of aromatic substrates (Gazaryan et al., 1994; Veitch et al., 1994; Veitch et al., 1995). The F230 mutations may disturb substrate binding to the enzyme, which reduces the substrate binding affinity of CiP.

Table 4-8. Kinetic parameters of the wild-type CiP and F230 mutant.

	K_m (μM)	k_{cat} (s^{-1})	k_{cat}/K_m ($\mu M^{-1}s^{-1}$)
CiP	6.20 ± 0.620	1.77 ± 0.0194	0.286 ± 0.0312
F230A	34.4 ± 3.70	2.02 ± 0.0855	0.0587 ± 0.0231

4. 3. 5 Molecular docking simulation

The molecular docking simulation for the wild-type CiP and F230A mutant presented that the F230 residue was located at the entrance to the heme pocket of CiP, and formed an aromatic-aromatic interaction with a phenol molecule in the modeled complex (Figure 4-5). However, the mutation of Phe to Ala disrupted this aromatic-aromatic interaction and the F230A mutant had a higher binding distance (13.2 Å) than the wild-type (11.3 Å) (Figure 4-5). This docking result indicates that the removal of the Phe residue at the entrance to the heme pocket of CiP can lead to a decreased binding affinity for aromatic substrates due to the disruption of a specific interaction between substrates and CiP. Our docking simulation and enzyme kinetics revealed that the Phe residue in the substrate binding pocket are responsible for binding of phenolic substrates, which is consistent with previous results of HRPC (Veitch et al., 1997; Veitch et al., 1995).

Although the F230A mutation decreased the catalytic efficiency (k_{cat}/K_m) (Table 4-7), the turn-over capacity for phenol of the F230A was enhanced by 16-fold, compared with wild-type (Table 4-4). These results suggest that the F230A mutant is a valuable biocatalyst that can improve the efficiency of polymerization in conditions where the enzyme suffers the enzyme inactivation by radical attack.

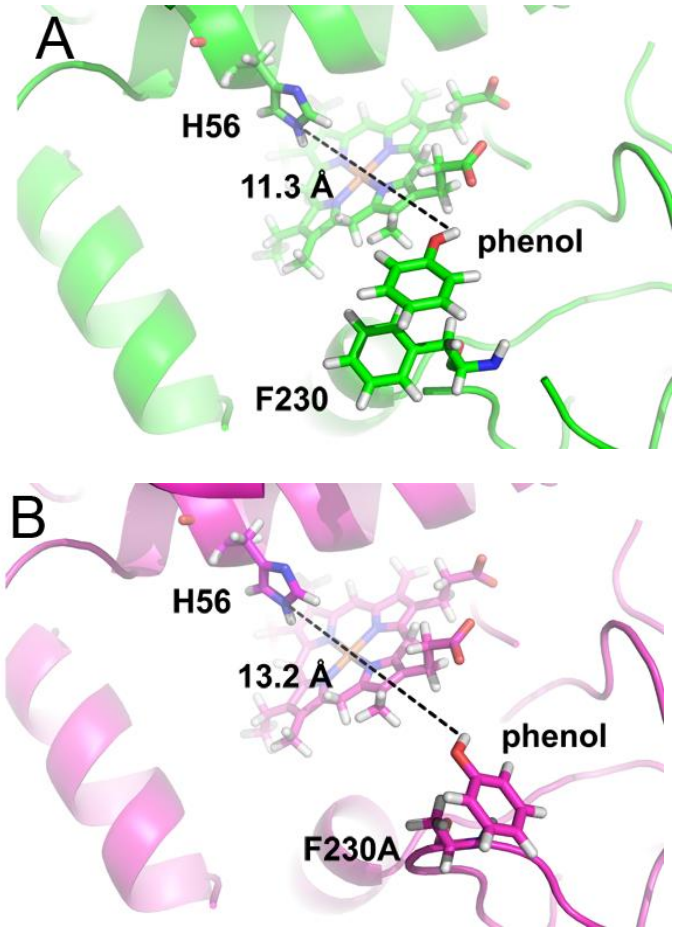

Figure 4-5. The modeled complexes of peroxidases and a phenol molecule. (A) The modeled complex of the wild-type CiP. (B) The modeled complex of the F230A mutant. Each distance indicates the distance between the εN atom of the catalytic His residue (His56) and the OH group of a phenol molecule.

4. 3. 6 Structure of CiP after the phenol modification

UV-Vis and CD spectral methods were used to further investigate the effect of the radical coupling on the conformational change of CiP. CD and absorbance spectra in UV and UV-Vis regions provide information on the structure of protein and prosthetic heme of peroxidase (Strickland, 1968). The position of the Soret absorption band of heme may provide information about possible deformation of the porphyrin, especially on the conformational change in the heme pocket (Herskovits and Jaillet, 1969; Rusling and Nassar, 1993). The absorbance spectra of CiP in the Soret (350-700 nm) region are shown in Figure 4-6. The UV-Vis spectra of the native CiP had a Soret maximum at 402 nm, and three smaller maxima at 497, 542, and 640 nm. The absorbance spectrum of radical-coupled CiP after the phenol oxidation reaction was almost similar to that of native CiP (Figure 4-6. A).

The CD spectra in the far-UV (190-260 nm) and near-UV (260-320 nm) regions are used to estimate protein secondary and tertiary structures, respectively (Fasman, 1996; Kelly et al., 2005). Figure 4-6. B shows the far-UV CD spectra of native and radical-coupled CiP. For both proteins, the spectrum was characterized by a negative band with double minima at 208 and 222 nm, which are typical for α-helix-rich structures (Myer, 1968). Upon radical coupling, inactivated CiP showed an almost identical far-UV CD spectrum to that of native CiP and the percentages of secondary structure elements of inactivated CiP were not altered (Table 4-9). Near-UV CD spectra can detect changes in the tertiary structure of proteins as near-UV region reflects

the environment of aromatic amino acids (Kelly et al., 2005). The native and radical-coupled CiP had very similar the near-UV CD spectra, and the global structure of CiP was not changed significantly by radical coupling (Figure 4-6. C).

Phe shows absorptions in the region of 260-270 nm, whereas Tyr and Trp absorb around 270-280 nm and 290-300 nm, respectively (Kelly et al., 2005). Near-UV CD spectra of native and inactivated CiP were shown in Figure 4-6. C, which had a slight decrease in the intensity of CD at around 260 nm and 305 nm after the oxidation reaction of phenol. Including F230 residue, other Phe and Trp residue(s) modified by radical coupling could influence the intensity of CD bands. All modified aromatic amino acids were not be detected in LC-MS/MS analysis. However, the absorbance changes in absorbance regions of Phe and Trp residue (Figure 4-6. C) indicate the possible modifications of other aromatic amino acids with phenoxyl radicals during the oxidation reaction of phenol. Because Trp, Tyr and Phe are the primary targets of radical attack (Stadtman, 1993), and are also known to be susceptible to the oxidative modification (Ivancich et al., 2013; Yukl et al., 2013).

There were no significant differences in the UV-Vis absorption and overall CD spectra of inactivated CiP after phenol oxidation, indicating that no considerable change in the interaction of the heme group with the protein moiety occurs and the native structure of CiP was retained during radical coupling (Figure 4-6 and Table 4-9). In addition, the wild-type CiP and F230 mutants showed similar UV-Vis absorption under high concentration of hydrogen peroxide without phenol (Figure 4-7), indicating the mutations of F230 residue could

not also change the local structure of porphyrin. The loss of catalytic activity of CiP during the phenol oxidation cannot therefore be due to structure disruption of enzyme.

The covalent binding between the Phe residue (F230) and phenoxyl radical was proved by mass and absorbance analysis (Figure 4-2 and 4-6). It is known that the formation of a phenyl radical from phenylalanine requires a very high oxidation potential. However, the formation of phenoxyl radical from the Phe residue can be observed in few oxygen-bridged diiron enzymes e.g., ribonucleotide reductases or methane monooxygenases (Baik et al., 2003; Kolberg et al., 2005). According to enzyme mechanism of ribonucleotide reductases, the Phe residue is firstly hydroxylated, and then further oxidized to a phenoxyl radical, which is coordinated one of the diiron. However, the formation of adduct between phenylalanine and phenoxyl radical observed in this study seems not to follow this mechanism, but LC-MS/MS results obtained in this work and previous literature (Chang et al., 1999) consistently confirmed the formation of the Phe adduct. Therefore further investigation will be required to reveal unknown mechanism of phenyl radical formation precisely.

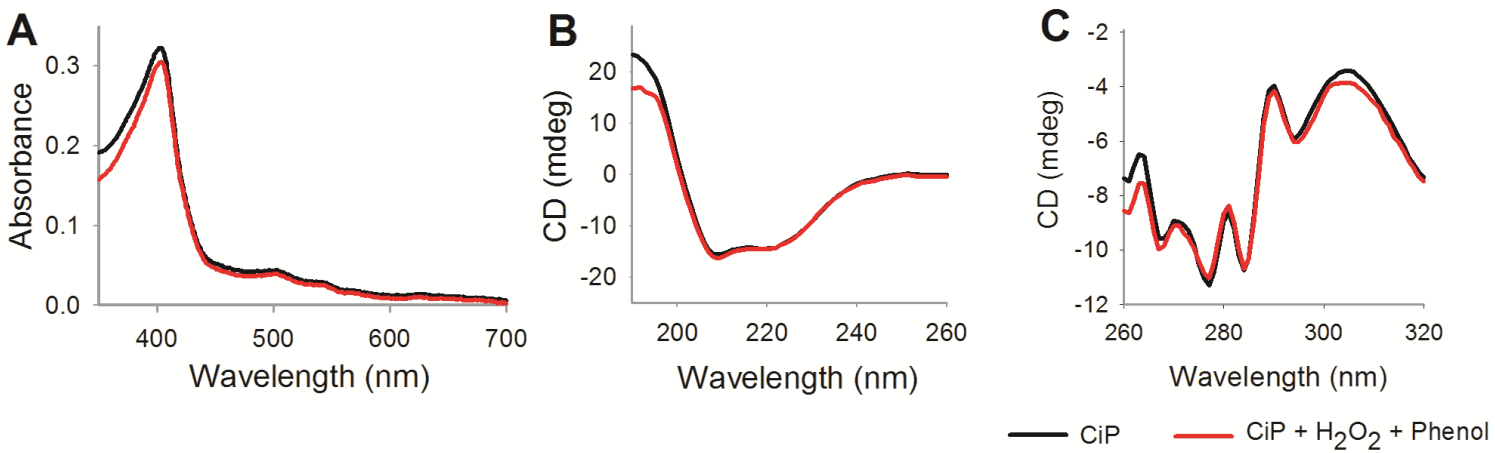

Figure 4-6. UV-Vis absorption and CD spectra of the native (black line) and inactivated CiP (red line). (A) UV-Vis absorption spectra were recorded in the wavelength range of 350-700 nm with a scanning precision of 1 nm. (B) Far-UV CD spectra were measure in the wavelength range of 190 to 260 nm in 1 nm intervals. (C) Near-UV CD spectra were recorded in the range from 260 to 320 nm in 1 nm intervals. Each CD spectrum was the average of 10 scans.

Table 4-9. Percentage of secondary structure elements of native and inactivated CiP.

Secondary structure Content (%)	α-helix	β-strand	Turns	Unordered
Native	42	2	7	49
Inactivated	42	2	7	49

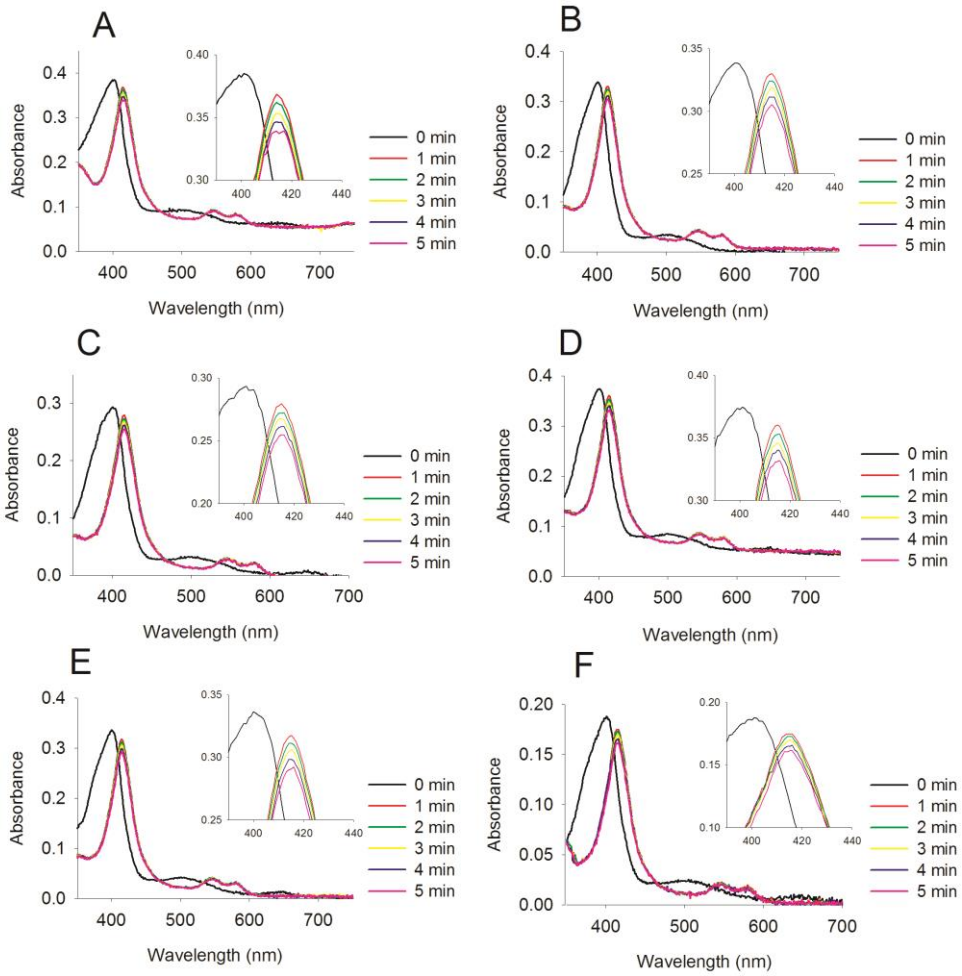

Figure 4-7. Time-dependent UV-Vis absorption spectra of wild-type CiP and F230 series mutants. (A) CiP. (B) F230A. (C) F230I. (D) F230L. (E) F230H. (F) F230W. The wile-type CiP and F230X mutants were treated with 5 mM H_2O_2. UV-Vis absorption spectra were recorded in the the wavelength range of 350-750 nm with a scanning precision of 1 nm.

4. 4 Conclusion

The present work showed that the covalent binding occurs between the phenoxyl radical and F230 residue of CiP during the oxidation reaction of phenol. Additionally, substitution of Phe residue with Ala avoided the radical coupling, and F230A mutation relieved the peroxidase inactivation by radical attack. It was first experimental evidence to reveal the specific radical coupling site, and the Ala substitution is an effective strategy to prevent the radical coupling. A novel strategy combining mass analysis and site-directed mutagenesis successfully identified an amino acid residue susceptible to radical attack and engineered radical-stable mutants. The design of a radical-stable peroxidase, which may be the starting point for engineering peroxidases against radical attack. Furthermore, the experimental results implied that the radical coupling with specific residue, especially Phe residue, is critical point in the radical-mediated peroxidase inactivation.

The radical coupling had no significant effect on the structure of peroxidase, which means that the peroxidase inactivation is accompanied with alternative mechanism rather than the structure destruction of enzyme. It was considered as alternative mechanism that the covalently bound phenoxyl radical bocks the entrance of the active site and limits the substrate access by the steric hindrance.

CHAPTER 5

ENGINEERING A HORSERADISH PEROXIDASE C STABLE TO RADICAL ATTACKS BY MUTATING MUTIPLE RADICAL COUPLING SITES

5. 1 Introduction

Peroxidases (EC 1.11.1.7) catalyze the oxidation of a wide variety of substrates, using hydrogen peroxide or other peroxides (Dunford, 1999). Peroxidases have a broad range of industrial applications in bioremediation, waste-water treatment, organic and polymer synthesis, food industry, pharmaceuticals industry, diagnostics and biosensors (Azevedo et al., 2003; Carlos Regalado et al., 2004). One of the major applications of peroxidases is in polymer synthesis (Hollmann and Arends, 2012). Specifically, horseradish peroxidase (HRP) has been extensively studied as a biocatalyst for the free radical polymerization of a variety of aromatic substrates (Gross et al., 2001). Within the environmental industry, HRP has been exploited to remove aromatic pollutants, such as phenolic compounds and azo dyes from wastewater, sediments and soil (Bhunia et al., 2001; Gholami-Borujeni et al., 2011; Wagner and Nicell, 2002). The chemical industry has also used HRP to synthesize a number of organic polymers (Dordick, 1992). For example, HRP can catalyze the synthesis of useful polymers such as polycardanol, polyanilline and poly(tyrosine)s (Fukuoka et al., 2002; Jin et al., 2001; Won et al., 2004). However, the rapid inactivation of HRP during oxidative polymerization of the phenolic compound often impedes its applications in industrial processes (Baynton et al., 1994; Nakamoto and Machida, 1992).

It is known that HRP is oxidized by hydrogen peroxide and then reduced to the native state via two sequential reduction steps involving the formation of two intermediates, Compounds I and II

(Jones, 2001). Compounds I and II accept one electron from an aromatic compound (AH_2) and generate a free radical product ($AH^{\bullet}$), and polyaromatic products can be formed from this radical product by polymerization. The crystal structure of HRPC revealed a hydrophobic patch of three phenylalanine residues (Phe68, Phe142, and Phe179) near the exposed heme edge, which is responsible for the superior ability of HRPC to form stable 1:1 complexes with aromatic substrates and product radicals (Gajhede et al., 1997).

Three possible mechanisms have been proposed for HRP inactivation during the oxidative polymerization of aromatic substrates: 1) reaction of HRP intermediates with hydrogen peroxide, 2) adsorption of HRP on polymeric products, and 3) attack of free radicals on HRP (Klibanov et al., 1983; Nakajima and Yamazaki, 1987; Nakamoto and Machida, 1992). Mechanism 1 involves the formation of the catalytically inactive intermediate of HRP, Compound III, from the reaction of Compound II with excess hydrogen peroxide (Nakajima and Yamazaki, 1987). In mechanism 2, the adsorption of HRP on precipitated polymeric products can gradually occlude the active sites of HRP and lead to inactivation of HRP (Nakamoto and Machida, 1992). Finally, the third mechanism involves the attack of free radicals on heme or polypeptide chains (Klibanov et al., 1983), which cause heme destruction (Mao et al., 2013) or the radical coupling of aromatic residues (Chang et al., 1999; Cohen-Yaniv and Dosoretz, 2009). HRP inactivation during the oxidative polymerization can be reduced by optimizing the reaction conditions. Hydrogen peroxide-mediated HRP inactivation can be alleviated by the addition of hydrogen peroxide in several portions (Hollmann and

Arends, 2012) or by the addition of an excess reducing substrate, such as phenol that prevents the formation of the Compound III, via competition with hydrogen peroxide for the same enzymatic form (Compound II) (Arnao et al., 1990; Hiner et al., 1995). In addition, it was found that HRP inactivation can also be mitigated by adding additives such as gelatin and polyethylene glycol (PEG). In particular, PEG can be used as the sacrificial polymer instead of the HRP protein (Mao et al., 2013; Wu et al., 1997).

Protein engineering has been applied to enhance the stability of peroxidases during the oxidation reaction. However, most studies have focused on improving the thermostability or stability against hydrogen peroxide (Morawski et al., 2001; Ryan and O'Fágáin, 2007). Despite evidence of HRP inactivation by radical coupling (Chang et al., 1999; Cohen-Yaniv and Dosoretz, 2009), there has been no report on engineering peroxidases' stability against radical-mediated inactivation.

In this study, a stable HRPC mutant against radical attack was developed based on a novel protein engineering strategy. HRPC incubation with hydrogen peroxide and phenol revealed that HRPC is predominantly inactivated to a larger extent by radical attack than by the action of hydrogen peroxide. Next, radical-vulnerable Phe residues were identified using mass spectrometry analysis of phenol-inactivated HRPC. Site-directed mutagenesis of four Phe residues resulted in a radical-robust quadruple mutant. High conservation of these Phe residues in homologous peroxidases implies similar radical inactivation of other peroxidases.

5. 2 Materials and Methods

5. 2. 1 Materials

All chemicals of analytical reagent grade or higher quality were purchased from Sigma-Aldrich (USA), unless otherwise stated. HPLC grade water and methanol were obtained from Burdick & Jackson (USA). Plasmid pET-21a and the BugBuster® Protein Extraction Reagent were purchased from Novagen (USA). Sequencing grade modified trypsin was purchased from Promega (USA). Soybean peroxidase (SBP), lactoperoxidase (LPO), and horseradish peroxidase isozyme A2 (HRP A2) were obtained from Sigma-Aldrich.

5. 2. 2 Expression of recombinant HRPC

The HRPC gene was synthesized by GenScript (USA). Site-directed mutagenesis of HRPC was conducted using mutational primers as previously described (Ho et al., 1989) (Table 5-1). The HRPC and mutated genes were cloned into pET21a, and transformed into the expression host, *E. coli* strain BL21 (DE3). *E. coli* was cultured in Luria-Bertani medium containing 50 μg/mL ampicillin until an OD_{600} of 0.6–0.8 was reached. Subsequently, protein expression was induced with 1 mM isopropyl-β-d-thiogalactopyranoside, and cultures were further incubated for 6 h. Cells were harvested by centrifugation at 10,000 *g* for 10 min at 4 °C.

5. 2. 3 Refolding of inclusion body and purification

Inclusion bodies (IB) were isolated using the BugBuster® Protein Extraction Reagent according to the manufacturer's instructions. Briefly, harvested cells were subsequently lysed using BugBuster reagent with benzonase nuclease. IB were collected by centrifugation and washed three times with 1:10 diluted BugBuster reagent. The washed IB were solubilized in 20 mM Tris-HCl (pH 8.0)/8 M urea. Refolding of recombinant HRPC (0.1 mg/mL) was carried out in refolding solution containing 20 mM Tris-HCl (pH8.0)/1.8 M urea/5 mM $CaCl_2$/20 μM bovine hemin/0.6 mM oxidized glutathione. Proteins were allowed to fully refold at 4 °C overnight. Subsequently, the refolded proteins were dialyzed twice against 20 mM Tris-HCl (pH 8.0) containing 1 mM $CaCl_2$, and insoluble material was removed by centrifugation at 16,000 *g* for 20 min. Refolded protein was loaded onto an anion-exchanged column (Mono Q® 5/50GL; ÄKTA FPLC System; GE Healthcare, USA) equilibrated with 20 mM Tris-HCl (pH 8.0), and elution was carried out using a linear NaCl gradient in the same buffer. The purified peroxidase was used for further enzymatic assays. Purified HRPCs showed RZ (A_{404}/A_{280}) values between 3.0 and 3.5. The protein concentration was determined by Bradford assay using a bovine serum albumin as the standard.

5. 2. 4 Peroxidase activity assay

Peroxidase activity was measured using 2,2'-azino-bis(3-ethylbenzthiazoline-6-sulphonic acid) (ABTS) as a substrate. An enzyme reaction was initiated by adding 50 μL of HRPC solution from the reaction mixture of phenol oxidation to 2 mL of reaction mixture (0.5 mM ABTS and 2.9 mM H_2O_2 in phosphate-citrate buffer, pH 5.0) and change in absorbance at 420 nm ($\mathcal{E}$ = 36,000 $M^{-1}cm^{-1}$) was monitored using UV-Vis spectrometry (Shimadzu, Japan) at room temperature. Kinetic parameters of HRPCs were determined by varying the concentration of guaiacol (0.1 to 1.5 mM), at fixed concentrations of hydrogen peroxide (200 μM) and HRPC (2 nM). The k_{cat} and K_m values were determined from initial velocity data and plotted as a function of substrate concentration. The molar extinction coefficient of guaiacol is 26,600 $M^{-1}cm^{-1}$ at 460 nm (Ozaki and Ortiz de Montellano, 1995).

5. 2. 5 Mass spectrometry analysis

Purified HRPC (12.5 nM) was incubated with 18 mM phenol and 18 mM H_2O_2 in 25 mL of 0.1 M phosphate buffer (pH 7.0). Reaction mixture was incubated for 40 min at room temperature with gentle stirring and centrifuged for 20 min at 13,000 g to remove polymerized precipitates. Subsequently, HRPC was precipitated using the acetone precipitation method. The HRPC precipitate was run on a 10% (w/v) SDS-PAGE gel, and the gel was stained with

colloidal Coomassie Brilliant Blue G-250 for 30 min. The protein band containing HRPC (35 kDa) was excised and digested with trypsin, as previously described (Gobom et al., 1999). The gel slice was washed 4–5 times with 200 μL of 1:1 acetonitrile/ 25 mM ammonium bicarbonate (pH 7.8) until it became clear. The gel slice was dried in a Speedvac concentrator, and then rehydrated in 30 μL of 25 mM ammonium bicarbonate (pH 7.8) containing 20 ng of trypsin. After incubation at 37 °C for 20 h, trypsin-digested peptides remaining in the gel matrix were extracted for 40 min at 30 °C with 20 μL of 50 % (v/v) aqueous acetonitrile containing 0.1 % (v/v) formic acid. The supernatant was evaporated in a Speedvac concentrator, and dissolved in 2 μL of 5% (v/v) aqueous acetonitrile solution containing 0.1 % (v/v) formic acid for mass spectrometric analysis. The peptides were analyzed by liquid chromatography-tandem mass spectrometry (LC-MS/MS) (ProteomTech Inc., Korea).

5. 2. 6 Spectroscopic analysis of HRPC

Purified HRPC was diluted to approximately 5 nM in 0.1 mM phosphate buffer (pH 7.0) and treated with 0.5 mM phenol or 0.5 mM hydrogen peroxide for 20 min at room temperature. After centrifugation at 13,000 *g* for 20 min to remove polymerized precipitates, the supernatant was filtered and concentrated. The spectral changes of HRPC were recorded in the range of 350–700 nm by a UV-Vis spectrophotometer (Multiskan GO; Thermo Scientific, USA). Circular dichroism (CD) spectra were obtained with 1 mg/ml

of sample protein and recorded on a J-815 CD spectropolarimeter (150-L Type; Jasco Inc., Japan) in 1 mM potassium phosphate (pH 7.0) at room temperature. Spectra of the far-UV, 190–260 nm, were measured using a quartz cell with 1 mm optical path length. Measurements were taken every 1 nm at a scan rate of 50 nm/min. The secondary structure percentages were analyzed using the CDSSTR algorithms at Dichroweb (http://www.cryst.bbk.ac.uk/cdweb/html/home.html) (Whitmore and Wallace, 2004).

5. 2. 7 Turnover capacity and radical stability

Phenol oxidation was initiated by adding hydrogen peroxide (0.5 mM of final concentration) to the reaction solution in 100 mM phosphate buffer (pH 7.0) containing 0.5 mM phenol and 0.5 nM peroxidases, and samples were withdrawn every 5 min to measure the concentration of residual phenol and determine residual peroxidase activity using ABTS as described above. Samples at each time were centrifuged for 15 min at 13,000 *g* to remove the polymerized precipitates. The supernatant was subjected to HPLC (Agilent model 1200 liquid chromatograph; Agilent Technologies, USA) with a diode-array detector working at 280 nm. Analysis was carried out using a Zorbax XDB-C18 column (150 × 0.3 mm, 3.5 m; Agilent Technologies) at 25 °C with a mobile phase of 0.3 % (v/v) acetic acid (70 %) and methanol (30 %) at a flow rate of 1.0 mL/min. The concentration of phenol was quantified using calibration curves prepared from external standards. The turnover capacity was

expressed as a ratio of exhausted phenol (ΔS) per enzyme consumed (ΔE) during a 20 min reaction.

5. 2. 8 Molecular docking simulation

Molecular docking simulations for HRPCs with a phenol molecule were performed using Discovery Studio (version 3.1; Accelrys Inc., USA). The structure of HRPC (PDB code: 2ATJ) was downloaded from the Protein Data Bank (http://www.rcsb.org), and a phenol molecule was constructed using the Fragment Builder tools of Discovery Studio. The wild-type and the quadruple mutant F68A/F142A/F143A/F179A of HRPC were simulated. The structure of the quadruple mutant was modeled in a SCRWL 3.0 program based on the combination of rotamer libraries (Canutescu et al., 2003). The CHARMM force field was applied to the molecules, and the CDOCKER module was used for molecular docking simulation. For docking the HRPC proteins, the initial position of the phenol molecule was aligned to the benzohydroxamic acid (BHA) of the wild-type HRPC (2ATJ), and the BHA was removed for further simulations. All possible complexes of HRPC mutants-phenol were generated. Residues within 8 Å from the initial docking position of the wild-type and corresponding sites on the mutant were selected for the binding site, and the other residues of the peroxidases were fixed. The molecular docking simulations were performed with the default parameters of the CDOCKER module. The top 10 hits with the lowest docking scores were selected for calculating the binding

free energy of the complexes. The binding free energy of the complexes was calculated using a Discovery Studio protocol with default parameters. The complex of HRPCs and a phenol molecule with the lowest binding free energy was used as the modeled docking structure for the structure analysis. The binding distance for HRPC was determined by calculating the distance between the εN atom of a His residue known as a catalytic residue (His42) (Rodriguez-Lopez et al., 1997), and the reactive OH group of phenol using the modeled structures of the complex.

5. 2. 9 Protein modeling of horseradish peroxidase isoenzyme A2

Arabidopsis Thaliana peroxidase isoenzyme A2 (ATP A2) shares a 93 % sequence identity with HRP A2 (UniProtKB: P80679.1). The crystal structure of ATP A2 (PDB code: 1PA2) was used as a template for the homology modelling of HRP A2. The structure of mature HRP A2 was modeled using the Fold and Function Assignment System server (Jaroszewski et al., 2005). The homology-modeled structure of HRP A2 contains heme and porphyrin molecules imported from the template.

Table 5-1. Primers used for site-directed mutagenesis of HRPC.

Primer	Sequence	Mutation sequence[a]	Mutation
Mutagenic primers	M1-F	5′- CGCACCGAAAAAGATGCGGCGGGCAACGCGAACAGCGCG-3′	F68A
	M1-R	5′- CGCGCTGTTCGCGTTGCCCGCCGCATCTTTTTCGGTGCG-3′	
	M2-F	5′- GCGAACCTGCCGGCGCCGGCGTTTACCCTGCCGCAGCTG-3′	F142A
	M2-R	5′- CAGCTGCGGCAGGGTAAACGCCGGCGCCGGCAGGTTCGC-3′	
	M3-F	5′- AACCTGCCGGCGCCGTTTGCGACCCTGCCGCAGCTGAAA-3′	F143A
	M3-R	5′- TTTCAGCTGCGGCAGGGTCGCAAACGGCGCCGGCAGGTT-3′	
	M4-F	5′- GGCAAAAACCAGTGCCGCGCGATTATGGATCGCCTGTAT-3′	F179A
	M4-R	5′- ATACAGGCGATCCATAATCGCGCGGCACTGGTTTTTGCC-3′	
	M5-F	5′- GCGAACCTGCCGGCGCCGGCGGCGACCCTGCCGCAGCTGAAA-3′	F142AF143A
	M5-R	5′- TTTCAGCTGCGGCAGGGTCGCCGCCGGCGCCGGCAGGTTCGC-3′	
Flanking primers	5′ *Nde*I	5′- CATATGCAGCTGACCCCGACCTTT-3′	
	3′ *EcoR*I	5′- GAATTCTTACACAAAATCCACCACT-3′	

[a]Mutated sequences are underlined.

5. 3 Results and Discussion

5. 3. 1 Inactivation of HRPC during the phenol oxidation

HRPC-mediated phenol oxidation reactions were performed to monitor the inactivation of peroxidase during the oxidation reaction of a phenol substrate (Figure 5-1). HRPC retained 70% of the initial activity in the presence of 0.5 mM hydrogen peroxide, whereas HRPC incubated with 0.5 mM phenol and 0.5 mM hydrogen peroxide was completely inactivated within 5 min. The addition of a reducing substrate, phenol, did not reduce but instead accelerated the peroxidase inactivation. This result indicates the presence of a more dominant factor than hydrogen peroxide for HRPC inactivation during the phenol oxidation. Previous studies have suggested the possibility that the phenoxyl radical is associated with the HRPC inactivation (Cohen-Yaniv and Dosoretz, 2009; Huang et al., 2005; Mao et al., 2013). However, there has been no attempt to evaluate the effect of the radical attack on the stability of peroxidases and to engineer radical-robust peroxidases by site-directed mutagenesis.

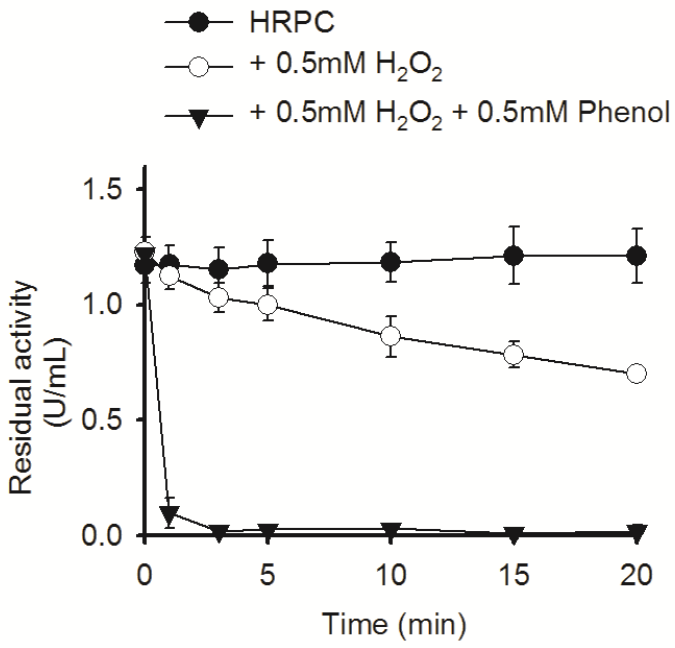

Figure 5-1. Residual activity of HRPC during the oxidation reaction of phenol. HRPC was incubated without phenol and H_2O_2 in the presence of 0.5 mM H_2O_2 and in the presence of 0.5 mM H_2O_2 and 0.5 mM phenol. Samples were withdrawn and the residual activities of HRPC were assayed using ABTS.

5. 3. 2 Peptide modification of HRPC by radical attack

Free radicals can attack and modify proteins. In particular, aromatic amino acids (e.g., phenylalanine, tryptophan, tyrosine and histidine) are known to be vulnerable to radical attacks. Radical species, such as the hydroxyl radical, can undergo an addition reaction to the aromatic rings of aromatic amino acids and form an adduct species (Hawkins and Davies, 2001). If the amino acid residue of HRPC is modified by a phenoxyl radical, HRPC may be predominantly inactivated by the phenoxyl radicals generated during the phenolic oxidation rather than by hydrogen peroxide. To test this hypothesis, the modification of HRPC by phenoxyl radicals was analyzed using mass spectrometry after HRPC-mediated phenol oxidation (Figure 5-2 and Tables 5-2, 5-3 and 5-4). HRPC was incubated in phosphate buffer (0.1 M, pH 7.0) containing 18 mM phenol and 18 mM hydrogen peroxide. The inactivated HPRC was separated from the reaction solution and subjected to LC-MS/MS after tryptic digestion. The modified fragments of inactivated HRPC were RDSLQAFLDLANANLPAPFFTLPQLK (residues 124–149) and FIMDRLYNFSNTGLPDPTLNTTYLQTLR (residues 179–206). Four Phe residues of HRPC i.e., F130, F142, F143, and F179 were modified by a single phenol or phenol oligomers, implying that radical coupling of these Phe residues may be associated with the rapid inactivation of HRPC during phenolic oxidation. In addition, the F142, F143, and F179 residues of HRPC play an important role in the binding affinity of aromatic substrates such as BHA via aromatic–aromatic interactions (Henriksen et al., 1998; Veitch et al., 1997).

Therefore, these Phe residues, vulnerable to modification by phenoxyl radicals, can be engineered to reduce the inactivation of HRPC during the phenolic oxidation.

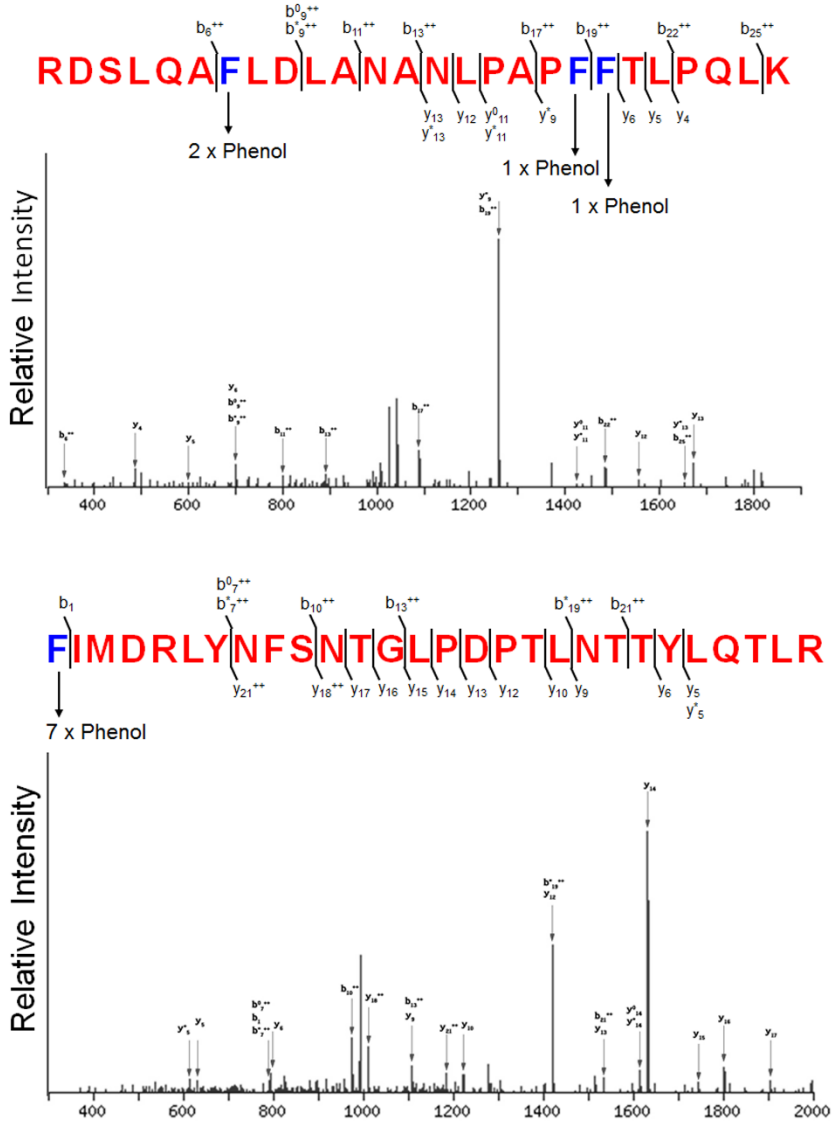

Figure 5-2. LC-MS/MS analysis of peptides from inactivated HRPC. Modified peptides from the inactivated HRPC were analyzed using mass spectrometry after incubation with 18 mM H_2O_2 and 18 mM phenol. MS/MS spectra were acquired from m/z 1151.703 and m/z 1322.777 of trypsin digest fragment of the inactivated HRPC. The primary structure of peptide was derived from de novo sequencing. The modified residue (Phe) with phenol is indicated on the figure.

Table 5-2. Modified residues of HRPC (m/z 1151.703) identified by mass spectrometry.

#	b	b^{++}	b*	b^{*++}	b^{0}	b^{0++}	Seq.	y	y^{++}	y*	y^{*++}	y^{0}	y^{0++}	#
1	157.108	79.058	140.082	70.545			**R**							**26**
2	272.135	136.571	255.109	128.058	254.125	127.566	**D**	3298.591	1649.799	3281.565	1641.286	3280.581	1640.794	**25**
3	359.167	180.087	342.141	171.574	341.157	171.082	**S**	3183.564	1592.286	3166.538	1583.772	3165.554	1583.280	**24**
4	472.251	236.629	455.225	228.116	454.241	227.624	**L**	3096.532	1548.770	3079.506	1540.256	3078.522	1539.764	**23**
5	600.310	300.659	583.283	292.145	582.299	291.653	**Q**	2983.448	1492.228	2966.422	1483.714	2965.437	1483.222	**22**
6	671.347	**336.177**	654.321	327.664	653.337	327.172	**A**	2855.389	1428.198	2838.363	1419.685	2837.379	1419.193	**21**
7	1186.520	593.764	1169.494	585.251	1168.510	584.759	**F**	2784.352	1392.680	2767.326	1384.167	2766.342	1383.675	**20**
8	1299.604	650.306	1282.578	641.793	1281.594	641.301	**L**	2269.179	1135.093	2252.153	1126.580	2251.169	1126.088	**19**
9	1414.631	707.819	1397.605	**699.306**	1396.621	**698.814**	**D**	2156.095	1078.551	2139.068	1070.038	2138.084	1069.546	**18**
10	1527.715	764.361	1510.689	755.848	1509.705	755.356	**L**	2041.068	1021.038	2024.042	1012.524	2023.058	1012.032	**17**
11	1598.753	**799.880**	1581.726	791.367	1580.742	790.875	**A**	1927.984	964.496	1910.957	955.982	1909.973	955.490	**16**
12	1713.780	857.393	1696.753	848.880	1695.769	848.388	**N**	1856.947	928.977	1839.920	920.464	1838.936	919.972	**15**
13	1784.817	**892.912**	1767.790	884.399	1766.806	883.907	**A**	1741.920	871.464	1724.893	862.950	1723.909	862.458	**14**
14	1899.844	950.425	1882.817	941.912	1881.833	941.420	**N**	**1670.883**	835.945	**1653.856**	827.432	1652.872	826.940	**13**
15	2012.928	1006.967	1995.901	998.454	1994.917	997.962	**L**	**1555.856**	778.432	1538.829	769.918	1537.845	769.426	**12**
16	2109.980	1055.494	2092.954	1046.981	2091.970	1046.489	**P**	1442.772	721.890	**1425.745**	713.376	**1424.761**	712.884	**11**
17	2181.018	**1091.012**	2163.991	1082.499	2163.007	1082.007	**A**	1345.719	673.363	1328.693	664.850	1327.709	664.358	**10**
18	2278.070	1139.539	2261.044	1131.026	2260.060	1130.534	**P**	1274.682	637.845	**1257.655**	629.331	1256.671	628.839	**9**
19	2517.165	**1259.086**	2500.138	1250.573	2499.154	1250.081	**F**	1177.629	589.318	1160.603	580.805	1159.619	580.313	**8**
20	2756.260	1378.633	2739.233	1370.120	2738.249	1369.628	**F**	938.535	469.771	921.508	461.258	920.524	460.766	**7**
21	2857.307	1429.157	2840.281	1420.644	2839.297	1420.152	**T**	**699.440**	350.224	682.413	341.710	681.429	341.218	**6**
22	2970.391	1485.699	2953.365	1477.186	2952.381	1476.694	**L**	**598.392**	299.700	581.366	291.187			**5**
23	3067.444	1534.226	3050.417	1525.712	3049.433	1525.220	**P**	**485.308**	243.158	468.282	234.645			**4**
24	3195.503	1598.255	3178.476	1589.742	3177.492	1589.250	**Q**	**388.255**	194.631	371.229	186.118			**3**
25	3308.587	1654.797	3291.560	1646.284	3290.576	1645.792	**L**	**260.197**	130.602	243.170	122.089			**2**
26							**K**	**147.113**	74.060	130.086	65.547			**1**

The matched fragment ions are presented and the ion series were in the upper row. The sequence of matched peptide is shown in 1 letter code and matched values are highlighter in bold.

Table 5-3. Modified residues of HRPC (m/z 1322.777) identified by mass spectrometry.

#	b	b^{++}	b*	b^{*++}	b^{0}	b^{0++}	Seq.	y	y^{++}	y*	y^{*++}	y^{0}	y^{0++}	#
1	**792.259**	396.633					**F**							**28**
2	905.343	453.175					**I**	3173.594	1587.300	3156.567	1578.787	3155.583	1578.295	**27**
3	1052.379	526.693					**M**	3060.510	1530.758	3043.483	1522.245	3042.499	1521.753	**26**
4	1167.406	584.206			1149.395	575.201	**D**	2913.474	1457.241	2896.448	1448.727	2895.464	1448.235	**25**
5	1323.507	662.257	1306.480	653.744	1305.496	653.252	**R**	2798.447	1399.727	2781.421	1391.214	2780.437	1390.722	**24**
6	1436.591	718.799	1419.564	710.286	1418.580	709.794	**L**	2642.346	1321.677	2625.320	1313.163	2624.336	1312.671	**23**
7	1599.654	800.331	1582.628	**791.817**	1581.644	**791.325**	**Y**	2529.262	1265.135	2512.235	1256.621	2511.251	1256.129	**22**
8	1713.697	857.352	1696.671	848.839	1695.687	848.347	**N**	2366.199	**1183.603**	2349.172	1175.090	2348.188	1174.598	**21**
9	1860.766	930.886	1843.739	922.373	1842.755	921.881	**F**	2252.156	1126.582	2235.129	1118.068	2234.145	1117.576	**20**
10	1947.798	**974.402**	1930.771	965.889	1929.787	965.397	**S**	2105.087	1053.047	2088.061	1044.534	2087.077	1044.042	**19**
11	2061.840	1031.424	2044.814	1022.911	2043.830	1022.419	**N**	2018.055	**1009.531**	2001.029	1001.018	2000.045	1000.526	**18**
12	2162.888	1081.948	2145.862	1073.434	2144.878	1072.942	**T**	**1904.012**	952.510	1886.986	943.997	1886.002	943.505	**17**
13	2219.910	**1110.458**	2202.883	1101.945	2201.899	1101.453	**G**	**1802.965**	901.986	1785.938	893.473	1784.954	892.981	**16**
14	2332.994	1167.000	2315.967	1158.487	2314.983	1157.995	**L**	**1745.943**	873.475	1728.917	864.962	1727.933	864.470	**15**
15	2430.046	1215.527	2413.020	1207.014	2412.036	1206.522	**P**	**1632.859**	816.933	**1615.833**	808.420	**1614.849**	807.928	**14**
16	2545.073	1273.040	2528.047	1264.527	2527.063	1264.035	**D**	**1535.806**	768.407	1518.780	759.894	1517.796	759.402	**13**
17	2642.126	1321.567	2625.100	1313.053	2624.116	1312.561	**P**	**1420.780**	710.893	1403.753	702.380	1402.769	701.888	**12**
18	2743.174	1372.091	2726.147	1363.577	2725.163	1363.085	**T**	1323.727	662.367	1306.700	653.854	1305.716	653.362	**11**
19	2856.258	1428.633	2839.231	**1420.119**	2838.247	1419.627	**L**	**1222.679**	611.843	1205.653	603.330	1204.668	602.838	**10**
20	2970.301	1485.654	2953.274	1477.141	2952.290	1476.649	**N**	**1109.595**	555.301	1092.568	546.788	1091.584	546.296	**9**
21	3071.348	**1536.178**	3054.322	1527.665	3053.338	1527.173	**T**	995.552	498.280	978.526	489.766	977.542	489.274	**8**
22	3172.396	1586.702	3155.370	1578.188	3154.386	1577.696	**T**	894.504	447.756	877.478	439.243	876.494	438.751	**7**
23	3335.459	1668.233	3318.433	1659.720	3317.449	1659.228	**Y**	**793.457**	397.232	776.430	388.719	775.446	388.227	**6**
24	3448.544	1724.775	3431.517	1716.262	3430.533	1715.770	**L**	**630.393**	315.700	**613.367**	307.187	612.383	306.695	**5**
25	3576.602	1788.805	3559.576	1780.291	3558.592	1779.799	**Q**	517.309	259.158	500.283	250.645	499.299	250.153	**4**
26	3677.650	1839.329	3660.623	1830.815	3659.639	1830.323	**T**	389.251	195.129	372.224	186.616	371.240	186.124	**3**

The matched fragment ions are presented and the ion series were in the upper row. The sequence of matched peptide is shown in 1 letter code and matched values are highlighter in bold.

Table 5-4. LC-MS/MS analysis of peptide from native and inactivated HRPC.

Peroxidase	Observed peak (m/z)	Molecular weights (Da)		Sequence and modification
		Expected	Calculated	
Native	1,372.974	2,743.933	2,743.459	DSLQAFLDLANANLPAPFFTLPQLK
	697.389	696.382	696.327	FIMDR
Inactivated	1,151.703	3,452.088	3,453.685	RDSLQAFLDLANANLPAPFFTLPQLK 2F with 1xPhenol,F with 4xPhenol
	1,322.777	3,965.308	3,963.838	FIMDRLYNFSNTGLPDPTLNTTYLQTLR F with 7xPhenol

5. 3. 3 Effect of radical modification on structure of HRPC

The effect of the phenoxyl radical reaction to HRPC due to the structural change of HRPC was investigated using the UV-Vis and CD spectral methods. Soret band absorption (350–700 nm) and CD spectra in the far-UV region (190–260 nm) were measured to analyze the changes in the heme pocket (Brems and Stellwagen, 1983) and secondary structures of HRPC (Norma, 2006), respectively. The absorbance spectra of HRPC in the absence and presence of phenol and hydrogen peroxide are shown in Figure 5-3. The UV/Vis spectrum of HRPC in the absence of phenol and hydrogen peroxide had a Soret maximum at 401 nm and two smaller maxima at 499 and 640 nm corresponding to peroxidase in its resting state (Strickland et al., 1968). After HRPC was incubated with phenol and hydrogen peroxide, the Soret absorbance of the HRPC was unchanged (Figure 5-3. A), indicating that the heme structure of HRPC is intact during the oxidation reaction of phenol. The CD spectra of HRPC in the absence of phenol and hydrogen peroxide showed a double minima at 209 and 222 nm (Figure 5-3, B), which is characteristic of the α-helix-rich structure (Myer, 1968), in agreement with another report for HRPC (Strickland et al., 1968). Following the phenolic oxidation reaction, no substantial change occurred in the far-UV CD band (Figure 5-3. B). The percentages of secondary structural elements calculated using the CDSSTR program (Johnson, 1999) are summarized in Table 5-5. No significant change in the α-helical content and other secondary structures of HRPC was observed. Based on these results, it can be speculated that the native structure of HRPC

is well retained upon radical coupling. This indicates that site-directed mutagenesis of the radical-vulnerable Phe residues can be an effective strategy to rescue HRPC from rapid inactivation, without drastic structural changes in HRPC.

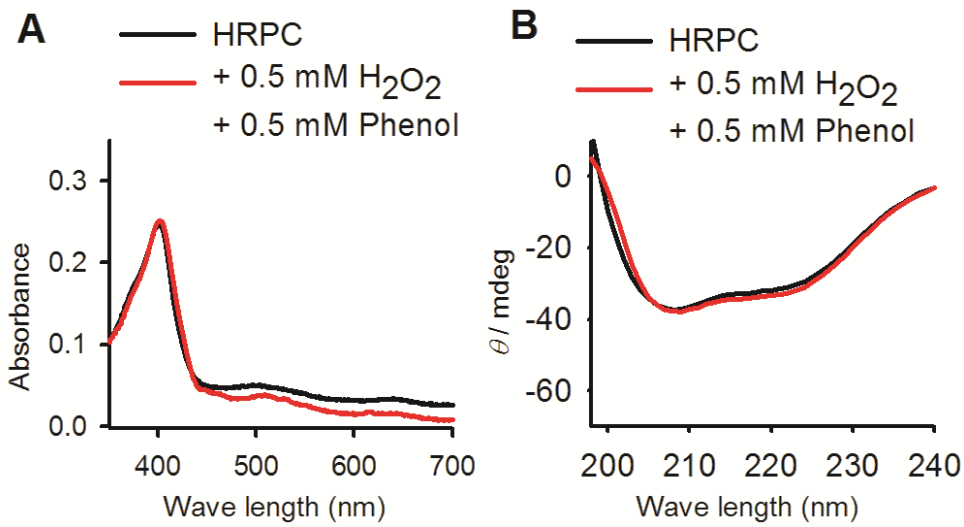

Figure 5-3. UV-Vis and CD spectra of HRPC before and after the phenol oxidation. (A) UV-Vis spectra of HRPC were recorded in the wavelength range of 350–700 nm. (B) Far-UV CD spectra of HRPC were recorded in the range from 190–260 nm. The contents of secondary structure of HRPC were calculated using CDSSTR software.

Table 5-5. Percentages of secondary structure elements of native and inactivated HRPC.

Secondary structure Contents (%)[a]	Native	Inactivated
α helix	42	42
β strand	30	30
Turns	7	7
Unordered	2.1	2.1

[a] The secondary structure contents of inactivated HRPC were calculated using the CDSSTR program.

5. 3. 4 Improving the radical stability of HRPC by site-directed mutagenesis of multiple Phe residues

Four Phe residues were substituted with a small hydrophobic residue, alanine, to design more radical-robust mutants by avoiding the modification by the phenoxyl radical. Four single mutants (F130A, F142A, F143A, and F179A) were constructed by site-directed mutagenesis. However, these Ala mutants exhibited no improvement in HRPC stability and phenol consumption during the phenol oxidation reaction (Figure 5-4 and Table 5-7), implying that elimination of single radical coupling site have no significant effect on the radical stability of HRPC due to the presence of other radical coupling sites in the active site. Therefore, multiple sites were mutated at the same time to investigate redundancy. The double mutant (F142A/F143A) and the triple mutant (F142A/F143A/F179A) could not maintain their peroxidase activity upon the phenol/hydrogen peroxide reaction (Figure 5-5). All Phe residues detected by LC-MS/MS analysis were mutated to Ala residues and the effect of this mutation was assessed. The F130A/F142A/F143A/F179A mutant exhibited marginal improvement in HRPC stability (Figure 5-5). This result suggests the presence of additional radical coupling sites not detected by our LC-MS/MS analysis, which are critical in HRPC inactivation in the phenol oxidation reaction.

In HRPC, Phe142, Phe143, and Phe179, are located at the entrance to the active site, and Phe130 is located at the enzyme surface, distant from the active site (Gajhede et al., 1997). Although our LC-

MS/MS analysis did not detect the modification of F68 by a phenoxyl radical, it might be a good idea to mutate F68 also located in the substrate-binding site of HRPC (Figure 5-6) (Henriksen et al., 1998). However, the F68A mutant was also completely inactivated within 10 min (Figure 5-4) and showed lower phenol-consumption rates and turnover capacities than the wild-type (Table 5-7), as other single mutants. Hence, the other quadruple mutant containing all single mutation sites located at the entrance to the active site was further constructed. Specific activities of the HRPC wild-type and quadruple mutant (F68A/F142A/F143A/F179A) towards ABTS were summarized in Table 5-6. Specific activities of the wild-type and quadruple mutant were 230 and 72 U/mg, respectively. The decrease was about 0.3-fold for the quadruple mutant for ABTS.

The quadruple mutant (F68A/F142A/F143A/F179A) retained 41% of its initial activity after 10 min of incubation and consumed almost 94% of the initial phenol to produce a phenol polymer (Figure 5-4). In addition, the F68A/F142A/F143A/F179A mutant exhibited a 1.7-fold and 17-fold higher turnover capacity compared with the wild-type and F130A/F142A/F143A/F179A mutant, respectively (Table 5-7). Although the radical coupling sites can be widely distributed in HRPC, the high stability of radical coupling site-eliminated mutant (F68A/F142A/F143A/F179A) alluded to radical coupling between the peroxidase and phenolic substrate in the active site being a critical cause of peroxidase inactivation during the oxidation reaction of the phenolic compound.

In addition, the radical binding sites of HRPC were F130, F142, F1143A and F179A, but F130A/F142A/F143A/F179A mutant

showed no effect on the peroxidase stability (Figure 5-5). When the all Phe residues at the entrance of active site (F68A, F142A, F143A, F179A) were changed to Ala, the stability of HRPC was increased (Figure 5-4). It implies the position of radical biding site is crucial for the peroxidase inactivation, and supports the phenoxyl radical bound to Phe residues at the entrance of the active site blocks the access of substrate and, consequentially, leads the peroxidase inactivation.

Table 5-6. Enzymatic specific activity of the in-vitro refolded recombinant HRPC and mutant.

Enzyme	Specific activity (U/mg)
HRPC	230
F68A/F142A/F143A/F179A	72

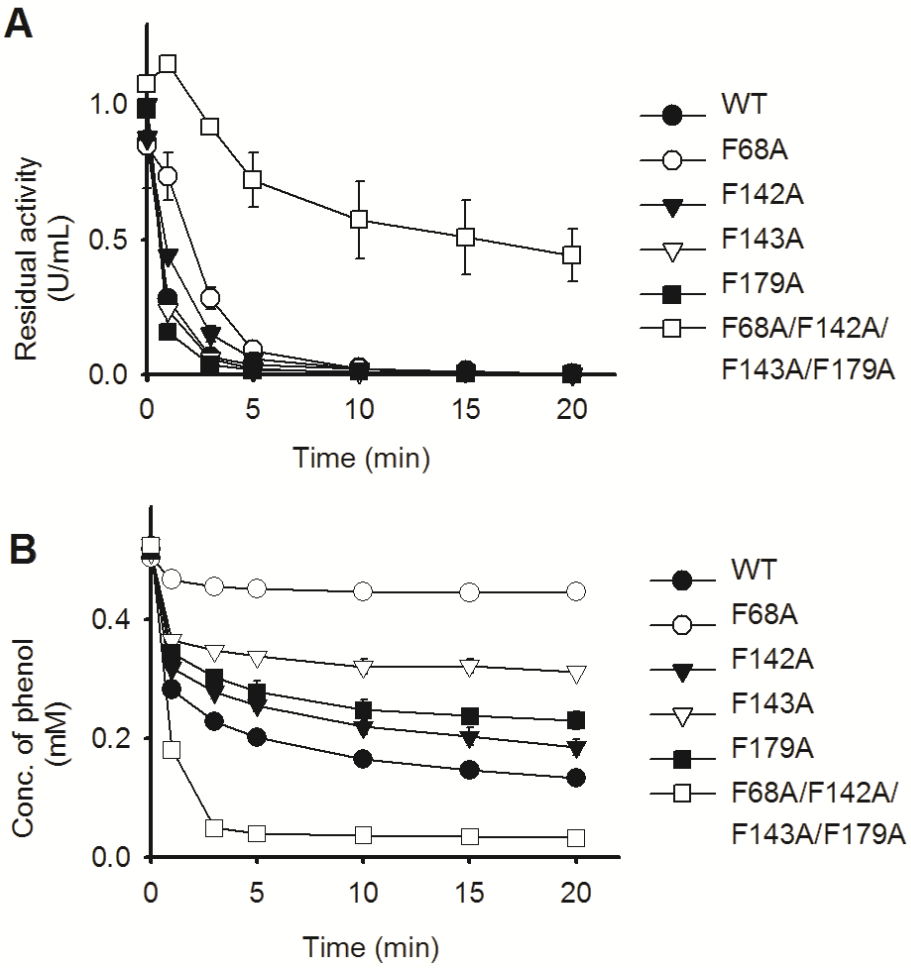

Figure 5-4. The stability of HRPC mutants during the oxidation reaction of phenol. (A) Residual activity of the HRPC wild-type (WT) and mutants. (B) Removal of phenol by the HRPC wild-type (WT) and mutants. The residual peroxidase activity was assayed using ABTS and the phenol concentrations were determined by HPLC.

Table 5-7. Turnover capacity of HRPC wild-type and mutants.

Peroxidase	Turnover capacity[a] (mM/U) (fold increase)
HRPC	0.46 (1.0)
F68A	0.06 (0.1)
F130A	0.09 (0.2)
F142A	0.39 (0.8)
F143A	0.20 (0.4)
F179A	0.30 (0.7)
F130A/F142A/F143A/F179A	0.06 (0.1)
F68A/F142A/F143A/F179A	0.78 (1.7)

[a]The turnover capacity is expressed as the ratio of exhausted phenol (mM) per consumed enzyme activity for 30 min of phenol oxidation reaction. Values are the means of three separate determinations.

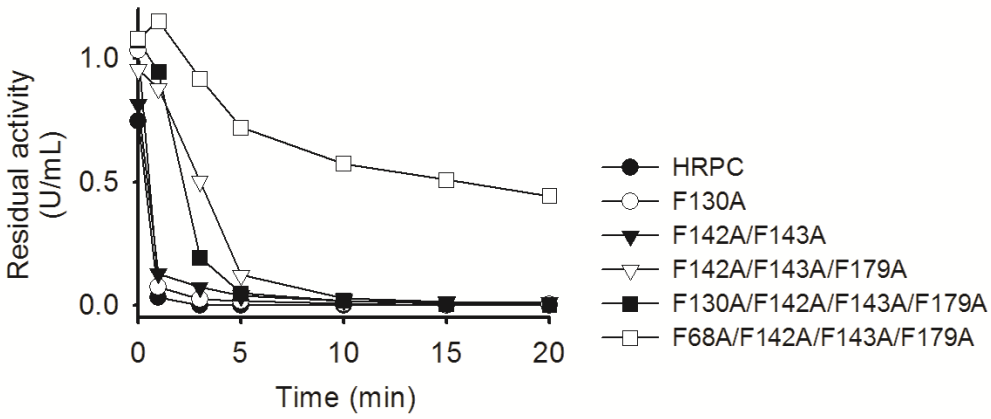

Figure 5-5. Residual activity of HRPC wild-type and mutants. Peroxidases were incubated with 0.5 mM H_2O_2, and 0.5 mM phenol in 0.1 M phosphate buffer (pH 7.0). Samples were withdrawn and the residual activities of the peroxidases were assayed using ABTS.

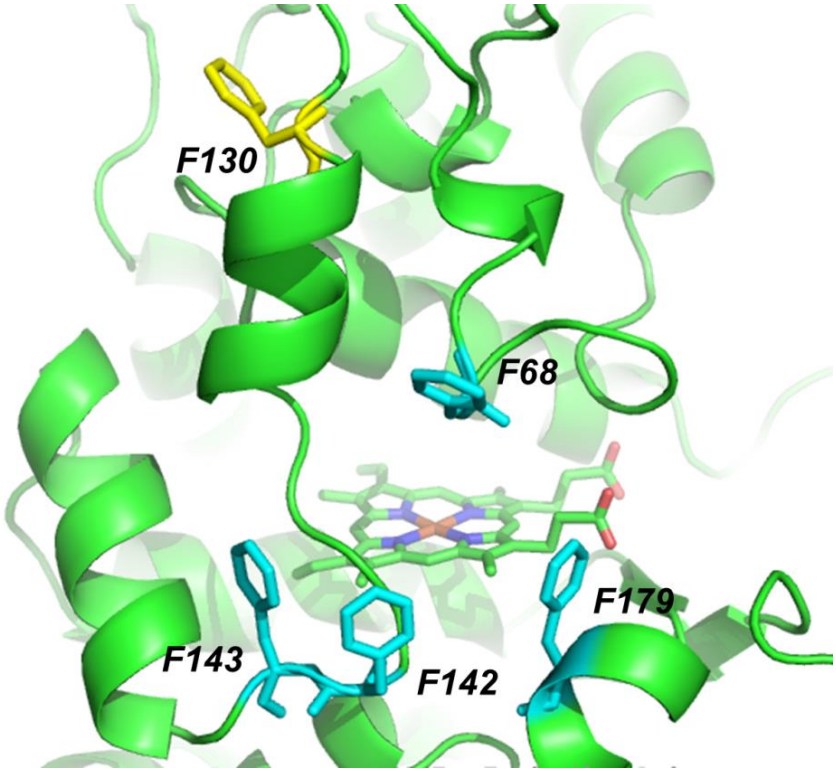

Figure 5-6. The Phe residues of HRPC. The Phe residues modified with phenoxyl radicals were F130, F142, F143, and F179. F68, F142, F143, and F179 were located in the substrate-binding site of HRPC.

5. 3. 5 Kinetic characterization of HRPC wild-type and mutants

A kinetic study was performed using guaiacol as the phenolic substrate. The kinetic parameters of the HRPC wild-type and mutants are summarized in Table 5-8. The kinetic parameters (K_m and k_{cat}) of the wild-type were 0.966 mM and 1.44 s^{-1}, respectively. Compared with the wild-type HRPC, the F130A mutant exhibited no differences in the kinetic parameters (0.966 mM and 1.41 s^{-1}), but the other four single mutants had higher K_m values (F68A: 1.06 mM, F142A: 2.04 mM, F143A: 1.72 mM, and F179A: 1.82 mM) and comparable k_{cat} values for guaiacol. Two quadruple mutants (F130A/F142A/F143A/F179A and F68A/F142A/F143A/F179A) showed much higher K_m values (2.16 mM and 2.69 mM). This result is consistent with the high dissociation constant (K_d) of the site-directed HRPC mutants F68A, F142A, F143A, and F179A for BHA found in previous studies (Gilfoyle et al., 1996; Veitch et al., 1997; Veitch et al., 1995). Except for the F230A mutant, the catalytic efficiency (k_{cat}/ K_m) of all HRPC mutants characterized in this study was lower than that of the wild-type due to high K_m values. In particular, the most radical-robust quadruple mutant (F68A/F142A/F143A/F179A) exhibited 0.6-fold lower catalytic efficiency than the wild-type (0.858 $mM^{-1}s^{-1}$ vs. 1.49 $mM^{-1}s^{-1}$). The kinetic study revealed that four Phe residues (F68, F142, F143, and F179) in the active site cooperatively contribute to the binding of aromatic substrates, elucidating the vulnerability of the F142, F143, and F179 residues to the radical modifications and high radical

stability of the quadruple mutant (F68A/F142A/F143A/F179A) (Figure 5-4. A). Moreover, the F130 residue distant from the active site is not involved in enzyme catalysis, i.e., substrate binding and thus, the modification of the F130 residue by a phenoxyl radical could not significantly affect the radical stability of the HRPC mutants (F142A/F143A/F179A vs. F130A/F142A/F143A/F179A) (Figure 5-5).

Table 5-8. Kinetic parameters of the HRPC wild-type and mutants.

Enzyme	K_m (mM)	k_{cat} (s^{-1})	k_{cat}/K_m ($mM^{-1}s^{-1}$)
HRPC	0.966 ± 0.0390	1.44 ± 0.0391	1.49 ± 0.0557
F68A	1.06 ± 0.0178	0.952 ± 0.222	0.897 ± 0.0134
F130A	0.966 ± 0.0151	1.41 ± 0.0234	1.46 ± 0.0147
F142A	2.04 ± 0.132	1.24 ± 0.118	0.608 ± 0.0426
F143A	1.72 ± 0.0945	1.55 ± 0.0794	0.896 ± 0.188
F179A	1.82 ± 0.0355	1.83 ± 0.058	1.01 ± 0.0128
F130A/F142A/F143A/F179A	2.16 ± 0.165	2.09 ± 0.0613	1.07 ± 0.0300
F68A/F142A/F143A/F179A	2.69 ± 0.177	2.30 ± 0.117	0.858 ± 0.0118

Values are the means of three separate determinations, and show the ± standard deviation of these means.

5. 3. 6 Molecular docking simulation of HRPC wild-type and quadruple mutant

Molecular docking simulations were performed for both wild-type HRPC and the quadruple mutant F68A/F142A/F143A/F179A. The docking simulations supported the importance of the aromatic residues for binding of the phenol molecule (Figure 5-7). The quadruple mutant had a greater binding distance (6.1 Å) and higher binding energy (-21.6 kcal/mol) than the wild-type (2.1 Å and -37.6 kcal/mol, respectively) (Table 5-8). The mutations of aromatic residues at the entrance to the heme pocket of HRPC can lead to a decreased binding affinity for aromatic substrates because of the disruption of aromatic–aromatic interactions between HRPC and substrates. According to the docking results, four Phe residues may form an aromatic–aromatic interaction with not only phenol but also with phenoxyl radicals.

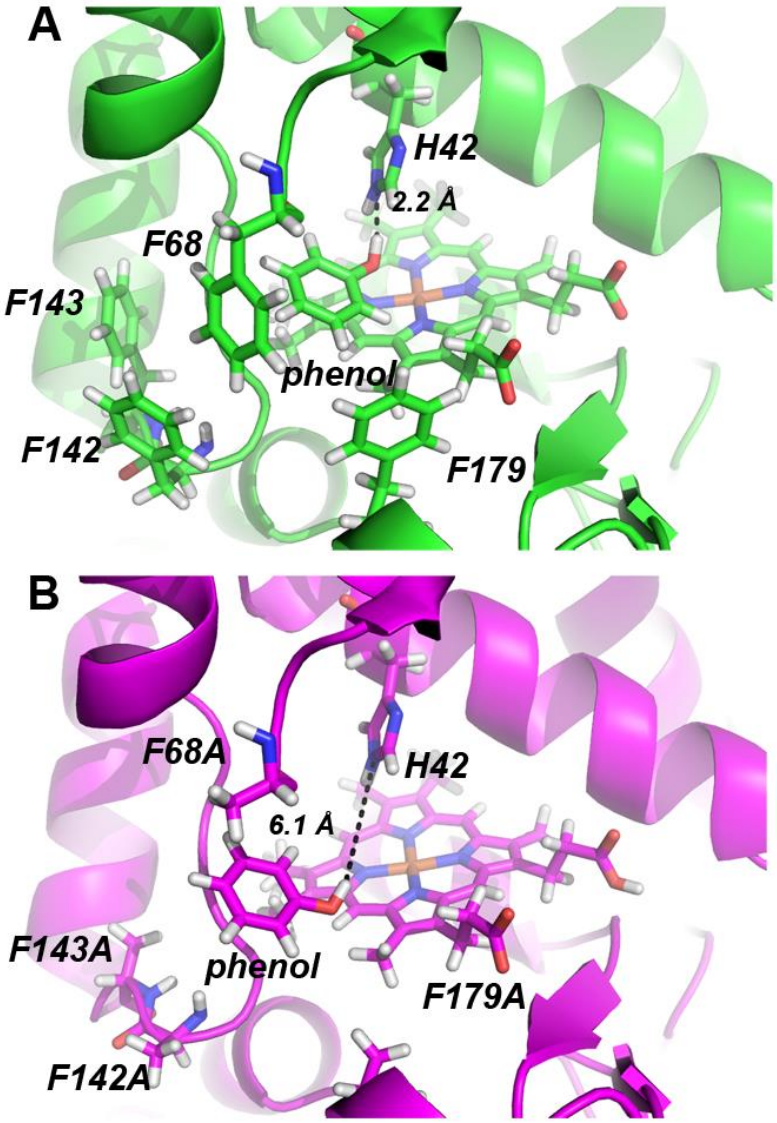

Figure 5-7. The modeled complexes of HRPCs and a phenol molecule. (A) The modeled complex of the HRPC wild-type with a phenol molecule. (B) The modeled complex of the HRPC quadruple mutant (F68A/F142A/F143A/F179A) with a phenol molecule. Each distance indicates the distance between the εN atom of the catalytic His residue (His42) and the OH group of a phenol molecule.

Table 5-9. The calculated binding free energy of the modeled complexes of the HRPC wild-type and mutant.

Enzyme	Binding free energy [a] (kcal mol^{-1})	Distance (Å)
wild-type	-37.6	2.2
F68A/F142A/F143A/F179A	-21.6	6.1

[a] The binding free energy of complexes was calculated by protocol of Discovery Studio 3.1.

5. 3. 7 Highly conversed Phe residues in homologous peroxidases

The radical stabilities of SBP, LPO, and HRP A2 were measured to investigate whether other peroxidases also exhibit rapid inactivation. As shown in Figure 5-8. A, SBP, LPO, and HRP A2 were also dramatically inactivated during the phenol oxidation reaction. Structural comparisons of the three peroxidases clearly showed that all three peroxidases have the Phe residue(s) peripheral to the entrance of the heme pocket, as does HRPC (Figure 5-8. B). Furthermore, sequence alignment of peroxidases revealed that the highly conserved Phe residue(s) in HRPC can also be found in other homologous peroxidases (Figure 5-9). These results imply that peroxidases may be inactivated during the phenol oxidation reaction by radical modification of the Phe residue(s). Therefore, multiple mutations of radical-vulnerable residues may provide a strategy to improve the radical stability of peroxidases.

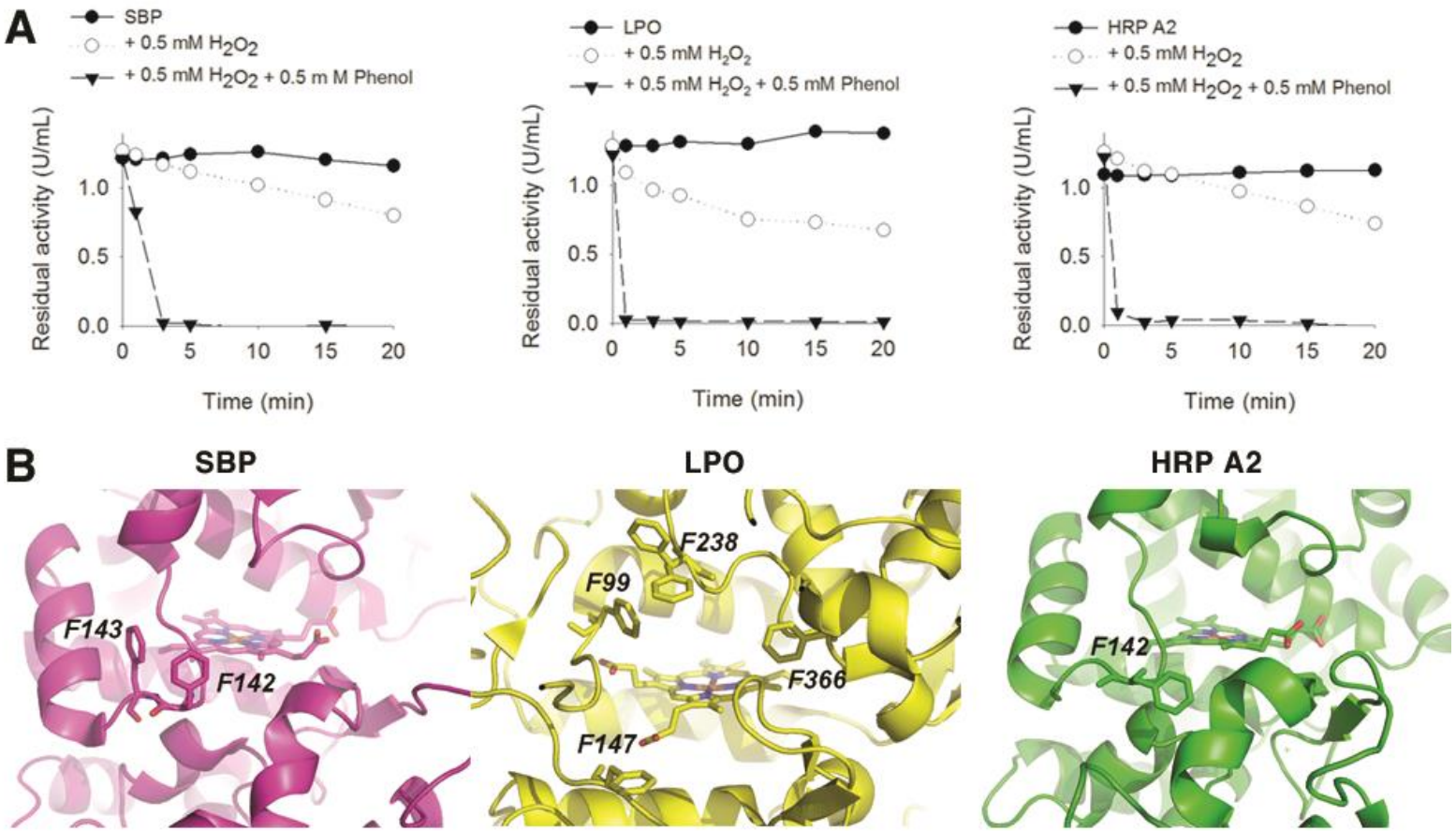
A
SBP
+ 0.5 mM H2O2
+ 0.5 mM H2O2 + 0.5 m M Phenol
Residual activity (U/mL)
Time (min)
LPO
+ 0.5 mM H2O2
+ 0.5 mM H2O2 + 0.5 mM Phenol
Residual activity (U/mL)
Time (min)
HRP A2
+ 0.5 mM H2O2
+ 0.5 mM H2O2 + 0.5 mM Phenol
Residual activity (U/mL)
Time (min)
B
SBP
F143
F142
LPO
F238
F99
F366
F147
HRP A2
F142

Figure 5-8. Radical stability and the conserved Phe residue(s) of SBP, LPO, and HRP A2. (A) Residual activity of SBP, LPO, and HRP A2 during the oxidation reaction of phenol. (B) The conserved Phe residue(s) at the entrance to the heme pocket of peroxidases. The crystal structure of SBP (PDB code: 1FHF) and LPO (PDB code: 3GC1) and the homology-modeled structure of HRP A2 were used for structural comparison.

```
                    *        20         *        40         *        60         *        80         *       100
A. rusticana        : -QLTPTFIDNSCPNVSNIVRDTIVNELRSDPRIAASILRLHFHDCFVNGCDASILLDNTTSFRTEKDAFGNANSARGFPVIDRMKAAVESACPRTVSCAD
A. thaliana         : -QLTPTFYDRSCPNVTNIVRETIVNELRSDPRIAASILRLHFHDCFVNGCDASILLDNTTSFRTEKDRFGNANSARGFPVIDRMKAAVERACPRTVSCAD
E. halophilum       : -QLTPTFYDTSCPSVFNIVRDTIVNELRSDPRIAASILRLHFHDCFVNGCDASILLDNTTSFRTEKDAAPNANSARGFPVIDRMKTAVEAACPRVVSCAD
B. napus            : -QLTPTFYDTSCPNVTNIVRATIVNELRSDPRIAASILRLHFHDCFVNGCDASILLDNTTSFRTEKDAVGNANSARGFPVIDTMKAAVERACPRTVSCAD
R. sativus var. niger : QPLSPDFYSRTCPRVFDIIRRTIVAELRSDPRIAASILRLHFHDCFVNGCDASILLDSSTSFRTEKDAAPNANSARGFDVIDRMKAEIEIACPRTVSCAD
P.  trichocarpa     : -QLTPTFYDQTCPNVSSIIRNVITETLVSDPRIAASLIRLHFHDCFVNGCDGSLLLDNTDTIESEKEAAGNNNSARGFEVVDRMKALLESACPATVSCAD
M. notabilis        : -QLTPTFYNETCPNVTSIVRGVIEGALQTDPRITASLLRLHFHDCFVIGCDGSLLLDNTATIESEKEAGGNNNSVRGFEVVDDIKTALENACPGTVSCAD

                    *       120         *       140         *       160         *       180         *       200
A. rusticana        : LLTIAAQQSVTLAGGPSWRVPLGRRDSLQAFLDLANANLPAPFFTLPQLKDSFRNVGLNRSSDLVALSGGHTFGKNQCRFIMDRLYNFSNTGLPDPTLNT
A. thaliana         : MLTIAAQQSVTLAGGPSWRVPLGRRDSLQAFLELANANLPAPFFTLPQLKASFRNVGLDRPSDLVALSGGHTFGKNQCQFILDRFYNFSNTGLPDPTLNT
E. halophilum       : ILTIAAQQSVNLAGGPSWRVPLGRRDSLQAFFDLSNANLPAPFFTLPQLKASFANVGLDRPSDLVALSGGHTFGKNQCQFIMDRLYNFSNTGLPDPTLNT
B. napus            : MLTIAAQQSVTLAGGPSWRVPLGRRDSLQAFFSLSNDNLPSPFFTLPELKASFGKVGLDRPSDLVALSGGHTFGKNQCQFIIGRLYNFSNTGLPDPTLNT
R. sativus var. niger : VLTIASQISVILSGGPGWQVPLGRRDSLRAFFDLANTALPSPFFTLAQLNASFAAVGLNRPSDLVALSGGHTFGKAQCQFVTPRLYNFNGTNRPDPSLNP
P.  trichocarpa     : ILTIAAEESVVLAGGPNWTVPLGRRDSTTASRAAANASLPAPFLTLDQLRESFTNVGLNNNTDLVALSGAHTFGRAKCSTFDFRLFDFNRTGAPDPSMDT
M. notabilis        : ILAIAAEESVNLSSGPSWTVRLGRRDSLIANRTLANENLPSPFLTLDQLKANFLKQGLN-TTDLVALSGGHTFGRAQCRFFSTRLYDFNSTGSPDPSLNT

                    *       220         *       240         *       260         *       280         *       300
A. rusticana        : TYLQTLRGLCPLNGNLSALVDFDLRTPTIFDNKYYVNLEEQKGLIQSDQELFSSPNATDTIPLVRSFANSTQTFFNAFVEAMDRMGNITPLTGTQGQIRL
A. thaliana         : TYLQTLRGLCPLNGNRSALVDFDLRTPTVFDNKYYVNLKERKGLIQSDQELFSSPNATDTIPLVRAYADGTQTFFNAFVEAMNRMGNITPTTGTQGQIRL
E. halophilum       : TYLQTLRGLCPRNGNQSVLVDFDLRTPTVFDNKYYKNLKELKGLIQTDQELFSSPNATDTVPLVRSYADGTEKFFNAFIEAMNRMGNITPLTGSQGQIRQ
B. napus            : TYLQTLRGLCPLNGNRSALVDFDLRTPTVFDNKYYVNLKEQKGLIQTDQELFSSPNATDTIPLVREYADGTQKFFDAFVEAMNRMGSITPLTGTQGEIRL
R. sativus var. niger : TYLTQLRGLCPQNGIGTVLVNFDPVTPGGFDNQYYTNLRNGRGLIQSDQELFSTPRA-FTIPLVEQYSNNRLVFFQAFAEAMIRMGNLKPLTGTQGEIRR
P.  trichocarpa     : TLLAALQKLCPENGNGSVITDLDVTTADAFDSKYYSNLQCNRGLLQTDQELFSTPGADDVIALVNAFSANQTAFFESFVESMIRMGNISPLTGTEGEIRL
M. notabilis        : TLLQTLRQICPQGGNDSAVTNLDQSTPDVFDKKYFSNLLLENGVLQTDQELYSTSGADT-APIVDAYSANQTAFFNSFVVSMIKMGNIGVLTATQGEIRS

                    *       320
A. rusticana        : NCRVVNSNSLLHDMVEVVDFVSSM
A. thaliana         : NCRVVNSNSLLHDVVDIVDFVSSM
E. halophilum       : NCRVVNSNSLLHDVVEIVDFVSSM
B. napus            : NCRVVNSNSLLQDVVELVDFVSSI
R. sativus var. niger : NCRVVNSRIRSVENE-DDGVVSSI
P.  trichocarpa     : NCRVVNANLAGPDSMLVSS-I---
M. notabilis        : NCRKVNGDISRLSSGGLVAEY---
```

Figure 5-9. Multiple sequence alignment of peroxidases derived from different plant species. The amino acid residues corresponding to F68, F142, F143 and F179 found in HRPC were highlighted with a grey background. Homologous peroxidases share 56–91% sequence identity and 72–97% sequence similarity with HRPC. AAA33377.1 (HRPC, *Armoracia rusticana*), CAA50677.1 (*Arabidopsis thaliana*), ABO93458.1 (peroxidase 32, *Eutrema halophilum*), AAY81665.1 (*Brassica napus*), ABY84191.1 (*Raphanus sativus* var. *niger*), AHL39106.1 (class III peroxidase, *Populus trichocarpa*), and EXC24761.1 (*Morus notabilis*).

5. 4 Conclusion

The multiple Phe residues of HRPC were modified with phenoxyl radicals, and these Phe residues were changes to Ala to prevent the radical binding. Hence, the quadruple mutant (F68A/F142A/F143A/F179A) showed the improved stability and turnover capacity in the phenol oxidation reaction. The new protein engineering strategy to eliminate the radical biding site successfully improved the radical stability of HRPC. In addition, the Phe residue(s) was conserved in other peroxidases that was inactivated by phenoxyl radical attack. It showed the engineering strategy suggested in this study could be applied to other peroxidase for improving the radical stability.

This study provides insights into the molecular mechanism of peroxidase inactivation by radical attack and into the design of radical-robust peroxidases during the oxidation reaction.

CHAPTER 6

IMPROVED PRACTICAL USEFULNESS OF PEROXIDASE FROM *COPRINUS CINEREUS* BY MUTIAON OF PHE230

6. 1. Introduction

In the previous two decades, there have been many attempts to use the enzymes as biocatalyst in industrial applications. Because enzymes show the remarkable versatility, regio-, chemo-, and entio-selectivity, which makes the enzyme-based reactions more economical and environmentally-friendly compared with conventional chemical reactions (Schmid et al., 2001). One of the enzymes group receiving industrial attention is peroxidases (Regalado et al., 2004). Peroxidases catalyze the oxidation of a wide variety of inorganic and organic substrates with reduction hydrogen peroxide. The ability of peroxidases to catalyze forming free-radicals which undergo spontaneous polymerization makes peroxidase useful in a number of applications (Regalado et al., 2004).

Some industrial processes using the peroxidase-based catalysis are the removal of phenolic compounds and synthetic dye from waste water and synthesis of various functional polymers (Regalado et al., 2004). Phenolic compounds and synthetic dyes are the common chemical pollutants in wastewater from various industrial origins such as textile, petrochemical, paper and chemical. They are should be removed from polluted water due to their toxicity. Phenol removal method using horseradish peroxidase was first proposed by Klibanov and colleagues (1980), and has been continuously improved since then. Synthetic dyes are generally resistant to microbial biodegradation and difficult to be degraded in waste water treatment plants, due to their complicated structure (Robinson et al., 2001). Hence, a number of studies have been focused

on developing the enzymes to be employed for removal of dye from polluted water (Husain, 2006). Many peroxidases such as lignin peroxidase, manganese peroxidase, soybean peroxidase, and HRP have been applied for enzymatic treatment to decolorize and degrade dye in wastewater (Heinfling et al., 1997; Nicell et al., 1993; Singh, 2006). Furthermore, another major application of peroxidase is as a mild catalyst in polymer synthesis (Kobayashi and Makino, 2009). Peroxidase-mediated polymerization process is expected to be an alternative route for the preparation of phenol polymers without the use of toxic formaldehyde, which is a monomer component for production of conventional phenolic resins (Dordick et al., 1987). Recently, new types of polymers have been successfully developed by peroxidase-mediated polymerization of phenol derivatives (Hollmann and Arends, 2012).

Among the most abundant peroxidases investigated, CiP has attracted attention due to its ease of production (Kim et al., 2009), high specific activity and broad substrate spectrum (Abelskov et al., 1997), compared with other peroxidases. CiP has been used successfully to remove the phenol and synthetic dye from waste water (Kauffmann et al., 1999; Yousefi and Kariminia, 2010), and to produce the useful polymers such as polycardanol and polybisphenol A (Kim et al., 2007; Kim et al., 2005). However, like other peroxidases, CiP also suffers from enzyme inactivation in the catalytic process (Chang et al., 1999; Kim et al., 2009).

In the previous work, the radical-stable CiP had been developed by site-directed mutagenesis of Phe 230 residue. The F230A mutant exhibited 80-fold improved stability, and the 16-fold

increased turnover capacity in the phenol oxidation reaction, compared with those of wild-type CiP. However, the substrate binding affinity and catalytic efficiency were reduced by F230A mutation, due to disruption of the specific interaction between the phenol substrate and Phe residue (Kim et al., 2014). It was remained as question that F230A mutant could show the high performance in the practical applications.

In this study, the radical-stable CiP, F230A mutant, was applied to some practical applications such as the removal of phenol from aqueous solution, the decolorization of Reactive Black 5, and the polymerization of phenol substrate. The effect of F230A mutation on the efficiency of each reaction, and the usefulness of F230A mutant as biocatalyst for the industrial process was evaluated.

6. 2. Materials and Methods

6. 2. 1 Materials

Phenol (99%), *m*-cresol, 3-methoxy phenol, acetic acid, and 2,2'-azino-bis(3-ethylbenzthiazoline-6-sulfonic acid) (ABTS) (98%, in diammonium salt form) were purchased from Sigma-Aldrich (USA). Hydrogen peroxide (H_2O_2, 30%, v/v) was obtained from Junsei Chemical Co., Ltd. (Japan). HPLC-grade water, methanol, ethanol acetonitrile, and isopropanol were supplied by Honeywell Burdick & Jackson (USA). A Bradford protein assay kit was purchased from Bio-Rad (USA).

6. 2. 2. Peroxidase

The expression and purification of *Coprinus cinereus* peroxidase (CiP) previously described (Kim et al., 2009). Briefly, the synthetic CiP gene was cloned in pPICZαA expression vector (Invitrogen, USA) and, expressed in *Pichia pastoris*. Expressed CiP was purified using an FPLC (GE Healthcare, USA) with a size exclusion column (SuperoseTM 6 10/300 GL, GE Healthcare, USA).

Peroxidase activity was measured using ABTS as a substrate. The reaction mixture containing 0.5 mM ABTS and 2.9 mM H_2O_2 in phosphate-citrate buffer (pH 5.0) and, the enzyme reaction was initiated by adding the enzyme solution. The absorbance change at

420 nm (ε =36,000 $M^{-1}cm^{-1}$) was measured using UV-Vis spectrometry (Shimadzu, Japan) at room temperature.

6. 2. 3 Peroxidase stability

The 1 U/mL of wild-type CiP and F230A mutant were incubated in each reaction mixture containing 0.5 mM phenol, *m*-cresol or 3-methoxy phenol in 0.1 M potassium phosphate buffer (pH 7.0) with 0.5 mM hydrogen peroxide. For the control reaction, wild-type CiP and F230A mutant were incubated in the 0.1 M potassium phosphate buffer (pH 7.0). The reaction solution was sampled every 5 min after the initiation of oxidation reaction of phenolic substrates, and then the residual peroxidase activity was measured using ABTS as described in above.

6. 2. 4 Removal of phenol

The wild-type CiP and F230A mutant were diluted with 0.1 M potassium phosphate buffer (pH 7.0) to give a final concentration of 10 U/mL. The phenol and hydrogen peroxide were added to the enzyme solutions to give a final concentration 0.5 mM, respectively, and then sample was withdrawn every 5 min. To determine the concentration of residual phenol, peroxidase-mediated reaction was stopped by adding the 1 volume of 1 M phosphoric acid. The precipitate was removed by centrifugation at 13,000 g for 20 min, and

then the phenol concentration was determined using high-performance liquid chromatography (HPLC) (Agilent model 1200 liquid chromatograph; Agilent Technologies, USA). Phenol was separated by Zorbax XDB-C18 column (150 × 0.3 mm, 3.5 m; Agilent Technologies, USA) with a diode-array detector working at 280 nm. The mobile phase was a mixture of methanol and water containing 0.1% glacial acetic acid (70:30 v/v) at a flow rate of 1.0 mL/min. The phenol concentration was quantified using calibration curves prepared from external standards. The removal efficiency was defined as follows:

$$\mathrm{RE}(\%)=\left(\frac{\text{Concentration of initial phenol}}{\text{Concentration of initial phenol}}-\frac{\text{Concentration of removal phenol}}{\text{Concentraion of initial phenol}}\right)\times 100$$

6. 2. 5 Decolorization of RB5

The peroxidase-mediated decolorization of RB5 was examined using the wild-type CiP and F230A mutant. Peroxidase were treated with 20 mg/L RB5 at pH 7.0 (0.1 M potassium phosphate buffer) in the presence of 0.5 mM hydrogen peroxide at room temperature. The peroxidase stability and the residual concentration of dye were investigated after different time intervals. The residual activity of peroxidase was measured using ABTS. The concentration of RB5 was determined by measuring the absorbance of dye solution at 596nm. Decolorization efficiency was defined as follows:

$$\mathrm{DE}(\%)=\left(\frac{\text{Absorbance of initial dye solution}}{\text{Absorbance of initial dye solution}}-\frac{\text{Absorbance of decolorized dye solution}}{\text{Absorbance of initial dye solution}}\right)\times 100$$

6. 2. 6 Phenol polymerization

Enzymatic polymerization of phenol was carried out in the various organic solvent-buffer mixtures. Reaction mixture consisted of 1 mM phenol and 0.5 mM hydrogen peroxide in the 50% v/v methanol, ethanol or isopropanol-buffer solutions. The enzyme solution (final concentration of 10 U/mL) added to each reaction mixture and incubated for 30 min at room temperature while stirring. The reaction mixture was separated into precipitate and supernatant by centrifuge at 13,000 g for 20 min. The supernatant of reaction mixture was subjected to analyze the residual concentration of phenol by HPLC. The settled materials were washed three times with distilled water to remove the enzymes and unreacted monomer. The water-insoluble material was dried in a vacuum, and then solved in tetrahydrofuran (THF) for the gel permeation chromatography (GPC) analysis. The molecular weights of phenol polymer were determined by GPC. GPC analysis was carried out using a refractive index detector under the following conditions: PL4 mixed BB columns (Tosoh, Japan) and THF as solvent at 0.5 mL/min. Calibration curves for GPC analysis were obtained using polystyrene standards.

Additionally, wild-type CiP and F230A mutant were incubated in the 50% v/v of various organic solvent (methanol, ethanol and isopropanol) in the presence or absence of 0.5 mM phenol and 0.5 mM hydrogen peroxide. The reaction solution was withdrawn every 5 min, and then the residual peroxidase activity was measured using ABTS.

6. 2. 7. Kinetic studies

The peroxidase (0.3 μM) was incubated in the variable concentration of guaiacol (0.4 to 20 mM) with 100 μM of hydrogen peroxide. The oxidation reaction rate of peroxidase was monitored by measuring a changes in absorbance at 470 nm (ε = 26,600 $M^{-1}cm^{-1}$). The k_{cat} and K_m of each peroxidase were derived by the Michaelis–Menten equation based on the corresponding Hanes–Woolf plots from three independent experiments.

6. 3. Results and Discussion

6. 3. 1. Phenol removal form aqueous solution

In previous study, the radical-stable mutant of CiP (F230A) was developed, and exhibited remarkably improved radical stability during the oxidation reaction of phenol (Kim et al., 2014). The wild-type CiP was inactivated by phenoxyl radical attack in a short time, however, the F230A mutant retained approximately 80% of its initial activity all over oxidation reaction time (Figure 6-1. A).

Not only phenol, also other substituted phenols are toxic organic pollutant in the industrial wastewater (Ayala et al., 2008). The stability of CiP and the F230A mutant were further investigated by using substituted phenols, *m*-cresol and 3-methoxyphenol. Figure 6-1 shows time-course experiments of the remaining activity of CiP and the F230A mutant incubated in 0.5 mM *m*-cresol or 0.5 mM 3-methoxyphenol in the presence of 0.5 mM hydrogen peroxide. In case of the wild-type enzyme, the activity was considerably decreased in both phenolic compounds. Otherwise, the F230A mutant showed greatly improved stability in the oxidation reaction compared with wild-type. After 20 min of incubation, the residual activities of F230A in *m*-cresol and 3-methoxyphenol were 86.4% and 48.1% of the initial activity, respectively (Figure 6-1. B and C). The high stability of mutant indicated the promise of F230A mutant as effective biocatalyst in the removal of phenolic compounds from the wastewater.

In addition, it had been suggested that F230 residue of CiP is the coupling site for phenoxyl radical, and F230A mutation prevents the peroxidase inactivation by blocking the radical coupling (Kim et al., 2014). Accordingly, the F230A mutation can effectively block the attack and coupling of other phenoxyl radical species, such as *m*-methylphenoxyl radical and 3-methoxyphenoxyl radical.

Enzymatic phenol removal was carried out to evaluate the phenol removal efficiency of F230A mutant. Wild-type CiP and F230A mutant were incubated with 0.5 mM phenol and 0.5 mM hydrogen peroxide, and the amount of removed phenol was calculated at regular time intervals (Figure 6-2). As expected, the efficiency of phenol removal of F230A was 4.5-fold higher than that of wild-type. The wild-type and F230A mutant eliminate 20% and 80% of phenol, respectively. Additionally, the removal reaction of phenol was almost completed for the first 5 minute.

.

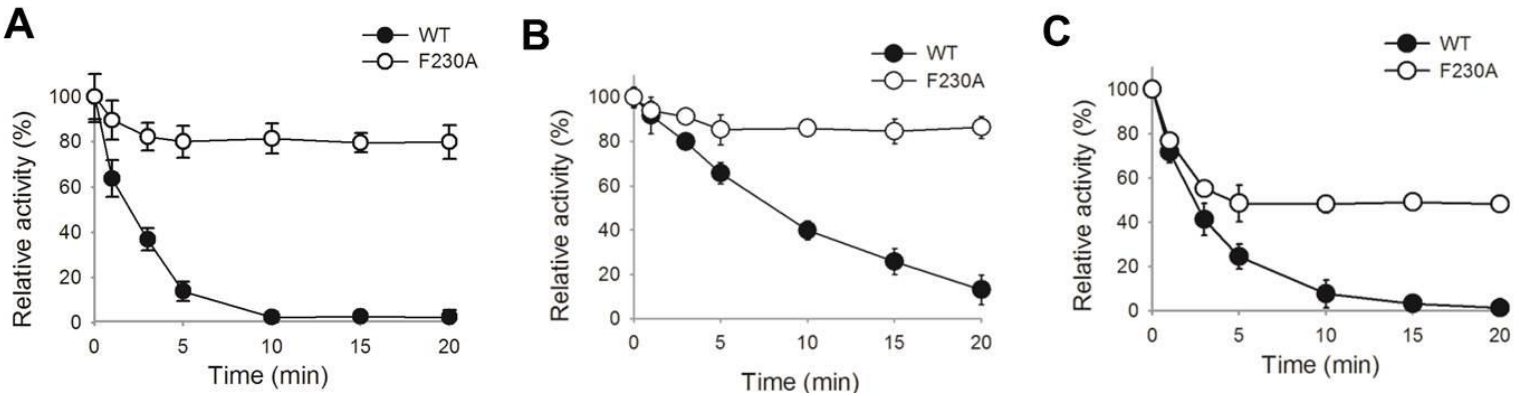

Figure 6-1. The stability of the wild-type CiP (WT) and F230A mutant during the oxidation reaction of phenolic substrates. (A) Residual peroxidase activity during the oxidation of phenol. (B) Residual peroxidase activity during the oxidation of *m*-cresol. (C) Residual peroxidase activity during the oxidation of 3-methoxyphenol. Peroxidase activity was measured, after incubation with 0.5 mM phenol, 0.5 mM *m*-cresol or 0.5 mM 3-methoxyphenol in the presence of 0.5 mM H_2O_2.

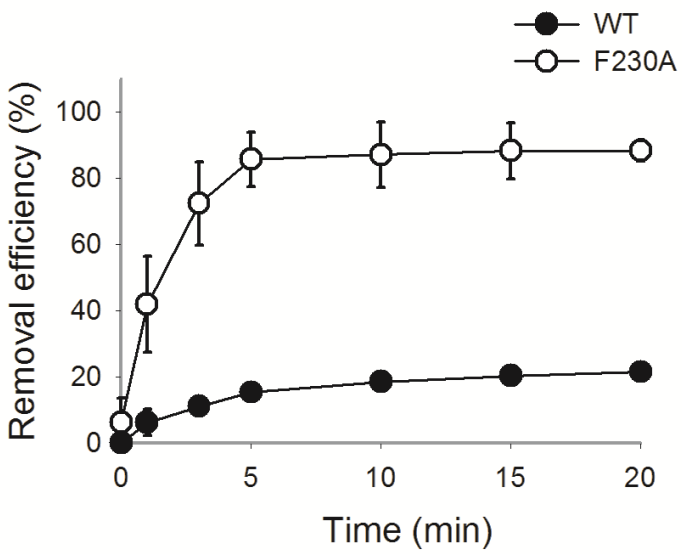

Figure 6-2. The phenol conversion of wild-type CiP (WT) and F230A mutant. The initial concentration of phenol was 0.5 mM.

6. 3. 2. Decolorization of Reactive Black 5

Peroxidases have also been extensively studied to apply to the decolorization of synthetic dye in industrial wastewater (Ong et al., 2011). Among the various dyes, Reactive Black 5 (RB5) is most used reactive dye for textile finishing and be dispelled into the river. The CiP was applied to the decolorization of RB5. The wild-type CiP and F230A mutant were incubated with 20 mg/L of RB5 in the presence of 0.5 mM hydrogen peroxide. The stability and the decolorization efficiency of peroxidase were presented in Figure 6-3. The wild-type and F230A mutant were inactivated upon the reaction of RB5 and hydrogen peroxide, which was resulted by free-radical intermediate formed from peroxidase catalysis (Figure 6-3. A). During the oxidation of RB5, the F230A maintained 67% of initial activity, whereas the residual activity of wild-type was continuously declined to 20% of initial activity. The F230A mutant showed the higher decolorization efficiency (77%) compared with wild-type (17%) (Figure 6-3. B). The enhanced stability of F230A mutant leads the higher decolorization efficiency of RB 5.

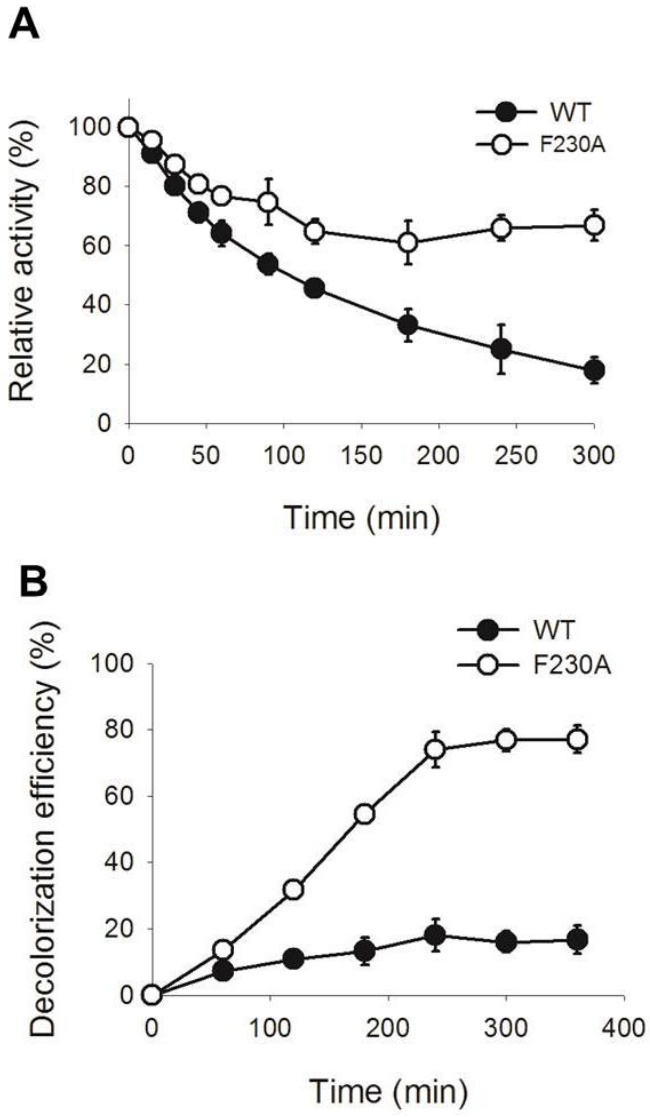

Figure 6-3. Comparison of activity and the decolorization efficiency of RB5 by CiP (WT) and F230A mutant. (A) Residual activity of wild-type and F230A mutant during the oxidation reaction of RB5. (B) The decolorization efficiency of RB5 by wild-type and the F230A mutant. Peroxidases were incubated in the presence of 0.5 mM H_2O_2, and 20 mg/L RB5.

6. 3. 3. Enzymatic polymerization of phenol

The peroxidase-mediated polymerization of phenol was evaluated in mixtures of phosphate buffer (pH 7.0) and various solvent-buffer mixtures. Peroxidase originating from *Coprinus cinereus* (CiP) was used to obtain the phenol polymer. The influence of the F230A mutation on the polymerization reaction of phenol and the properties of the phenolic polymer were investigated. The polymerization reaction of phenol was conducted in various water-miscible organic solvent/phosphate buffer (50:50, v/v) mixtures with 1 mM phenol and 0.5 mM hydrogen peroxide. Three water-miscible organic solvents with different hydrophobicities (log *P*), methanol (log *P*: -0.82), ethanol (log *P*: -0.31), and isopropanol (log *P*: 0.34), were used in this reaction. When the enzymatic polymerization is carried out in organic solvent, high-molecular-mass polymers can be obtained due to increase in the solubility of phenolic oligomers (Klibanov, 2001).

The consumption of phenol was compared between the wild-type CiP and F230A mutant under the various solvent-buffer mixtures. shows the concentration of residual phenol after the polymerization reaction. Wild-type CiP and F230A oxidized similar amounts of phenol monomers (50% of total phenol) in the phosphate buffer, whereas F230A consumed more phenol substrate than wild-type in all of the solvent-buffer mixtures. Although the wild-type oxidized up to 20% of the total phenol in all of the solvent-buffer mixtures, the F230A mutant consumed 95% of phenol in the methanol-buffer mixture and 50% of the total phenol content in the

ethanol- and isopropanol-buffer mixtures (Figure 6-4).

The phenolic polymer produced in the 50% (v/v) solvent-buffer mixtures was analyzed using GPC, and the molecular weight (Mw) distribution of the phenolic polymer are shown in Table 6-1. The Mw phenolic polymers synthesized by the wild-type enzyme in each solvent-buffer mixture ranged from approximately 1,500 to 3,000 Da. Although the Mw of the polymer in 50% methanol (3,115 Da) was higher than that synthesized in phosphate buffer (2,186 Da), a slight decline in the Mw of polymers synthesized in 50% ethanol (1,588 Da) and isopropanol (1,569 Da) was observed. For F230A, lower or similar Mw polymers were obtained in phosphate buffer (1,619 Da) or methanol compared to the wild-type (2,186 Da), whereas the highest Mw phenolic polymer of 8,850 Da was obtained in 50% isopropanol. In addition, the Mw of the polymers increased from 1,588 to 5,900 Da in the 50% buffer-ethanol mixture using the F230A mutant. The Mw of the phenolic polymer was affected by the nature of the organic solvent media. Although the wild-type CiP yielded phenolic polymers with a low Mw in all of the solvent-buffer mixtures, the F230A mutant yielded polymerized products with a higher Mw in the more hydrophobic aqueous solvent mixtures. The higher Mw phenolic polymer can be dissolved in more hydrophobic solvents, which may be the reason why the highest Mw polymer was polymerized in an isopropanol-buffer mixture. A previous report showed the relationship between the hydrophobicity (log *P*) of the organic solvent and the Mw of poly(bisphenol A) polymerized by CiP and found that the poly(bisphenol A) with the highest Mw was produced in the most hydrophobic solvent (isopropanol) among the

examined various organic solvents (Kim et al., 2007).

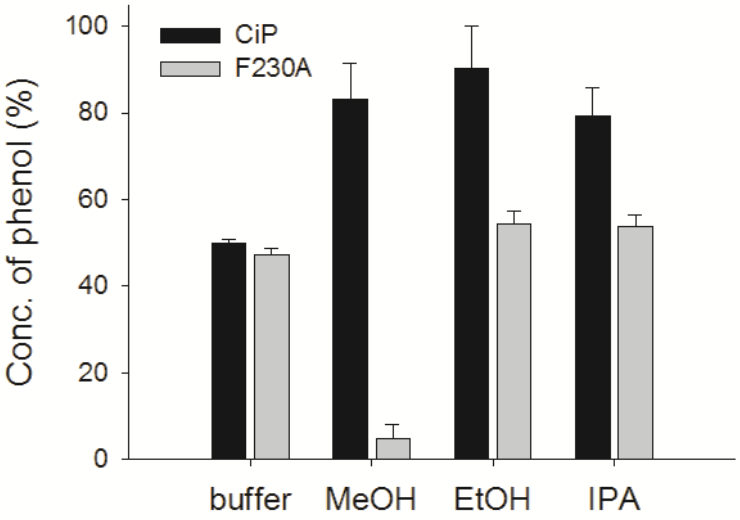

Figure 6-4. Residual phenol concentration of wild-type CiP and F230A mutant after the phenol oxidation reaction. The phenol concentration was measured after incubation with 1 mM phenol and 0.5 mM H_2O_2, in the 50% v/v of various organic solvent-buffer mixtures.

Table 6-1. Molecular weight distribution of the phenolic polymers synthesized by the wild-type CiP and the F230A mutant.

Peroxidase[a]	Solvents[b]	Mn[c]	Mw[d]	Pd[e]
CiP	Buffer	1555	2186	1.4057
	Methanol	2294	3115	1.3581
	Ethanol	1525	1588	1.0414
	Isopropanol	1447	1519	1.0496
F230A	Buffer	1269	1619	1.2761
	Methanol	1977	3080	1.5578
	Ethanol	3285	5900	1.7963
	Isopropanol	4273	8850	2.0709

[a] 10 U/ml of peroxidases was used.

[b] The solvents are composed of a 50:50 mixture of the organic solvent and phosphate buffer.

[c] Number average molecular weight.

[d] Weight average molecular weight.

[e] Polydispersity.

6. 3. 4. Effect of organic solvent on enzyme stability

To study the effect of the peroxidase stability on the phenolic polymer synthesis, the enzyme stability against the organic solvent was investigated. Peroxidases were incubated in 50% (v/v) methanol, ethanol, and isopropanol, and their residual activities were then measured (Figure 6-5). The results show that the activities of the wild-type CiP and F230A mutant were diminished in all of the solvent-buffer mixtures (Figure 6-5. B, C and D). The extent of enzyme inactivation due to the organic solvents followed the order methanol > ethanol > isopropanol. In many cases, the hydrophobicity of the solvent can influence the stability of a protein, and solvents with high log *P* values causes less inactivation of biocatalysts (Laane et al., 1987; Ó'Fágáin, 2003). he log *P* values of each alcohol were followed methanol (-0.82) > ethanol (-0.31) > isopropanol (0.34), which indicated that the stability of CiP was dependent on the hydrophobicity of the solvent.

In addition, the stability of the F230A mutant was lower than the wild-type in all of the solvent-buffer mixtures. In previous reports, the solvent stabilities of lipases and proteases were successfully improved by changing their surface hydrophobicity, and improving the hydrophobicity on the enzyme surface enhanced the stability of the enzyme in organic media (Schwehm et al., 1998; Monsef Shokri et al., 2014; Van den Burg et al., 1994). The Phe230 residue of CiP forms a hydrophobic patch with Pro91, Gly94, Ile153, Pro156, Gly191, and Leu192 for substrate binding (Tsukamoto et al. 1999; Wariishi et al., 2000). The hydropathy value of Ala (1.8) is lower than that of Phe (2.8)

(Kyte and Doolittle, 1982), and the smaller hydrophobic side chain of Ala causes reduced hydrophobic interactions with other hydrophobic residues in the hydrophobic patch. An Ala substitution weakens the hydrophobicity of the hydrophobic patch on the surface of CiP, which may destabilize the surface structure and result in the low stability of the F230A mutant in organic solvents.

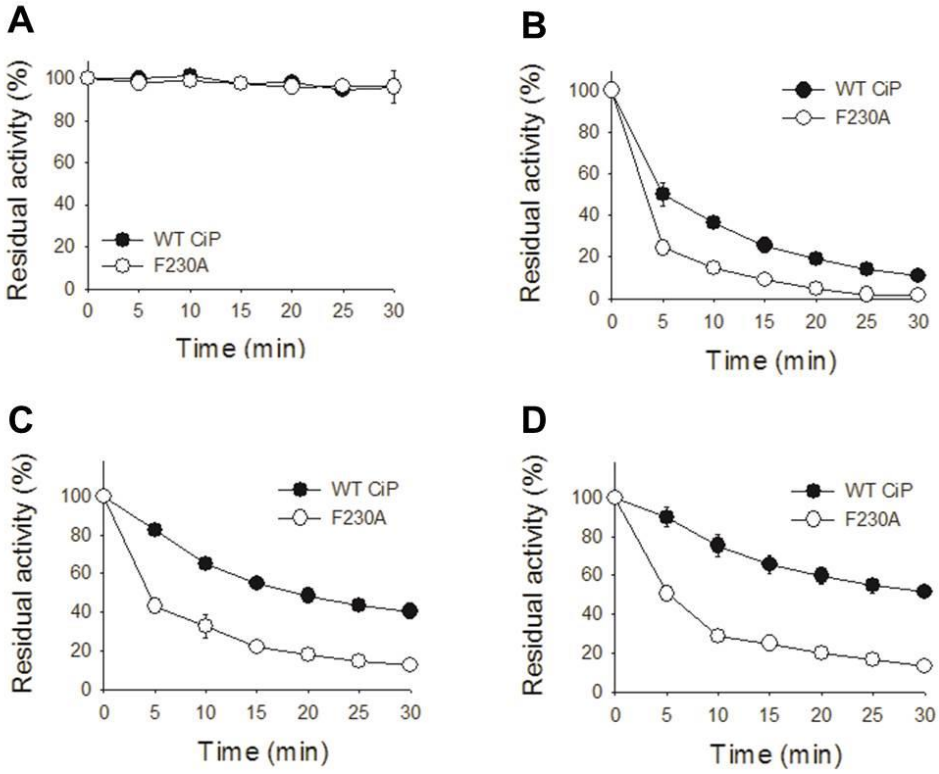

Figure 6-5. Residual activity of wild-type CiP and F230A mutant in the 50% various organic solvents-buffer mixtures. The wild-type CiP and F230A mutant were incubated in (A) 0.1 M phosphate buffer (pH 7.0), (B) 50% v/v methanol (C) 50% v/v ethanol (D) 50% v/v isopropanol.

6. 3. 5. Enzyme stability during phenol oxidation in solvent mixtures

The peroxidase-mediated polymerization reaction of phenol was performed in the organic solvent-buffer mixtures, and the radical-stability of the peroxidases was observed during the oxidation of phenols in aqueous organic solvent mixtures (Figure 6-6). After the phenol oxidation catalyzed by CiP was carried out in the phosphate buffer, the wild-type and F230A mutant lost 50% and 10% of their initial activity, respectively (Figure 6-6. A). Inactivation by radials was observed in both the wild-type and F230A mutant. However, the wild-type suffered more severe inactivation due to phenoxyl radical attack. The F230A mutant is a radical-robust CiP that is highly stable during the oxidation reaction of phenols

When the peroxidases were incubated with phenol and hydrogen peroxide under the 50% (v/v) organic solvent-buffer conditions, the F230A mutant exhibited a lower stability than that of wild-type. In addition, the inactivation rate of peroxidase due to radicals in the solvent mixtures (Figure 6-6. B, C and D) was very similar to that by the solvent (Figure 6-5. B, C, D). The F230A mutant exhibited a high stability during the oxidation reaction of phenol in the buffer, whereas it did not exhibit stability in organic solvent-buffer mixtures. Moreover, there was no significant difference in the degree of enzyme inactivation by the organic solvent and radicals. This result indicates that the organic solvent-mediated inactivation have a greater influence on the peroxidase activity than radical-mediated inactivation, when peroxidase catalyzes the polymerization

of phenol in 50% organic solvent-buffer mixtures.

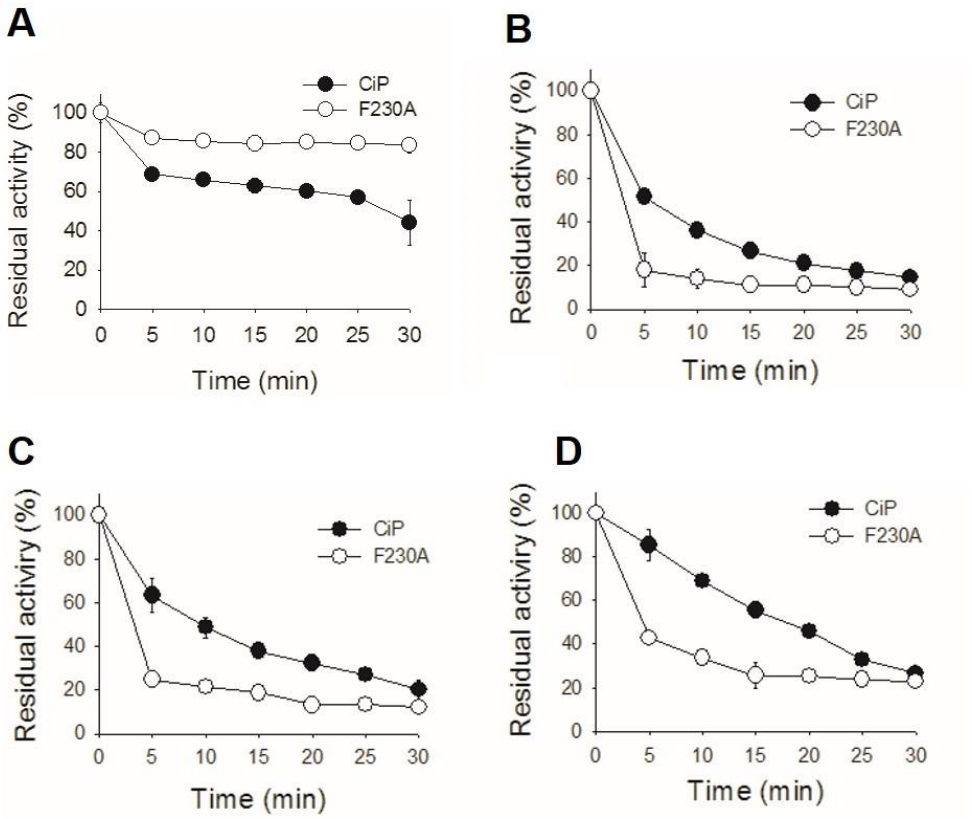

Figure 6-6. Residual stability of wild-type CiP and F230A mutant during the oxidation reaction of phenol in the 50% various organic solvents-water mixtures. The wild-type CiP and F230A mutant were incubated in (A) 0.1 M phosphate buffer (pH 7.0), (B) 50% v/v methanol, (C) 50% v/v ethanol, (D) 50% v/v isopropanol, in the presence of 1 mM phenol and 0.5 mM H_2O_2.

6. 3. 6. Kinetic study

The kinetic parameters of wild-type and F230A were determined using the guaiacol, and depicted in Table 6-2. F230A mutation results in various changes in the kinetic parameters of peroxidase. The turnover number (k_{cat}) of the peroxidase increase from 5.61 to 15.3 s^{-1} due to the F230A mutation. A reduction in the substrate affinity (K_m: 5.41 μM) and catalytic efficiency (k_{cat}/K_m: 2.83 $\mu M^{-1}s^{-1}$) of F230A mutant compared to the wild-type was also observed. The low K_m value of F230A is due to an interruption of the aromatic-aromatic interaction between the Phe residue and the phenolic substrate, which has been well described by molecular docking simulations (Kim et al., 2014).

Although the k_{cat}/K_m of F230A was lower than that of wild-type, the phenolic polymer with the highest Mw was synthesized by the F230A mutant in 50% isopropanol (Table 6-1). In the Figure 6-2, wild-type CiP and F230A mutant completely oxidize the maximum amount of oxidizable phenol substrate in the total oxidation reaction within 5 minutes. Therefore, peroxidase-mediated polymerization would also be completed within a very short time. In addition, in the early phase of the polymerization reaction in the solvent-buffer mixtures, the gap between the residual activity of the wild-type CiP and the F230A mutant was not considerabl (Figure 6-5 and 6-6). As a result, the short reaction time and higher k_{cat} value of the F230A mutant may lead to the production of the large Mw polymer in ethanol- and isopropanol. Likewise, the wild-type may produce the lower Mw phenolic polymer even in the solvent-buffer mixture due

to their low k_{cat} value.

Table 6-2. Kinetic parameters of the wild-type CiP and F230A mutant with guaiacol.

	K_m (μM)	k_{cat} (s^{-1})	k_{cat}/K_m ($\mu M^{-1}s^{-1}$)
CiP	1.14±0.0456	5.61±0.100	4.94±0.120
F230A	5.41±0.240	15.3±0.544	2.83±0.0284

6. 4. Conclusion

In this study, the radical-stable mutant (F230A) was applied to practical applications to evaluate its usefulness as biocatalyst industrial filed. The high stability of the F230A mutant retained during the oxidation of various phenolic substrates including phenol, *m*-cresol and 3-methoxypehnol. This feature could be an advantageous for the treatment of industrial wastewater contaminated with diverse phenolic compounds. In addition, F230A mutant exhibited the higher performance in the removal of phenol, the decolorization of dye, and the phenol polymer synthesis, compared with wild-type CiP. Although a decline in the stability of the F230A mutant against solvents and radicals was observed, this study shows the promise of the F230A CiP mutant as an effective biocatalyst in organic polymer synthesis.

CHAPTER 7

OVERALL DISCUSSIONS AND RECOMMENDATIONS

Clearly, peroxidases have promise for applications, but commercial processes based on peroxidases have been restricted mainly due to the inactivation of peroxidases during the reaction process. The low stability of peroxidases has been a difficult challenge to overcome; however, there have been numerous efforts to improve peroxidase stability through the protein engineering method. Accordingly, information on the inactivation mechanism of peroxidases is essential for the rational design of site-directed variants to prevent inactivation.

In the first part of this study, a dominant inactivation mechanism for peroxidase during phenol oxidation was proposed using the two model enzymes, CiP and HRPC. Among the inactivation factors suggested in previous studies, excessive hydrogen and phenolic polymers had a weak influence on peroxidase stability, whereas phenoxyl radicals greatly affected peroxidase inactivation. The modification of polypeptides and the maintenance of high intact heme content after the oxidation reaction of phenol imply that the modification of amino acid residue with phenoxyl radicals is the major reason for peroxidase inactivation rather than heme modification/destruction. It is strongly suggested that the inactivation of a peroxidase during the oxidation of phenolic compounds occurs by a covalent modification of the peroxidase polypeptide chain with phenoxyl radicals.

In the second part of this study, the inactivation model

suggested in this study was proved through experimental evidence using CiP. The specific radical coupling site (F230) of CiP was identified, and the F230A mutant showed the highest stability against radical inactivation during phenol oxidation. The F230A mutated residue was not modified with phenoxyl radicals, which implies that the substitution with Ala of the radical binding site efficiently blocked the radical coupling. Furthermore, the lack of structural changes after radical coupling means that the radical coupling led the peroxidase inactivation by an alternative mechanism rather than by the structure destruction of the enzyme. Hence, it was suggested that the F230-phenol radical adduct inactivated CiP by blocking the substrate access to the active site of the enzyme. In addition, a novel strategy (eliminating the radical binding site by substitution with Ala) was proposed for enhancing the peroxidase stability. However, in order to validate the general applicability of this inactivation mechanism and protein design strategy to other enzymes, more enzymes should be radical-stabilized by this strategy.

In the third part of this study, the peroxidase inactivation model was proved using another peroxidase, HRPC, and a novel protein engineering approach was applied to HRPC. The phenylalanine residues that are vulnerable to modification by the phenoxyl radicals were identified, and the F68A/F142A/F143A/F179A mutant of HRPC demonstrated dramatic enhancement of radical stability. A significant structure disruption was not observed upon radical coupling. These results supported the inactivation model involving radical coupling with a

specific residue (Phe) and the blocking of the access channel of the enzyme's active site. It was shown that engineering the radical-vulnerable residues to eliminate multiple radical coupling can be a good strategy to improve the stability of peroxidases against radical attack. Furthermore, structure and sequence alignment revealed that radical-vulnerable Phe residues of HRPC are conserved in homologous peroxidases, which showed that the novel engineering strategy can be applied to other peroxidases to improve radical stability.

In the fourth part of this study, the practicality of the engineered peroxidase mutant was evaluated. The radical-stable CiP (F230A) was applied to the major practical applications, such as the removal of phenol, the decolorization of dye, and the synthesis of polymers. The F230A mutant showed excellent reaction efficiency in all reactions. From a practical point of view, the F230A mutant of CiP is a more useful biocatalyst for industrial applications.

This study provides the first experimental evidence demonstrating the molecular mechanism of peroxidase inactivation by radical coupling. Moreover, a new engineering strategy was suggested to improve peroxidase stability against the free phenoxyl radicals generated from phenol oxidation reactions. Radical-stable peroxidases were successfully developed, which confirmed the inactivation mechanism associated with radical coupling. Nevertheless, some questions remain unanswered. It was revealed

that the radical coupling at the specific Phe residues is critical in the radical-meditated inactivation of peroxidase. However, how the attached phenoxyl radical inactivates the peroxidase remains unclear. It was assumed that the access channel of the active site was blocked by radical coupling in this study, since the protein structure was not changed upon radical coupling. Direct experimental evidence will be required to prove and elucidate the inactivation model in more detail. Further mass analysis will be needed to confirm the chemical structures between the phenoxyl radicals and peroxidases (CiP and HRPC). This experimental result will determine whether the hydroxylation of Phe residue is involved in the phenoxyl radical coupling process. In addition, the X-ray crystal structure of the complex of phenol with phenoxyl radical-modified peroxidase will clarify the suggested inactivation mechanism of blocking the access channel of the active site by radical coupling.

Additional experimental results (other radical-stable peroxidase variants engineered through eliminating the radical binding site) are necessary to strengthen and generalize the inactivation mechanism. The radical-stable CiP mutant (F230A) showed excellent potential in the practical applications, but this mutant had lower stability in the organic solvent media. The organic solvent stability is coupled to the structural stability of the folded state; therefore, the F230A mutation would weaken the structural stability of the enzyme. In order to investigate the effect of the Ala substitution on the folding state, it is necessary to analyze the changes in the protein structure based on the crystal structure of the radical-stable peroxidase mutant. Additionally, this structure analysis will

provide a perspective on strengthening the structural stability of the enzyme closely connected to the organic solvent and thermal stability. In this study, the radical stability of peroxidases was successfully improved, but other weaknesses (e.g. low stability against organic solvent and heat) still exist as obstacles to the utilization of peroxidase. Hence, a combination of engineering strategies should be applied to develop high-performance peroxidases.

BIBLIOGRAPHIES

Abelskov, A.K., Smith, A.T., Rasmussen, C.B., Dunford, H.B., and Welinder, K.G. (1997). pH dependence and structural interpretation of the reactions of *Coprinus cinereus* peroxidase with hydrogen peroxide, ferulic acid, and 2,2'-azinobis. Biochemistry *36*, 9453-9463.

Adediran, S.A., and Lambeir, A.M. (1989). Kinetics of the reaction of compound II of horseradish peroxidase with hydrogen peroxide to form compound III. Eur J Biochem *186*, 571-576.

Aitken, M.D. (1993). Waste treatment applications of enzymes: opportunities and obstacles. Chem Eng J *52*, B49-B58.

Aitken, M.D., and Heck, P.E. (1998). Turnover capacity of *Coprinus cinereus* peroxidase for phenol and monosubstituted phenols. Biotechnol Prog *14*, 487-492.

Al-Ansari, M.M., Modaressi, K., Taylor, K.E., Bewtra, K.K., and Biswas, N. (2010). Soybean peroxidase-catalyzed oxidative polymerization of phenols in coal-tar wastewater: comparison of additives. Environ Eng Sci *27*, 967-975.

Al-Ansaria, M.M., Steevensza, A., Al-Aasma, N., Taylora, K.E., Bewtrab, J.K., and Biswasb, N. (2009). Soybean peroxidase-catalyzed removal of phenylenediamines and benzenediols from water. Enzyme Microb Technol *45*, 253-260.

Ammosova, T.N., Ouporov, I.V., Rubtsova, M.Y., Ignatenko, O.V., Egorov, A.M., Kolesanova, E.F., and Archakov, A.I. (1997). Epitope mapping of horseradish peroxidase (isoenzyme C). Biochemistry (Mosc) *62*, 440-447.

Antoniotti, S., and Dordick, J.S. (2005). Peroxidase-catalyzed coupling of solid-supported ortho-methoxyphenols. Adv Synth Catal *347*, 1119-1124.

Arnao, M., Acosta, M., Delrio, J., Varon, R., and Garciacanovas, F. (1990). A kinetic study on the suicide inactivation of peroxidase by hydrogen peroxide .

Biochim Biophys Acta Protein Struct Mol Enzymol *1041*, 43-47.

Ator, M.A., and Ortiz de Montellano, P.R. (1987). Protein control of prosthetic heme reactivity. Reaction of substrates with the heme edge of horseradish peroxidase. J Biol Chem *262*, 1542-1551.

Ayala, M., Pickard, M.A., and Vazquez-Duhalt, R. (2008). Fungal enzymes for environmental purposes, a molecular biology challenge. J Mol Microbiol Biotechnol *15*, 172-180.

Azevedo, A.M., Martins, V.C., Prazeres, D.M., Vojinović, V., Cabral, J.M., and Fonseca, L.P. (2003). Horseradish peroxidase: a valuable tool in biotechnology. Biotechnol Annu Rev *9*, 199-247.

Baik, M.H., Newcomb, M., Friesner, R.A., and Lippard, S.J. (2003). Mechanistic studies on the hydroxylation of methane by methane monooxygenase. Chem Rev *103*, 2385-2419.

Bao, X., Huang, X., ., Lu, X., and Li, J.J. (2014). Improvement of hydrogen peroxide stability of Pleurotus eryngii versatile ligninolytic peroxidase by rational protein engineering. Enzyme Microb Technol *10*, 52-58.

Baunsgaard, L., Dalbøge, H., Houen, G., Rasmussen, E.M., and Welinder, K.G. (1993). Amino acid sequence of *Coprinus macrorhizus* peroxidase and cDNA sequence encoding *Coprinus cinereus* peroxidase. A new family of fungal peroxidases. Eur J Biochem *213*, 605-611.

Baynton, K.J., Bewtra, J.K., Biswas, N., and Taylor, K. (1994). Inactivation of horseradish peroxidase by phenol and hydrogen peroxide: a kinetic investigation. Biochim Biophys Acta Protein Struct Mol Enzymol *1206*, 272-278.

Bhunia, A., Durani, S., and Wangikar, P.P. (2001). Horseradish peroxidase catalyzed degradation of industrially important dyes. Biotechnol Bioeng *72*, 562-567.

Blodig, W., Smith, A.T., Doyle, W.A., and Piontek, K. (2001). Crystal structures of pristine and oxidatively processed lignin peroxidase expressed in *Escherichia*

coli and of the W171F variant that eliminates the redox active tryptophan 171. Implications for the reaction mechanism. J Mol Biol *305*, 851-861.

Bollag, J.M. (1992). Decontaminating soil with enzymes. Environ Sci Technol *26*, 1876-1881.

Bornscheuer, U.T., and Buchholz, K. (2005). Highlights in biocatalysis – historical landmarks and current trends. Eng Life Sci *5*, 309-323.

Brems, D.N., and Stellwagen, E. (1983). Manipulation of the observed kinetic phases in the refolding of denatured ferricytochromes c. J Biol Chem *258*, 3655-3660.

Canutescu, A.A., Shelenkov, A.A., and Dunbrack, R.L.J. (2003). A graph-theory algorithm for rapid protein side-chain prediction. Protein Sci *12*, 2001-2014.

Carlos Regalado, B.E., García-Almendárez, M.A., and Duarte-Vázquez (2004). Biotechnological applications of peroxidases. Phytochem Rev *3*, 243-256.

Chandra, R., and Abhishek, A. (2011). Bacterial decolorization of black liquor in axenic and mixed condition and characterization of metabolites. Biodegradation *22*, 603-611.

Chang, H.C., Doerge, D.R., Hsieh, C., Lin, Y., and Tsai, F. (2011). The covalent binding of genistein to the non-prosthetic-heme-moiety of bovine lactoperoxidase leads to enzymatic inactivation. Biomed Environ Sci *24*, 284-290.

Chang, H.C., Holland, R.D., Bumpus, J.A., Churchwell, M.I., and Doerge, D.R. (1999). Inactivation of *Coprinus cinereus* peroxidase by 4-chloroaniline during turnover: comparison with horseradish peroxidase and bovine lactoperoxidase. Chem Biol Interact *123*, 197-217.

Chen, G.X., and Asada, K. (1990). Hydroxyurea and *p*-aminophenol are the suicide inhibitors of ascorbate peroxidase. J Biol Chem *265*, 2775-2781.

Cherry, J.R., Lamsa, M.H., Schneider, P., Vind, J., Svendsen, A., Jones, A., and

Pedersen, A.H. (1999). Directed evolution of a fungal peroxidase. Nat Biotechnol *17*, 379-384.

Childs, R.E., and Bardsley, W.G. (1975). The steady-state kinetics of peroxidase with 2,2'-azino-di-(3-ethyl-benzthiazoline-6-sulphonic acid) as chromogen. Biochem J *145*, 93-103.

Choi, Y.J., Chae, H.J., and Kim, E.Y. (1999). Steady-state oxidation model by horseradish peroxidase for the estimation of the non-inactivation zone in the enzymatic removal of pentachlorophenol. J Biosci Bioeng *88*, 368-373.

Cohen-Yaniv, V., and Dosoretz, C.G. (2009). Fate of horseradish peroxidase during oxidation of monobrominated phenols. J Chem Technol Biotechnol *84*, 1559-1566.

Colonna, S., Gaggero, N., Richelmi, C., and Pasta, P. (1999). Recent biotechnological developments in the use of peroxidases. Trends Biotechnol *17*, 163-168.

Dalboge, H., Jensen, E.B., and Welinder, K.G. (1992). A process for producing heme proteins, .

Damhus, T., Gotfredsen, S.E., and Kirk, O. (1989). A detergent additive for bleaching fabric.

DeSimone, L.D., and Popoff, F. (2000). Eco-efficiency: the business link to sustainable development (Cambridge MA: The MIT Press).

Divi, R.L., and Doerge, D.R. (1994). Mechanism-based inactivation of lactoperoxidase and thyroid peroxidase by resorcinol derivatives. Biochemistry *33*, 9668-9674.

Dordick, J.S. (1992). Enzymatic and chemoenzymatic approaches to polymer synthesis. Trends Biotechnol *10*, 287-290.

Dordick, J.S., Marletta, M.A., and Klibanov, A.M. (1987). Polymerization of phenols catalyzed by peroxidase in nonaqueous media. Biotechnol Bioeng *30*,

31-36.

Dunford, H.B. (1999). Heme peroxidase (New York: John Wiley and Sons Inc.).

Dunford, H.B. (2010). Peroxidases and catalases: biochemistry, biophysics, biotechnology and physiology., 2nd edn (John Wiley & Sons, INC.).

Fasman, G.D. (1996). Circular dichroism and the conformational analysis of biomolecules (New York: Plenum Press).

Feng, W., Taylor, K.E., Biswas, N., and Bewtra, J.K. (2013). Soybean peroxidase trapped in product precipitate during phenol polymerization retains activity and may be recycled. J Chem Technol Biotechnol *88*, 1429-1435.

Fukuoka, T., Tachibana, Y., Tonami, H., Uyama, H., and Kobayashi, S. (2002). Enzymatic polymerization of tyrosine derivatives. Peroxidase- and protease-catalyzed synthesis of poly(tyrosine)s with different structures. Biomacromolecules *3*, 768-774.

Gajhede, M., Schuller, D.J., Henriksen, A., Smith, A.T., and Poulos, T.L. (1997). Crystal structure of horseradish peroxidase C at 2.15 Å resolution. Nat Struct Biol *4*, 1032-1038.

Gazaryan, I.G., Doseeva, V.V., Galkin, A.G., and Tishkov, V.I. (1994). Effect of single-point mutations Phe41→ His and Phe143→ Glu on folding and catalytic properties of recombinant horseradish peroxidase expressed in *E. coli*. FEBS Lett *354*, 248-250.

Gholami-Borujeni, F., Mahvi, A.H., Nasseri, S., Faramarzi, M.A., Nabizadeh, R., and Alimohammadi, M. (2011). Enzymatic treatment and detoxification of acid orange 7 from textile wastewater. Appl Biochem Biotechnol *165*, 1274-1284.

Ghoul, M., and Chebil, L. (2012). Enzymatic polymerization of phenolic compounds by oxidoreductases (New York,: Springer).

Gilfoyle, D.J., Rodríguez-López, J.N., and Amith, A.T. (1996). Probing the aromatic-donor-binding site of horseradish peroxidase using site-directed

mutagenesis and the suicide substrate phenylhydrazine. Eur J Biochem *236*, 714-722.

Gobom, J., Nordhoff, E., Mirgorodskaya, E., Ekman, R., and Roepstorff, P. (1999). Sample purification and preparation technique based on nano-scale reversed-phase columns for the sensitive analysis of complex peptide mixtures by matrix-assisted laser desorption/ionization mass spectrometry. J Mass Spectrom *34*, 105-116.

Gross, G.G., Janse, C., and Elstner, E.F. (1977). Involvement of malate, monophenols, and the superoxide radical in hydrogen peroxide formation by isolated cell walls from horseradish (*Armoracia lapathifolia* Gilib.). 136 *3*.

Gross, R.A., Kumar, A., and Kalra, B. (2001). Polymer synthesis by in vitro enzyme catalysis. Chem Rev *101*, 2097-2142.

Halliwell, B. (1978). Lignin synthesis: The generation of hydrogen peroxide and superoxide by horseradish peroxidase and its stimulation by manganese (II) and phenols. Planta *140*, 81-88.

Hamid, M., and Khalil-ur-Rehman (2009). Potential applications of peroxidases. Food Chem *115*, 1177-1186.

Hammel, K.E., and Cullen, D. (2008). Role of fungal peroxidases in biological ligninolysis. Curr Opin Plant Biol *11*, 349-355.

Harazono, K., Kondo, R., and Sakai, K. (1996). Bleaching of hardwood kraft pulp with manganese peroxidase from *Phanerochaete sordida* YK-624 without addition of MnSO(inf4). Appl Environ Microbiol *62*, 913-917.

Hawkins, C.L., and Davies, M.J. (2001). Generation and propagation of radical reactions on proteins. Biochim Biophys Acta *1504*, 196-219.

Heinfling, A., Bergbauer, M., and Szewzyk, U. (1997). Biodegradation of azo and phthalocyanine dyes by *Trametes versicolor* and *Bjerkandera adusta*. Appl Microbiol Biotechnol *48*, 261-266.

Heinfling, A., Martínez, M.J., Martínez, A.T., Bergbauer, M., and Szewzyk, U. (1998). Transformation of industrial dyes by manganese peroxidases from *Bjerkandera adusta* and *Pleurotus eryngii* in a manganese-independent reaction. Appl Environ Microbiol *64*, 2788-2793.

Henriksen, A., Schuller, D.J., Meno, K., Welinder, K.G., Smith, A.T., and Gajhede, M. (1998). Structural interactions between horseradich peroxidase C and the substrate benzhydroxamic acid determined by x-ray crystallography. Biochemistry *37*, 8045-8060.

Herskovits, T.T., and Jaillet, H. (1969). Structural stability and solvent denaturation of myoglobin. Science *163*, 282-285.

Hiner, A.N., Hernández-Ruíz, J., García-Cánovas, F., Smith, A.T., Arnao, M.B., and Acosta, M. (1995). A comparative study of the inactivation of wild-type, recombinant and two mutant horseradish peroxidase isoenzymes C by hydrogen peroxide and *m*-chloroperoxybenzoic acid. Eur J Biochem *234*, 506-512.

Hiner, A.N., Rodríguez-López, J.N., Arnao, M.B., Lloyd Raven, E., García-Cánovas, F., and Acosta, M. (2000). Kinetic study of the inactivation of ascorbate peroxidase by hydrogen peroxide. Biochem J *348*, 321-328.

Ho, S.N., Hunt, H.D., Horton, R.M., Pullen, J.K., and Pease, L.R. (1989). Site-directed mutagenesis by overlap extension using the polymerase chain reaction. Gene *77*, 51-59.

Hollmann, F., and Arends, I.W. (2012). Enzyme Initiated Radical Polymerizations. Polymers *4*, 759-793.

Huang, Q., Huang, Q., Pinto, R.A., Griebenow, K., Schweitzer-Stenner, R., and Weber, W.J.J. (2005). Inactivation of horseradish peroxidase by phenoxyl radical attack. J Am Chem Soc *127*, 1431-1437.

Huang, Q., and Weber, W.J.J. (2005). Transformation and removal of bisphenol A from aqueous phase via peroxidase mediated oxidative coupling reactions:

efficacy, products, and pathways. Environ Sci Technol *39*, 602-6036.

Husain, Q. (2006). Potential applications of the oxidoreductive enzymes in the decolorization and detoxification of textile and other synthetic dyes from polluted water: a review. Crit Rev Biotechnol *26*, 201-221.

Ikeda, R., Tanaka, H., Uyama, H., and Kobayashi, S. (2000). Enzymatic synthesis and curing of poly(cardanol). Polym J *32*, 589-593.

Itakura, H., Oda, Y., and Fukuyama, K. (1997). Binding mode of benzhydroxamic acid to *Arthromyces ramosus* peroxidase shown by X-ray crystallographic analysis of the complex at 1.6 Å resolution. FEBS Lett *412*, 107-110.

Ivancich, A., Donald, L.J., Villanueva, J., Wiseman, B., Fita, I., and Loewen, P.C. (2013). Spectroscopic and kinetic investigation of the reactions of peroxyacetic acid with Burkholderia pseudomallei catalase-peroxidase, KatG. Biochemistry *52*, 7271-7282.

Jacks, T.J., Cotty, P.J., and Hinojosa, O. (1991). Potential of animal myeloperoxidase to protect plants from pathogens. Biochem Biophys Res Commun *178*, 1202-1204.

Jaroszewski, L., Rychlewski, L., Li, Z., Li, W., and Godzik, A. (2005). FFAS03: a server for profile-profile sequence alignments. Nucleic Acids Res *33*, w284-285.

Jauregui, J., Valderrama, B., Albores, A., and Vazquez-Duhalt, R. (2003). Microsomal transformation of organophosphorus pesticides by white rot fungi. Biodegradation *14*, 397-406.

Jin, Z., Su, Y., and Duan, Y. (2001). A novel method for polyaniline synthesis with the immobilized horseradish peroxidase enzyme. Synth Met *122*, 237-242.

Johnson, W.C. (1999). Analyzing protein circular dichroism spectra for accurate secondary structures. Proteins *35*, 307-312.

Jones, P. (2001). Roles of water in heme peroxidase and catalase mechanisms. J

Biol Chem *276*, 13791-13796.

Kauffmann, C., Petersen, B.R., and Bjerrum, M.J. (1999). Enzymatic removal of phenols from aqueous solutions by *Coprinus cinereus* peroxidase and hydrogen peroxide. J Biotechnol *73*, 71-74.

Kelly, S.M., Jess, T.J., and Price, N.C. (2005). How to study proteins by circular dichroism. Biochim Biophys Acta *1751*, 119-139.

Khmelnitsky, Y.L., Budde, C., Arnold, J.M., Usyatinsky, A., Clark, D.S., and Dordick, J.S. (1997). Synthesis of water-soluble paclitaxel derivatives by enzymatic acylation. J Am Chem Soc *119*, 11554-11555.

Kilbanov, A.M., Alberti, B.N., Morris, E.D., and Felshin, L.M. (1980). Enzymatic removal of toxic phenols and anilines from waste waters. J Appl Biochem *2*, 414-421.

Kim, H.S., Cho, D.H., Won, K., and Kim, Y.H. (2009). Inactivation of *Coprinus cinereus* peroxidase during the oxidation of various phenolic compounds originated from lignin. Enzyme Microb Technol *45*, 150-155.

Kim, S.J., Joo, J.C., Kim, H.S., Kwon, I., Song, B.K., Yoo, Y.J., and Kim, Y.H. (2014). Development of the radical-stable *Coprinus cinereus* peroxidase (CiP) by blocking the radical attack. J Biotechnol *189*, 78-85.

Kim, S.J., Lee, J.A., Joo, J.C., Yoo, Y.J., Kim, Y.H., and Song, B.K. (2010). The development of a thermostable CiP (*Coprinus cinereus* peroxidase) through in silico design. Biotechnol Prog *26*, 1038-1046.

Kim, Y.H., An, E.S., Park, S.Y., Lee, J., Kim, J.H., and Song, B.K. (2007). Polymerization of bisphenol a using *Coprinus cinereus* peroxidase (CiP) and its application as a photoresist resin. J Mol Catal, B Enzym *44*, 149-154.

Kim, Y.H., An, E.S., Song, B.K., Kim, D.S., and Chelikani, R. (2003). Polymerization of cardanol using soybean peroxidase and its potential application as anti-biofilm coating material. Biotechnol Lett *25*, 1521-1524.

Kim, Y.H., Won, K., Kwon, J.M., Jeong, H.S., Park, S.Y., An, E.S., and Song, B.K. (2005). Synthesis of polycardanol from a renewable resource using a fungal peroxidase from *Coprinus cinereus*. J Mol Catal, B Enzym *34*, 33-38.

Kirby, N., Mc Mullan, G., and Marchant, R. (1995). Decolourisation of an artificial textile effluent by *Phanerochaete chrysosporium*. Biotechnol Lett *17*, 761-764.

Kjalke, M., Andersen, M.B., Schneider, P., Christensen, B., Schülein, M., and Welinder, K.G. (1992). Comparison of structure and activities of peroxidases from *Coprinus cinereus*, *Coprinus macrorhizus* and *Arthromyces ramosus*. Biochim Biophys Acta *1120*, 248-256.

Klibanov, A.M. (2001). Improving enzymes by using them in organic solvents. Nature *409*, 241-246.

Klibanov, A.M., Tu, T.M., and P., S.K. (1983). Peroxidase-catalyzed removal of phenols from coal-conversion waste waters. Science *221*, 259-261.

Klibanov, A.M., Tu, T.M., and Scott, K.P. (1982). Peroxidase-catalyzed removal of phenols from coal-conversion waste waters. Science *221*, 259-261.

Kobayashi, S., and Makino, A. (2009). Enzymatic polymer synthesis: an opportunity for green polymer chemistry. Chem Rev *109*, 5288-5353.

Kohler, H., and Jenzer, H. (1989). Interaction of lactoperoxidase with hydrogen peroxide. Formation of enzyme intermediates and generation of free radicals. Free Radic Biol Med *6*, 323-339.

Kolberg, M., Logan, D.T., Bleifuss, G., Pötsch, S., Sjöberg, B.M., Gräslund, A., Lubitz, W., Lassmann, G., and Lendzian, F. (2005). A new tyrosyl radical on Phe208 as ligand to the diiron center in *Escherichia coli* ribonucleotide reductase, mutant R2-Y122H. Combined x-ray diffraction and EPR/ENDOR studies. J Biol Chem *280*, 11233-11246.

Kyte, J., Doolittle, R.F. (1982). A simple method for displaying the hydropathic character of a protein. J Mol Biol 157, 105-132.

Laane, C., Boeren, S., Vos, K., and Veeger, C. (1987). Rules for optimization of biocatalysis in organic solvents. Biotechnol Bioeng *30*, 81-87.

Li, Q.S., Ogawa, J., Shimizu, S., (2001) Critical role of the residue size at position 87 in H_2O_2- dependent substrate hydroxylation activity and H_2O_2 inactivation of cytochrome P450BM-3. Biochem Biophys Res Commun *280*, 1258-1261.

Lim, C.H., and Yoo Y.J. (2000). Synthesis of ortho-directed polyaniline using horseradish peroxidase. Process Biochem *36*, 23-241.

Longoria, A., Tinoco, R., Vázquez-Duhalt, R. (2008) Chloroperoxidase-mediated transformation of highly halogenated monoaromatic compounds. Chemosphere *72*, 485-490.

Ma, X.Y., and Rokita, S.E. (1988). Role of oxygen during horseradish peroxidase turnover and inactivation. Biochem Biophys Res Commun *157*, 160-165.

Mahanwar, P.A., and Kale, D.D. (1998). Effect of cashew nut shell liquid (CNSL) on properties of phenolic resins. J Appl Polym Sci *61*, 2107-2111.

Mamatha, J., Vedamurthy, A.B., and Shruthi, S.D. (2012). Degradation of phenol by turnip root enzyme extract. J Microbiol Biotech Res *2*, 426-430.

Mao, L., Luo, S., Huang, Q., and Lu, J. (2013). Horseradish Peroxidase Inactivation: Heme Destruction and Influence of Polyethylene Glycol. Sci Rep *4*.

Masuda, M., Sakurai, A., and Sakakibara, M. (2001). Effect of enzyme impurities on phenol removal by the method of polymerization and precipitation catalyzed by *Coprinus cinereus* peroxidase. Appl Microbiol Biotechnol *57*, 494-499.

McEldoon, J.P., Pokora, A.P., and Dordick, J.S. (1995). Lignin peroxidase-type activity of soybean peroxidase. Enzyme Microb Technol *17*, 359-365.

Miyazaki, C., and Takahashi, H. (2001). Engineering of the H_2O_2-binding pocket region of a recombinant manganese peroxidase to be resistant to H_2O_2.

FEBS Lett *509*, 111-114.

Monsef Shokri, M., Ahmadian, S., Akbari, N., Khajeh, K. (2014). Hydrophobic substitution of surface residues affects lipase stability in organic solvents. Mol Biotechnol *56,* 360-368.

Morawski, B., Quan, S., and Arnold, F.H. (2001). Functional expression and stabilization of horseradish peroxidase by directed evolution in Saccharomyces cerevisiae. Biotechnol Bioeng *76*, 99-107.

Morita, Y., Yamashita, H., Mikami, B., Iwamoto, H., Aibara, S., Terada, M., and Minami, J. (1988). Purification, crystallization, and characterization of peroxidase from *Coprinus cinereus*. J Biochem *103*, 693-699.

Muñoz, C., Guillén, F., Martínez, A.T., and Martínez, M.J. (1997). Laccase isoenzymes of *Pleurotus eryngii:* characterization, catalytic properties, and participation in activation of molecular oxygen and Mn_2^+ oxidation. Appl Environ Microbiol *63*, 2166-2174.

Myer, Y.P. (1968). Conformation of cytochromes. II. Comparative study of circular dichroism spectra, optical rotatory dispersion, and absorption spectra of horse heart cytochrome c. J Biol Chem *249*, 2115-2122.

Nakajima, R., and Yamazaki, I. (1980). The conversion of horseradish peroxidase C to a verdohemoprotein by a hydroperoxide derived enzymatically from indole-3-acetic acid and by *m*-nitroperoxybenzoic acid. J Biol Chem *255*, 2067-2071.

Nakajima, R., and Yamazaki, I. (1987). The mechanism of oxyperoxidase formation from ferryl peroxidase and hydrogen peroxide. J Biol Chem *262*, 2576-2581.

Nakamoto, S., and Machida, N. (1992). Phenol removal from aqueous solutions by peroxidase-catalyzed reaction using additives. Water Res *26*, 49-54.

Nakayama, T., and Amachi, T. (1999). Fungal peroxidase: its structure, function, and application. J Mol Catal, B Enzym *6*, 185-198.

Nicell, J.A., Al-Kassim, L., and Bewtra, J.K. (1993). Wastewater treatment by enzyme catalyzed polymerization and precipitation. Water Res *27*, 1629-1639.

Norma, J.G. (2006). Using circular dichroism spectra to estimate protein secondary structure. Nat Protoc *1*, 2876-2890.

O'Carra, P. (1975). Porphyrin and Metalloporphyrins (Amsterdam, The Netherlands: Elsevier Scientific Publishing Co.).

Ó'Fágáin, C. (2003). Enzyme stabilization—recent experimental progress. Enzyme Microb Technol *33*, 137-149.

Oguchi, T., Tawaki, S., Uyama, H., Kobayashi, S. (1999). Soluble polyphenol. Macromol Rapid Comm *20*, 401-403.

Ong, S., Keng, P., Lee, W., Ha, S., and Hung, Y. (2011). Dye waste treatment. Water *3*, 157-176.

Ortiz de Montellano, P.R., David, S.K., Ator, M.A., and Tew, D. (1988). Mechanism-based inactivation of horseradish peroxidase by sodium azide. Formation of meso-azidoprotoporphyrin IX. Biochemistry *27*, 5470-5476.

Ozaki, S., and Ortiz de Montellano, P.R. (1995). Molecular engineering of horseradish peroxidase: Thioether sulfoxidation and styrene epoxidation by Phe-41 leucine and threonine mutants. J Am Chem Soc *117*, 7056-7064.

Park, S.Y., Kim, Y.H., Won, K., and Song, B.K. (2009). Enzymatic synthesis and curing of polycardol from renewable resources. J Mol Catal, B Enzym *57*, 312-316.

Patrick, M.J., and Jakob, W. (2000). A method for enzymatic treatment of wool.

Pedersen, G., Christensen, B.E., and Schneider, P. (1993). Heme group attached to cysteine in a given specific sequence of 14 amino acids. (Google Patents).

Perkins, D.N., Pappin, D.J., Creasy, D.M., and Cottrell, J.S. (1999). Probability-based protein identification by searching sequence databases using mass

spectrometry data. Electrophoresis *20*, 3551-3567.

Petersen, J.F.W., Kadziola, A., and Larsen, S. (1994). Three-dimensional structure of a recombinant peroxidase from *Coprinus cinereus* at 2.6 Å resolution. FEBS Lett *339*, 291-296.

Phani Kumar, P., Paramashivappa, R., Vithayathil, P.J., Subba Rao, P.V., and Srinivasa Rao, A. (2002). Process for isolation of cardanol from technical cashew (*Anacardium occidentale* L.) nut shell liquid. J Agric Food Chem *50*, 4705-4708.

Piontek, K., Smith, A.T., and Blodig, W. (2001). Lignin peroxidase structure and function. Biochem Soc Trans *29*, 111-116.

Pricelius, S., Ludwig, R., Lant, N.J., Haltrich, D., and Guebitz, G.M. (2011). In situ generation of hydrogen peroxide by carbohydrate oxidase and cellobiose dehydrogenase for bleaching purposes. Biotechnol J *6*, 224-230.

Regalado, C., García-Almendárez, B.E., and Duarte-Vázquez, M.A. (2004). Biotechnological applications of peroxidases. Phytochem Rev *3*, 243-256.

Reihmann, M., and Ritter, H. (2006). Synthesis of phenol polymers using peroxidases. Adv Polymer Sci *194*, 1-49.

Robinson, T., McMullan, G., Marchant, R., and Nigam, P. (2001). Remediation of dyes in textile effluent: a critical review on current treatment technologies with a proposed alternative. Bioresour Technol *77*, 247-255.

Rodriguez-Lopez, J.N., Smith, A.T., and Thorneley, R.N. (1997). Effect of distal cavity mutations on the binding and activation of oxygen by ferrous horseradish peroxidase. J Biol Chem *272*, 389-395.

Rusling, J.F., and Nassar, A.E. (1993). Enhanced electron transfer for myoglobin in surfactant films on electrodes. J Am Chem Soc *115*, 11891-11897.

Russ, R., Zelinski, T., and Anke, T. (2002). Benzylic biooxidation of various toluenes to aldehydes by peroxidase. Tetrahedron Lett *43*, 791-793.

Ryan, B.J., and O'Fágáin, C. (2007). Effects of single mutations on the stability of horseradish peroxidase to hydrogen peroxide. Biochimie *89*, 1029-1032.

Ryu, K., Mceldoon, J.P., and Dordick, J.S. (1995). Kinetic characterization of a fungal peroxidase from *Coprinus cinereus* in aqueous and organic media. Biocatal Biotransformation *13*, 53-63.

Sakurai, A., Masuda, M., and Sakakibara, M. (2003). Effect of surfactants on phenol removal by the method of polymerization and precipitation catalysed by *Coprinus cinereus* peroxidase. J Chem Technol Biotechnol *78*, 952-958.

Schmid, A., Dordick, J.S., Hauer, B., Kiener, A., Wubbolts, M., and Witholt, B. (2001). Industrial biocatalysis today and tomorrow. Nature *409*, 258-268.

Schwehm, J.M., Kristyanne, E.S., Biggers, C.C., Stites, W.E., (1998). Stability effects of increasing the hydrophobicity of solvent-exposed side chains in staphylococcal nuclease. Biochemistry 37, 6939-6948.

Seelbach, K., van Deurzen, M.P., van Rantwijk, F., Sheldon, R.A., and Kragl, U. (1997). Improvement of the total turnover number and space-time yield for chloroperoxidase catalyzed oxidation. Biotechnol Bioeng *55*, 283-288.

Shan, J., and Cao, S. (2000). Enzymatic polymerization of aniline and phenol derivatives catalyzed by horseradish peroxidase in dioxane. Polym Adv Technol *11*, 288-293.

Shiro, Y., Kurono, M., and Morishima, I. (1986). Presence of endogenous calcium ion and its functional and structural regulation in horseradish peroxidase. J Biol Chem *261*, 9382-9390.

Shutava, T., Zheng, Z., John, V., and Lvov, Y. (2004). Microcapsule modification with peroxidase-catalyzed phenol polymerization. Biomacromolecules *5*, 914-921.

Sigoillot, C., Camarero, S., Vidal, T., Record, E., Asther, M., Pérez-Boada, M., Martínez, M.J., Sigoillot, J.C., Asther, M., Colom, J.F., *et al.* (2005). Comparison of different fungal enzymes for bleaching high-quality paper pulps. J

Biotechnol *115*, 333-343.

Simmons, K.E., Minard, R.D., and Bollag, J.M. (1987). Oligomerization of 4-chloroaniline by oxidoreductases. Environ Sci Technol *21*, 999-1003.

Singh, H. (2006). Mycoremediation: Fungal Bioremediation. (Johne Wiley and Sons Publication).

Singh, P., Sulaiman, O., Hashim, R., Rupani, P.F., and Peng, L.C. (2010). Biopulping of lignocellulosic material using different fungal species: a review. Rev Environ Sci Biotechnol *9*, 141-151.

Smith, A.T., N., S., Dacey, S., Edwards, M., Bray, R.C., Thorneley, R.N., and Burke, J.F. (1990). Expression of a synthetic gene for horseradish peroxidase C in *Escherichia coli* and folding and activation of the recombinant enzyme with Ca^{2+} and heme. J Biol Chem *265*, 13335-13343.

Stadtman, E.R. (1993). Oxidation of free amino acids and amino acid residues in proteins by radiolysis and by metal-catalyzed reactions. Annu Rev Biochem *62*.

Steevensz, A., Al-Ansari, M.M., Taylor, K.E., Bewtra, J.K., and Biswas, N. (2009). Comparison of soybean peroxidase with laccase in the removal of phenol from synthetic and refinery wastewater samples. J Chem Technol Biotechnol *84*, 761-769.

Steevensz, A., Mousa Al-Ansari, M., Taylor, K.E., Bewtra, J.K., and Biswas, N. (2012). Oxidative coupling of various aromatic phenols and anilines in water using a laccase from *Trametes villosa* and insights into the 'PEG effect'. J Chem Technol Biotechnol *87*, 21-32.

Strickland, E.H. (1968). Circular dichroism of horseradish peroxidase and its enzyme-substrate compounds. Biochim Biophys Acta *151*, 70-75.

Strickland, E.H., Kay, E., Shannon, L.M., and Horwitz, J. (1968). Peroxidase isoenzymes from horseradish roots. 3. Circular dichroism of isoenzymes and apoisoenzymes. J Biol Chem *243*, 3560-3565.

Tsukamoto, K., Itakura, H., Sato, K., Fukuyama, K., Miura, S., Takahashi, S., Ikezawa, H., and Hosoya, T. (1999). Binding of salicylhydroxamic acid and several aromatic donor molecules to Arthromyces ramosus peroxidase, investigated by X-ray crystallography, optical difference spectroscopy, NMR relaxation, molecular dynamics, and kinetics. Biochemistry *38*, 12558-12568.

Valderrama, B., Ayala, M., and Vazquez-Duhalt, R. (2002). Suicide inactivation of peroxidases and the challenge of engineering more robust enzymes. Chem Biol *9*, 555-565.

Van den Burg, B., Dijkstra, B.W., Vriend, G., Van der Vinne, B., Venema, G., Eijsink, V.G. (1994). Protein stabilization by hydrophobic interactions at the surface. Eur J Biochem 220, 981-985.

van de Velde, F., van Rantwijk, F., and Sheldon, R.A. (1999). Selective oxidations with molecular oxygen, catalyzed by chloroperoxidase in the presence of a reductant. J Mol Catal, B Enzym *6*, 453-461.

van de Velde, F., van Rantwijk, F., and Sheldon, R.A. (2001). Improving the catalytic performance of peroxidases in organic synthesis. Trends Biotechnol *19*, 73-80.

Van Deurzen, M.P.J., Seelbach, K., van Rantwijk, F., Kragl, U., and Sheldon, R.A. (1997). Chloroperoxidase: Use of a hydrogen peroxide-stat for controlling reactions and improving enzyme performance. Biocatal Biotransformation *15*, 1-16.

Veitch, N.C. (2004). Horseradish peroxidase: a modern view of a classic enzyme. Phytochemistry *65*, 249-259.

Veitch, N.C., Gao, Y., Smith, A.T., and White, C.G. (1997). Identification of a critical phenylalanine residue in horseradish peroxidase, Phe179, by site-directed mutagenesis and ^{1}H-NMR: implications for complex formation with aromatic donor molecules. Biochemistry *36*, 14751-14761.

Veitch, N.C., Gilfoyle, D.J., White, C.G., and Smith, A.T. (1996). Plant

Peroxidases: biochemistry and physiology (Switzerland: University of Geneva).

Veitch, N.C., Tams, J.W., Vind, J., Dalbøge, H., and Welinder, K.G. (1994). NMR studies of recombinant *Coprinus peroxidase* and three site-directed mutants. Implications for peroxidase substrate binding. Eur J Biochem *222*, 909-918.

Veitch, N.C., Williams, R.J., Bone, N.M., Burke, J.F., and Smith, A.T. (1995). Solution characterisation by NMR spectroscopy of two horseradish peroxidase isoenzyme C mutants with alanine replacing either Phe142 or Phe143. Eur J Biochem *233*, 650-658.

Villegas, J.A., Mauk, A.G., and Vazquez-Duhalt, R. (2000). A cytochrome c variant resistant to heme degradation by hydrogen peroxide. Chem Biol *7*, 237-244.

Vyas, B.R., and Molitoris, H.P. (1995). Involvement of an extracellular H_2O_2-dependent ligninolytic activity of the white rot fungus *Pleurotus ostreatus* in the decolorization of Remazol brilliant blue R. Appl Environ Microbiol *61*, 3919-3927.

Wagner, M., and Nicell, J.A. (2002). Detoxification of phenolic solutions with horseradish peroxidase and hydrogen peroxide. Water Res *36*, 4041-4052.

Wallace, G., and Fry, S.C. (1999). Action of diverse peroxidases and laccases on six cell wall-related phenolic compounds. Phytochemistry *52*, 769-773.

Ward, G., Belinky, P.A., Hadar, Y., Bilkis, I., and Dosoretz, C.G. (2002). The influence of non-phenolic mediators and phenolic co-substrates on the oxidation of 4-bromophenol by lignin peroxidase. Enzyme Microb Technol *30*, 490-498.

Wariishi, H., Akileswaran, L., and Gold, M.H. (1988). Manganese peroxidase from the basidiomycete *Phanerochaete chrysosporium*: spectral characterization of the oxidized states and the catalytic cycle. Biochemistry *27*, 5365-5370.

Wariishi, H., and Gold, M.H. (1989). Lignin peroxidase compound III: Formation, inactivation, and conversion to the native enzyme. FEBS Lett *243*,

165-168.

Wariishi, H., and Gold, M.H. (1990). Lignin peroxidase compound III. Mechanism of formation and decomposition. J Biol Chem *265*, 2070-2077.

Wariishi, H., Nonaka, D., Johjima, T., Nakamura, N., Naruta, Y., Kubo, S., Fukuyama, K. (2000) Direct binding of hydroxylamine to the heme iron of *Arthromyces ramosus* peroxidase. Substrate analogue that inhibits compound I formation in a competetive manner. J Biol Chem 275, 32919-32924.

Welinder, K.G. (1979). Amino acid sequence studies of horseradish peroxidase. Amino and carboxyl termini, cyanogen bromide and tryptic fragments, the complete sequence, and some structural characteristics of horseradish peroxidase C. Eur, J Biochem *96*, 483-502.

Welinder, K.G. (1992). Superfamily of plant, fungal and bacterial peroxidases. Curr Opin Struct Biol *2*, 388-393.

Welinder, K.G., Mauro, J.M., and Nørskov-Lauritsen, L. (1992). Structure of plant and fungal peroxidases. Biochem Soc Trans *20*, 337-340.

Whitmore, L., and Wallace, B.A. (2004). DICHROWEB, an online server for protein secondary structure analyses from circular dichroism spectroscopic data. Nucleic Acids Res *32*, W668-673.

Won, K., Kim, Y.H., An, E.S., Lee, Y.S., and Song, B.K. (2004). Horseradish peroxidase-catalyzed polymerization of cardanol in the presence of redox mediators. Biomacromolecules *5*, 1-4.

Wong, D.W.S. (1995). Food enzymes: structure and mechanism (NY: Chapman and Hall).

Wu, J., Taylor, K.E., Bewtra, J.K., and Biswas, N. (1993). Optimization of the reaction conditions for enzymatic removal of phenol from wastewater in the presence of polyethylene glycol. . Water Res *27*, 1701-1706.

Wu, Y., Taylor, K.E., Biswas, N., and Bewtra, J.K. (1997). Comparison of

additives in the removal of phenolic compounds by peroxidase-catalyzed polymerization. Water Res *31*, 2699-2704.

Wu, Y., Taylor, K.E., Biswas, N., and Bewtra, J.K. (1998). A model for the protective effect of additives on the activity of horseradish peroxidase in the removal of phenol. Enzyme Microb Technol *22*.

Yang, B.Y., Gray, J.S., and Montgomery, R. (1996). The glycans of horseradish peroxidase. Carbohydr Res *287*, 203-212.

Yousefi, V., and Kariminia, H. (2010). Statistical analysis for enzymatic decolorization of acid orange 7 by *Coprinus cinereus* peroxidase. Int Biodeterior Biodegradation *64*, 245-252.

Yu, J., Taylor, K.E., Zou, H., Biswas, N., and Bewtra, J.K. (1994). Phenol conversion and dimeric intermediates in horseradish peroxidase-catalyzed phenol removal from water. Environ Sci Technol *28*, 2154-2160.

Yukl, E.T., Williamson, H.R., Higgins, L., Davidson, V.L., and Wilmot, C.M. (2013). Oxidative damage in MauG: implications for the control of high-valent iron species and radical propagation pathways. Biochemistry *52*, 9447-9455.

국 문 초 록

퍼옥시다제는 다양한 방향족 화합물을 산화시키는 효소촉매작용으로, 많은 생물공학분야와 생합성분야에 유용하게 사용될 수 있다. 하지만 페놀화합물의 산화반응과정에서 보여지는 퍼옥시다제의 낮은 안정성으로 인해, 이 효소의 사용에는 많은 제약이 따른다. 퍼옥시다제의 낮은 안정성은 불완전 반응을 초래하여 생산율을 감소시키고, 생산단가를 높인다. 지금까지 퍼옥시다제의 비활성에 관한 많은 연구가 이루어 졌으며, 퍼옥시다제의 비활성화 메커니즘으로 과산화수소, 페놀 중합체, 자유래디컬 중간물질(free radical intermediate)과의 상호작용에 의한 메커니즘이 제기되고 있다. 이 중 과산화수소와 페놀 중합체에 의한 비활성화 메커니즘은 많은 실험적 증거들로 증명이 되었지만, 아직까지 자유래디컬에 의한 비활성화 메커니즘은 상대적으로 연구가 미진하다. 따라서 본 연구에서는 페놀 화합물의 산화 과정 동안 퍼옥시다제 비활성화를 일으키는 주요한 비활성화 메커니즘을 규명하고 하였다. 더불어 퍼옥시다제의 비활성화 메커니즘을 기반으로 단백질 공학적 기법을 도입하여 안정성이 향상된 퍼옥시다제를 개발하고자 하였다.

첫째로, 코프리너스 시네레우스 유래의 퍼옥시다제(CiP)와 겨자무에서 유래한 퍼옥시다제(HRPC)를 대상으로, 페놀산화반응 중 효소의 비활성화를 일으키는 주요 인자를 규명하였다. 두 퍼옥시다제에 과산화수소나 페놀 중합체를 각각 처리하였을 경우보다, 과산화수소와 페놀을 동시에 처리했을 때 효소의 비활성화가 매우 크게 나타나는

것을 확인하였다. 또한 페놀산화반응 후 비활성화 효소의 분자량을 확인한 결과, 퍼옥시다제 폴리펩타이드의 분자량이 다소 증가하였으며, 비활성화된 퍼옥시다제에서 추출한 헴(heme)은 대부분이 산화되지 않은 온전한 상태를 보여주었다. 이러한 결과는 페놀산화반응 중 생성되는 페녹실래디컬(phenoxyl radical)과 효소의 폴리펩타이드와의 결합이 효소 비활성화의 주요 인자임을 보여준다.

둘째로, CiP의 래디컬 결합부위를 밝히고, 페놀산화반응 중 일어나는 래디컬에 의한 비활성화 메커니즘을 구체적으로 제안하였다. 비활성화된 CiP의 질량분석을 통하여, F230 잔기에 페녹실래디컬이 결합된 것을 확인하였으며, 해당 아미노산 잔기를 래디컬과 반응성이 낮은 알라닌 아미노산 잔기로 치환하여 F230A 돌연변이형을 제작하였다. F230A 돌연변이형은 페놀산화과정 동안 처음 활성의 80%를 유지하며, 야생형과 달리 매우 높은 안정성을 보여주었다. 더불어 래디컬 결합 전후의 퍼옥시다제의 단백질 구조 변화를 비교해 본 결과, 단백질 구조에는 거의 변화가 없음을 확인하였다. 즉, 래디컬에 의한 비활성화는 래디컬 결합에 의한 효소의 구조변형에 기인한 것이 아니라, 래디컬의 결합으로 인해 효소 기질이 효소 활성자리(active site)에 결합하지 못한 결과라고 추측할 수 있다.

셋째로, 또 다른 퍼옥시다제인 HRPC를 대상으로 래디컬에 대한 안정성을 향상시켜, 퍼옥시다제 비활성화 메커니즘을 추가적으로 증명하였다. HRPC 내의 래디컬 결합에 취약한 페닐알라닌 잔기들을 확인하고, 래디컬의 결합을 막기 위해 알라닌 잔기로 모두 치환하였다. 실험 결과, F68A/F142A/F143A/F179A 돌연변이형은 페놀산화 반응

동안 처음 활성의 41%를 유지하며 야생형에 비해 높은 안정성을 보여주었다. 또한 페놀산화 과정 중 비활성화되는 다른 퍼옥시다제에서도 래디컬 결합에 취약한 페닐알리닌 아미노산 잔기들이 효소의 활성자리 입구에 보존되어 있었다. 이러한 사실은 래디컬 결합 사이트의 위치가 퍼옥시다제의 비활성화에 매우 결정적임을 보여준다. 또한 본 연구에서 제시한 새로운 단백질 디자인 전략(protein design strategy)이 실제 두 퍼옥시다제의 안정성을 성공적으로 향상시켜 그 유효함을 보여주었으며, 다른 단백질의 안정성 향상개발도 중요한 전략으로 쓰일 것으로 기대된다.

넷째로, 래디컬에 대한 안정성이 증대된 CiP의 F230A 돌연변이형을 실제 응용분야(페놀 제거, 염색화합물의 탈색, 페놀 중합반응)에 적용해 보았다. F230A 돌연변이형은 야생형에 비해 페놀제거율이 4.5 배, 염색화학물(Reactive Black 5)의 탈색율이 5 배 증가하였다. 또한 페놀 중합반응에서는 50% (v/v) 농도의 이소프로판올 용액에서 가장 높은 분자량(8850 Da)의 페놀중합체를 형성하였다. 본 연구에서 개발한 래디컬에 대한 안정성이 향상된 돌연변이형 퍼옥시다제가 실제 산업분야에서도 생화학 촉매로서 성공적으로 사용 될 수 있는 가능성을 보여준다.

본 연구에서는 산업적으로 유용한 두 종류의 퍼옥시다제 (CiP와 HRPC)를 모델효소로 이용하여, 기존과 다른 래디컬에 의한 퍼옥시다제의 비활성화 메커니즘을 제안하였다. 또한 래디컬 결합 사이트를 제거하는 새로운 단백질 디자인 방법을 적용하여, 실제 CiP와 HRPC의 래디컬에 대한 안정성을 증가시켰다. 이러한 전략은 지금까지 제기되지 않은 새로운 접근방법으로, 기존 효소 설계 방법보다

효과적일 것으로 기대된다. 또한, 본 연구에서 제안한 레디컬에 의한 비활성화 메커니즘은 안정한 효소를 얻기 위한 연구에 큰 도움을 줄 것이며, 산업적으로 유용한 효소 설계에도 적용될 수 있어 학문적, 산업적 응용이 기대된다.

주 제 어 : 퍼옥시다제의 비활성화, 래디컬에 대한 안정성, 래디컬 결합, 질량분석법, 위치선택적 돌연변이, 코프리너스 시네레우스 퍼옥시다제 (*Coprinus cinereus* peroxidase), 겨자무 퍼옥시다제 (Horseradish peroxidase)

학 번 : 2010-31018